Predicting cooling loads in hot and humid climates using machine-learning approaches

Bingyan Jia

A Thesis

in

the Department

of

Building, Civil and Environmental Engineering

Presented in Partial Fulfilment of the Requirements

for the Degree of

Master of Applied Science (Building Engineering) at

Concordia University

Montreal, Quebec, Canada

May 2021

© Bingyan Jia 2021

CONCORDIA UNIVERSITY

SCHOOL OF GRADUATE STUDIES

This is to certify that the thesis prepared

By: Bingyan Jia

Entitled: Predicting cooling loads in hot and humid climates using machine-learning approaches

and submitted in partial fulfilment of the requirements for the degree of

Master of Applied Science (Building Engineering)

complies with the regulations of the University and meets the accepted standards with respect to originality and quality.

Signed by the final Examining Committee:

_____ Chair

Dr. Hua Ge

_____ Examiner

Dr. Hua Ge

_____ Examiner

Dr. Mazdak Nik-Bakht

_____ Supervisor

Dr. Liangzhu (Leon) Wang

_____ Supervisor

Dr. Ibrahim Galal Hassan

Approved by: _____

Chair of Department or Graduate Program Director: Dr. Ashutosh Bagchi

_____ 2021   _____

Dean of Faculty: Dr. Mourad Debbabi

ABSTRACT

Predicting cooling loads in hot and humid climates using machine-learning approaches

Bingyan Jia

In residential, buildings cooling accounts for a significant amount of energy in hot, humid areas. In Qatar, cooling accounts for more than 60% of the country's generated electricity. In previous years, overestimating cooling loads has led to wasted equipment costs and negatively impacted indoor thermal comfort. District cooling systems have gained popularity recently, both in Qatar and worldwide, due to advances in chillers, heat exchangers, and control systems. To determine the district cooling plant's size and operation, it is vital to estimate building-level cooling loads. An accurate and fast prediction of building-level cooling loads is required to assist decision-making. There are several challenges in modeling building cooling loads, such as lack of detailed information regarding the buildings (e.g., building envelope), cooling energy data for validation, and computational effort. Furthermore, in multi-apartment residential buildings connected to a district or centralized cooling system, individual charging requires improvement. To save money and time on individual metering and charging, apartment-level cooling loads prediction is also required. Moreover, an apartment-level meta-model may be useful for optimizing building energy use and retrofit analysis at the apartment level.

This study aims to develop building- and apartment-level meta-models using machine learning approaches to predict the cooling load. Four machine-learning approaches are applied: multiple linear regression, support vector regression, artificial neural networks, and extreme gradient boosting. Critical parameters identified using sensitivity analysis are used as independent variables, which simultaneously consider the building envelope, climate, and internal heat gain parameters. New building energy models are created to test the meta-models' performance.

ACKNOWLEDGEMENTS

I would like to thank all those who helped me throughout my graduate study in Concordia University. Firstly, I would like to express my great appreciation to my supervisors Dr. Liangzhu (Leon) Wang and Dr. Ibrahim Hassan. Advice given by them helps a lot in the research during my graduate study. I sincerely appreciate their time and effort during this time. Secondly, I would like to express my special thanks to Danlin Hou, who helped to develop the sensitivity analysis method. And I learned so many research skills from her. I would also like to thank various colleagues in the group, Dr. Kamal Athar, Dr. Sambhaji Kadam, and Dongxue Zhan, for their assistance and support. It is a wonderful journey to work with them. Finally, I wish to thank my friend Milan Mao, Jianning Quan, and Miao Feng for their support and encouragement.

TABLE OF CONTENTS

LIST OF FIGURES

LIST OF TABLES

NOMENCLATURE

ANN	Artificial neural network
CART	Classification and regression trees
CDD	Cooling degree days
CSP	Cooling setpoint
CV(RMSE)	Coefficient of variation of the root mean squared error
EPD	Equipment power density
FEMP	Federal energy management program
GA	Genetic algorithms
GBDT	Gradient boosting decision tree
IPMVP	International performance measurement and verification protocol
LHS	Latin hypercube sampling
LPD	Lighting power density
MLR	Multiple linear regression
NMBE	Normalized mean bias error
OCC	Number of occupants
R^2	R Square
RBF	Radial basis functions
RC	Relative compactness
RF	Random forests
SA	Sensitivity analysis
SHGC	Solar heat gain coefficient for window glazing
SR	Solar reflectance of interior diffusing blinds roll
SVI	Sensitivity value index
SVM	Support vector machines
SVR	Support vector regression
TMY	Typical meteorological year
WWR	Window-to-wall ratio

1 Introduction

1.1 Problem statement

Building energy consumption is becoming a critical issue worldwide. Countries experiencing hot/humid climates are facing challenges to maintain indoor thermal comfort and air quality in an energy-efficient way. An area where the cooling degree days (CDD) (10 °C) is 3,000 or more hours and the average temperature in the coldest month is greater than 10 °C, and dry bulb humidity is greater than 50% usually is considered as hot and humid climate [1]. Qatar is a rapidly modernizing country in the Middle East. As of 2016, Qatar has the fourth highest GDP per capita in the world, according to the International Monetary Fund [2]. The weather in Qatar can be considered hot and humid. From the typical meteorological year (TMY) weather data, the CDD in Qatar is more than 7,000 hours. As shown in Figure 1, the dry bulb temperature in Qatar can reach up to 45°C during summer, while remains above 15°C in winter. The relative humidity almost reaches 100%.

Qatar is experiencing rapid population and industrial growth, which has led to an influx of foreign workers and the migration of residents to cities. This dramatic population growth has led to a significant increase in energy demand. The total generated electricity has been estimated at 49,873 GWh in 2019 with an average rate of annual increase of 5.2% [3]. Air conditioning comprises 60–70% of Qatar's total electricity demand [4], of which the residential sector accounts for two-thirds [5].The district cooling system has grown in popularity in Qatar and worldwide due to its potential to save about 40% of the electricity compared with stand-alone cooling system.

With over 80% of the nation's population living in capital Doha or its surrounding suburbs, Lusail is a new city that is being built from scratch as an extension of Doha. The city will accommodate 200,000 residents and 170,000 employees in the future [6]. As part of the government's Vision 2030 [7] sustainable development plan, the district cooling system in Lusail city is designed to

save 65 million tons of CO_2 a year. It has been observed that in Qatar, many building developers overestimate building cooling consumption, resulting in wasted district cooling plant capacity and affecting the comfort index in the conditioned indoor environment. To assist decision-making by district cooling plant stakeholders, accurate and fast prediction and analysis of building-level cooling energy needs are required.

In multi-apartment residential buildings connected to a district or centralized cooling system, individual charging for each apartment's energy consumption is essential. It is directly related to the interests of the apartment owners and building managers. In Qatar, for the end-users of a central district cooling system, a flat charge is applied based on the per unit volume of apartments. Actual cooling energy is affected by the units' setpoints, occupant behavior, schedule, and the month of the year. This charging approach is unreasonable because it is irrespective of all the factors mentioned. As such, there is no economic incentive for occupants to save energy. Therefore, a more reasonable charging method is desirable. However, individual charging is challenging due to the multiple factors involved, including meteorology, policy, and energy management [8]. Separate charging usually requires individual meters or other devices to be installed, which consumes time and money. In Europe, the installation fee for an apartment with an individual metering system varies between 300 € to 3,000 € per year, with running costs between 20 € and 60 € per year [8]. Currently, Lusail city is still under construction, and historical data on cooling demand is unavailable. Furthermore, an extensive survey is infeasible, which has made this research much more challenging.
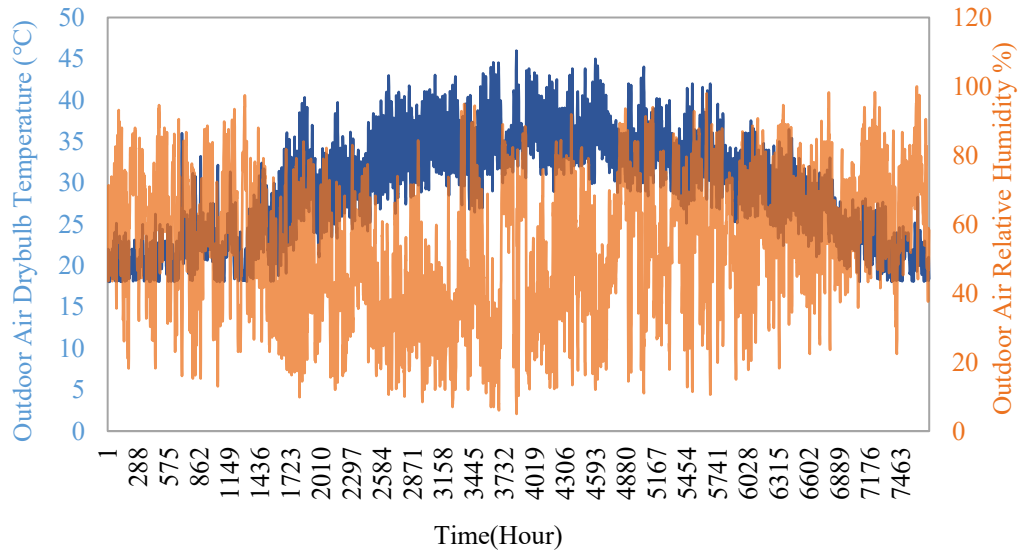
Figure 1. Qatar's annual dry bulb temperature and relative humidity.

1.2   Research objectives

To tackle the two problems discussed in Section 1.1, the research has two objectives:

 (1) To estimate residential building energy use at the district scale, a meta-model is developed that can predict the building-level cooling load for different residential buildings. The selected building is a high-rise typical residential tower located in the Lusail city of Qatar. Eighteen building energy models are created using EnergyPlus based on the selected building, and 11,700 cases are generated by changing the critical parameters defined by sensitivity analysis. The input-output dataset is used to develop the meta-models by applying four machine-learning approaches. (2) To understand the apartment-level cooling load, the selected building is modeled in detail using EnergyPlus. The building contains 138 apartments. In the energy model, each apartment is modeled as one thermal zone. In this way, we can estimate differences in the cooling load of apartments located on separate floors and at different orientations. The meta-models are

3

subsequently developed based on the apartment-level cooling load following the same process. A

new building energy model is established to validate the meta-model.

2 Literature Review

2.1 Factors influencing building thermal loads

This section is focused on analyzing and identifying the influencing factors on thermal loads (mainly cooling loads) or energy consumption. The main categories of factors can be summarized as climate parameters, building thermal-physical characteristics, and building operation parameters. These three categories gather the pool of factors that define the thermal loads of a building.

2.1.1 Climate parameters

In energy simulation, climate parameters are the primary inputs. Examples of climate parameters are temperature (including dry and wet bulb temperatures), relative humidity, solar radiation, dewpoint temperature, wind speed, and wind direction. Each climatic element could affect the building's energy performance in one or more aspects [9]. For example, the temperature may influence heating and cooling loads, and solar radiation has an impact on cooling and lighting loads.

A study conducted by Swhli et al. detected heating load by analyzing five climate parameters: dry bulb temperature, dewpoint temperature, radiation, diffuse radiation, and wind speed [10]. Dry bulb temperature was revealed to be the most significant heating load factor, while dewpoint temperature had the least influence. Afshari et al. studied a fifteen-floor building in Abu-Dhabi [11]. The results revealed that air temperature and relative humidity represent weather data in hot and arid climates. Adel et al. analyzed the impact of weather conditions on peak electricity demand in Qatar [12]. Their results failed to show a correlation between daily peak load and daily maximum humidity. However, the daily maximum temperature and daily peak load were summarized as a linear relationship. Radhi et al. studied the relationship between weather data and

building energy performance [9]. The climatic elements included dry and wet bulb temperatures, wind speed, wind direction, atmospheric pressure, net long, precipitation, solar radiation, cloud cover, and sunshine duration. The electricity consumption simulation results, using previous weather data, showed a 14.5% difference compared to present weather conditions, demonstrating the influence of weather on building energy demand.

2.1.2 Building thermal-physical characteristics

The thermal-physical characteristics of built structures include the typology and building envelope. Typology parameters include building shape, orientation, aspect ratio, and the number of floors. The building envelope includes roof system, wall assembly, glazing, doors and foundation (Figure 2).
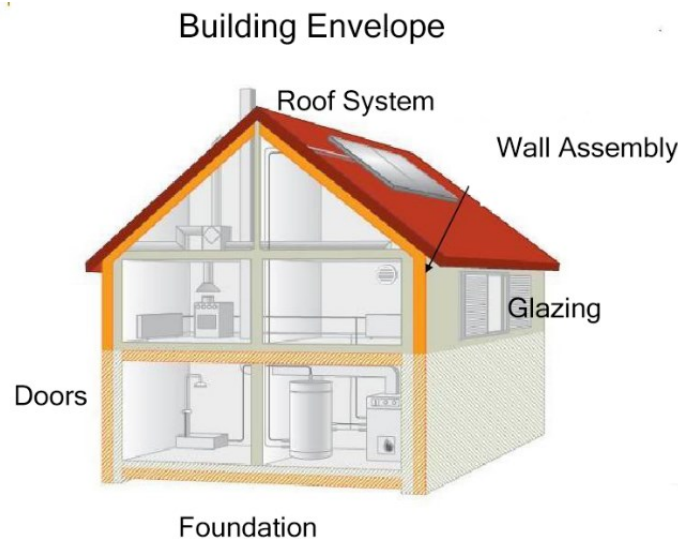
Figure 2. The building envelope (adapted from [13]).

Building shape and orientation have been considered in several studies. Ourghi et al. provided a method of studying the impact of building shape on the annual cooling load of an office block [14]. The results indicated a strong correlation between building shape and cooling load:

$$\frac{E_t}{E_{ref}} = 1 + a \times WWR \times SHGC\left(\frac{1 - RC}{RC}\right) \qquad (1-1)$$

where E_t is building energy consumption, and E_{ref} is the total building energy consumption for the reference building, which has the same floor area and volume as the studied building. Adnan AlAnzi et al. also estimated the influence of building shape on cooling energy use [15]. Several building shapes (including rectangular, L-shape, U-shape, and H-shape) were considered, as well as aspect ratios, window-to-wall ratios, and glazing types. A correlation was found:

$$E_t = E_{ref} \times \left\{ A + B \times \left(WWR \times SHGC \times \frac{1}{RC} \right) \times 2 + C \times \left(WWR \times SHGC \times \frac{1}{RC} \right) + D \times \frac{1}{RC} \right\} \qquad (1-2)$$

where E_t is building energy use, and E_{ref} is the total building energy use for a square building (reference building) with the same floor area and volume of the studied building. Andersson et al. investigated the influence of building orientation on heating and cooling load, using BLAST to simulate a prototype residential building in 25 climates in the United States [16]. The study offered the following conclusions: (1) the east and west orientations produced a higher total load than the south, (2) the east and west orientations produced a higher total load than the north, (3) the north orientation produced a higher total load than the south in all but the hottest U.S. climates, (4) cooling load peaked for the west orientation, and (5) increasing shading over windows tended to diminish the effects of orientation changes. Chi et al. also explored the relationship between building orientation and energy consumption using a case study in Sizhai [17]. They cited several findings: (1) the test case with a north orientation required minimal electricity consumption, (2) electricity consumption for artificial lighting at the south orientation was lower than for the north, (3) the difference in total annual electricity cost was 150 kWh between the best and worst cases.
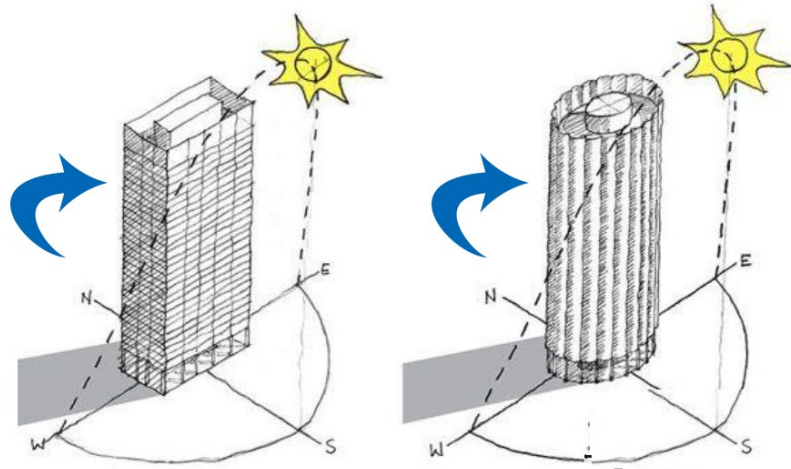
Figure 3. Building shape and orientation (adapted from [18]).

Window-related parameters, such as glass type, and window attachment have also been studied. Tibi studied the impact of glass selection on a high-rise residential building's annual cooling load [19]. Compared to the typical curtain wall glass, the selected glass type (single glazing and double glazing) reduced the cooling load between 5.6% and 9.7%. Huang and Niu conducted an energy simulation using EnergyPlus to investigate the impact of a silica aerogel glazing system on space cooling load [20]. It was observed that solar heat gain through window areas accounted for 80% of the cooling load caused by the building envelope in hot climates. This study demonstrated that the application of a silica aerogel glazing system could reduce the annual cooling load in a typical commercial building by 4%. Assem and AI-Mumin investigated the influence of glazing type on the cooling peak load [21]. Their research revealed that when the glazing type changed to clear double-pane glazing, the cooling peak load reduction was 6.8% for clear low-emissivity, 15.5% for tinted low- emissivity, and 27.5% for reflective low- emissivity glazing. Tan et al. investigated the impact of window attachments on residential buildings' energy use by applying the WINDOW and THERM programs developed by Lawrence Berkeley National Laboratory [17]. The study

illustrated that window attachments with high reflectance and low transmission, were more suitable for use in cooling-dominated climates. In the heating-dominated city, window attachments with low reflectance and high solar transmission were preferable.

Several studies have investigated wall thickness, insulation, and the materials included in the building envelope. Bojic et al. explored the effects of doors and walls on the cooling load in high-rise residential buildings in Hong Kong [22]. Using HTB2 software, the study investigated the yearly cooling load by changing different doors and walls (i.e., wall thickness and composition). Based on the research, the authors made the following observations: (1) the lowest cooling load was obtained when the insulation is added to the living and dining room partitions, (2) additional concrete in thermally insulated walls decreased the yearly cooling load, (3) thermal insulation should be introduced when the thickness ofexterior walls are 25 cm, (4) increased concrete thickness in exterior walls should be abandoned as a design strategy, (5) concrete thickness of 20 cm should be avoided, and (6) uniform distribution may be favorable when the concrete thickness is 30cm. Bojic et al. used HTB2 software to investigate the influence of exterior wall insulation on annual cooling load [23]. They demonstrated that additional thermal insulation applied to an apartment interior was most successful in reducing annual cooling. Furthermore, increasing the thickness of concrete and thermal insulation in external walls may produce a slight increase in the annual cooling load. Solgi et al. analyzed the effect on the cooling load of phase change materials (PCMs) as a thermal mass material [24]. The study was based on a typical office building equipped with an HVAC system and night purge ventilation, in a hot, arid climate. From the study results, it was noted that PCMs could significantly contribute to reducing the cooling load. However, the application of PCMs on the ground floor would increase the cooling load. Ji Hun Park et al. analyzed the impact on energy consumption and thermal comfort of a shading system using PCMs

[25]. When PCMs were applied to the shading system, the cooling energy consumption decreased by 44%, and the number of thermal comfort hours improved by 34%. Wu et al. developed a model to investigate the influence of phase change humidity control material (PCHCM) on indoor hygrothermal conditions and building energy use in office buildings in different climates [26]. They demonstrated that PCHCM greatly influenced building energy performance in Paris and Atlanta climates, which have a broad temperature and humidity difference between day and night. Yang and Li explained the relationship between thermal mass and cooling load by analyzing a simple office building model with air conditioning during the daytime and free cooling at night [27]. The study showed that only an appropriate amount of thermal mass in terms of both thermal properties and convective heat transfer together with suitable outdoor suitable outdoor climates will benefit the most.

There are some other relevant studies. Qiao and Liu explored the relationship between building greening and energy consumption [28]. They built a simulation model using NASA satellite data. The regression results indicated that building energy consumption decreased by 7.8% for every 0.1 increase in the normalized differential vegetation index (NDVI), which proved that building greening reduced energy consumption. Schiavon et al. explored the relationship between cooling load and raised floor systems [29]. This study was based on an office building located in San Francisco and used EnergyPlus to evaluate the summer design's day cooling-load profile. The authors observed that the raised floor system affects the zone cooling load profile and the peak cooling load over the range of -7 to $+40\%$. However, the overall impact was reduced with the presence of carpeting, ranging from 0 to 5% greater for the raised floor than without it.

2.1.3 Building operation parameters

Building operation parameters refer to the setpoint, occupancy rate, lighting density, equipment power density, ventilation rate, and HVAC system operation, all of which significantly impact building energy consumption.

Occupant behavior is a significant factor regarding building cooling load. Poor performance of occupants can significantly influence energy efficiency. Jia et al. investigated the impact of window operation on the cooling load within a high-rise residential building in Hong Kong [30]. They compared building simulation results with a post-occupancy evaluation survey. The results showed that the cooling loads of residential units with different window operating behavior varied up to 11%. Friess et al. generated energy savings of 40% by changing the interior setpoint of a typical villa in United Arab Emirates (UAE) from 22 °C to 25 °C in the living areas and from 21 °C to 24 °C in the bedrooms [31]. Afshin et al. studied a fifteen-story mixed-use building in Abu Dhabi [11]. By increasing the setpoint from 22 °C to 23 °C, then 24 °C, 25 °C, and 26 °C, the annual cooling load reduced by 8%, 16%, 23%, and 29% respectively. Several studies indicate that occupancy data can help predict building cooling load. Simon et al. investigated occupancy area and rate, using them to mimic building cooling load by applying a probabilistic entropy-based neural (PENN) model [32]. Employing weather data acquired from the Hong Kong Observatory and building data from an office block, the authors demonstrated that building occupancy data can significantly improve model prediction accuracy. Furthermore, Simon et al. adopted the multi-layer perceptron (MLP) model to predict cooling load, noting that building occupancy rate significantly impacted building cooling load predictions and greatly improved the accuracy of cooling-load profile simulations [33].

Lam et al. used DOE-2.1E software to analyze the impact of lighting density on heating and cooling loads in office buildings in five climate zones in China [34]. Heat dissipation from electric

lighting could lower the heating load in winter but established a major cooling load component during the summer. The influence of lighting density on the cooling load was several times greater than on the heating load. Taleb studied natural ventilation as an energy-efficient solution in Dubai, using a villa as a case study [35]. Operating the air condition only during the summer months and using natural ventilation in winter achieved energy savings of 30%. The HVAC system operation can also impact a building's cooling load. Deng et al. studied the energy performance of a chilled water system within a high-rise office building in China [36]. The results indicated that greater temperature differences, the energy efficiency of typical devices, and lower terminal resistance could improve the energy efficiency of a chilled water system.

2.2   Building energy simulation models

Figure 4 presents three categories of models used to assess building energy performance: white-box, black-box, and grey-box [37]. White-box refers to physics-based models, also known as thermal models. Black-box models are data-driven, statistical simulations that learn from data to predict building energy without detailed building information. Grey-box describes hybrid models that combine statistical and physics-based approaches [37]. Black-box models are also termed meta-models. Since black-box and grey-box models are both data-driven, two main approaches are used in building energy simulation: physical modeling and data-driven approaches [38].
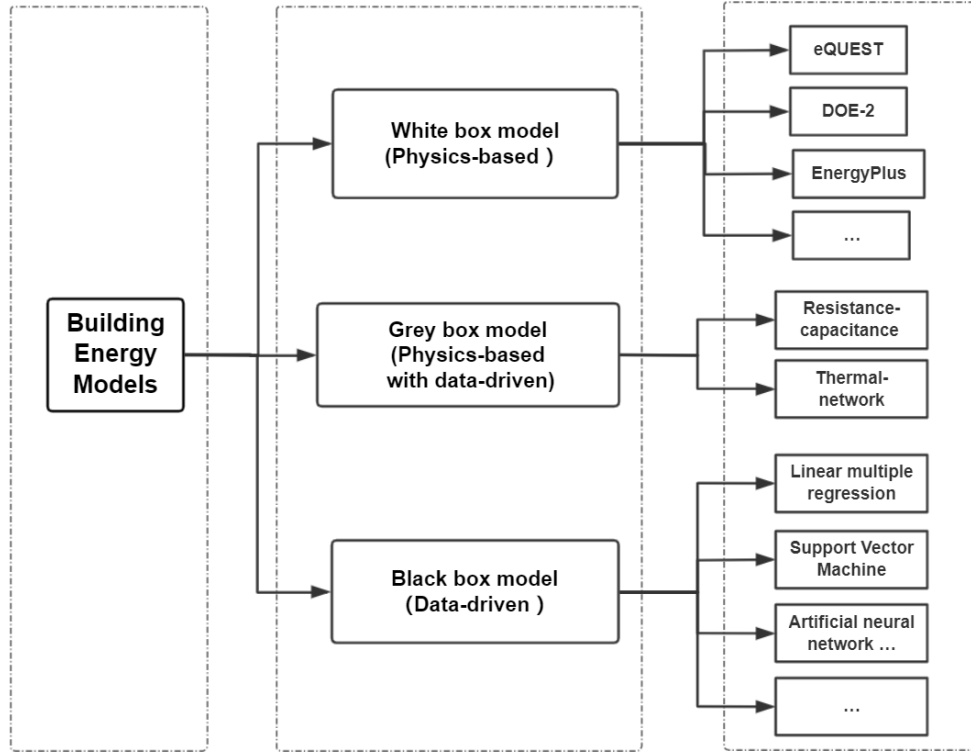
Figure 4. A summary of building energy models.

2.2.1 Physics-based approaches

Physics-based approaches are based on detailed modeling of building physics (e.g., wall heat transfer, air exchange, and air temperatures). This method frequently requires detailed information, such as the parameters for weather condition, building structure, building systems and building equipment from design plan, manufacture catalog or on-site measurement [39]. Such approaches are based on the physical behavior of heat transfer [37]. The equation is written as follows [37]:

$$\emptyset_{int} + \emptyset_{source} = \emptyset_{out} + \emptyset_{stock} \qquad (1-3)$$

where $\emptyset_{int}$ is the heat flux entering the system, $\emptyset_{source}$ is the heat flux source, $\emptyset_{out}$ is the heat flux leaving the system, and $\emptyset_{stock}$ is the stored heat flux. Conduction through walls, convection, longwave and shortwave radiation, and ventilation are the fluxes that take place in the heat transfer.

13
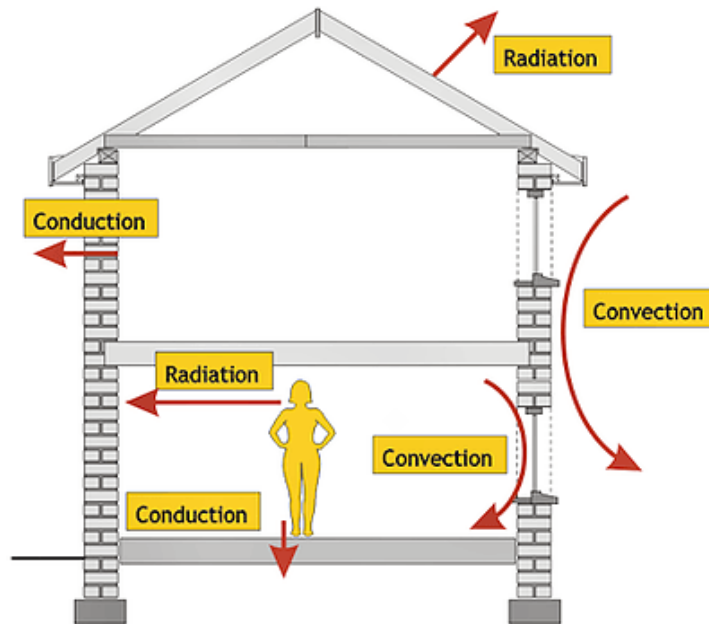
Figure 5. Examples of heat transfer [40].

Lots of physic-based tools have been developed over the years to evaluate building energy consumption, such as BSim [41], DOE-2 [42], ESP-r [43], IDA ICE [44], IES VE [45], eQUEST [46], EnergyPlus [47], and TRNSYS [48]. These softwires allow to size the building HVAC system and analyze the building energy consumption. Crawley and Hand[49] reviewed 20 building energy simulation programs and compared their capabilities on several aspects. Several popular software are compared as follow [49]:

Table 1 Comparison of physic-based models

Features	DeST [50]	DOE-2 [42]	EnergyPlus [47]	eQUEST [46]	ESP-r [43]	TRNSYS [48]
Interior surface convection			√		√	√
Internal thermal mass	√	√	√	√	√	√
Design day sizing calculations	√	√	√	√		

Number of outside surface convection algorithms	1	1	4	1	2	1
Single zone infiltration	√	√	√	√	√	√
Natural ventilation	√		√	√	√	√
Ideal HVAC system	√		√		√	√
User-configurable HVAC systems	√		√		√	√

2.2.2 Data-driven approaches

Black-box models could use a building's historical energy consumption to analyze the relationship between building information and energy data. Information obtained from smart energy meters, building management systems, and weather stations is used as input data. Due to a lack of data available for residential buildings, such approaches typically focus on commercial buildings [37]. Soheil et al. used statistical models to provide a systematic review of building performance forecasting [38]. Multiple linear regression [51], self-regression methods [51], autoregressive with exogenous (ARX) model [52], and artificial neural network(ANN) [53]–[55] are used in the studies. When historical building consumption data is unavailable, meta-models are usually used to predict building energy use. A meta-model is derived from physics-based models; it is usually developed as a correlation between input and output datasets and obtained through physics-based model simulations. Compared to physics-based models, this method is easier to use although more challenging to develop. When many simulations are required, however, meta-models may significantly relieve computing costs while maintaining acceptable levels of accuracy. For meta-model development, a rough description of the building geometry is sufficient.

If data is the fuel of data-driven models, machine learning is the powerful engine. Machine learning can "learn" by themselves once the learning algorithm is determined. This makes the model more adaptable to the uncertain [56]. Tom Mitchell provides a modern definition of machine learning: "A computer program is said to learn from experience E with respect to some class of tasks T and performance measure P, if its performance at tasks in T, as measured by P, improves with experience E." [57].

In machine-learning problems, the training data x_i is used to predict a target variable y_i. A linear model, for example, may be explained using the following equation:

$$\hat{y_i} = \sum_j \theta_j x_{ij} \qquad (2-1)$$

where θ_j represents the parameters that need to learn from the data. The model training process finds the parameters θ that best fit the training data x_i and the target variable y_i. During the training process, the objective function must be defined to measure how effectively the model is trained. The objective function may be described in the following equation:

$$obj(\theta) = L(\theta) + \Omega(\theta) \qquad (2-2)$$

where $L(\theta)$ is the training loss function, the mean squared error is a common choice for $L(\theta)$, and $\Omega(\theta)$ is the regularization term that helps to avoid model overfitting. The meta-models are developed using machine-learning algorithms. Many reviews discuss the use of such algorithms. In a review of the use of machine-learning algorithms in data-driven building energy prediction, Kadir et al. noted that 47% of the studies used artificial neural networks (ANNs), and 25% employed support vector machines (SVMs) to develop their models [38]. Yildiz et al. compared physic-based models with meta-models, including autoregressive and machine-learning models [58]. They applied the models to forecast a building's electricity load. The results indicated that ANNs with Bayesian regulation backpropagation performed best. Nadia et al. reviewed meta-

models using ANNs to simulate building performance [59]. Artificial neural network meta-models are widely used in the analysis of residential and office buildings energy performance. Heating or cooling energy load, comfort index, and indoor microclimate are the main outputs of the meta-models. Ying et al. conducted a comprehensive review to develop data-driven models in general procedures, including feature engineering and data-driven algorithms [60]. They summarized that the main machine-learning algorithms used to model building performance are linear regression, regression trees, support vector regression (SVR), and ANNs. A more detailed review may be found in papers [61]–[63].

2.2.2.1 Meta-model applications

A meta-model may be used in early building design. In a study by Hygh et al., a multivariate linear regression model based on building design parameters was developed to understand building performance at the design stage [64]. The meta-model was used for optimizing the design. The results demonstrated that the model could fit the EnergyPlus simulation results except during Miami's heating season. Gharably et al. extended the model developed by Hygh et al. [64] to include additional buildings with alternative shapes [65]. The relative error between the model and EnergyPlus results was less than 10%. Philipp et al. applied a component-based approach using ANN models to support flexible design [66]. Although these papers have reviewed many parameters related to the building envelope, internal gain parameters such as occupancy have not been discussed.

Besides early building design, meta-models are widely used in sensitivity analysis and model calibration. Five machine-learning models are regularly used in model calibration: Bayesian inference, multiple linear regression (MLR) [67]–[69], SVMs [70], ANNs [71]–[73], multivariate adaptive regression splines [74], and the Gaussian process [68], [69], [74]–[76].

17

Meta-models are also used to optimize building performance and predict energy use. Regarding building performance optimizations, Facundo et al. proposed a method to solve multi-objective building performance problems using ANN-based meta-models [77]. A typical single-family house in Argentina was used as a case study. Seyed et al. applied ANN to a simulation-based multi-objective optimization [78]. A case study was developed using a university building and the proposed model's accuracy was evaluated. Most studies predict the energy for an individual building [37]. Romani et al. developed several meta-models to evaluate the heating and cooling energy needs for a single-family house in Morocco [79]. The results indicated that the Gaussian process, ANNs, and multivariate adaptive regression splines produced more accurate meta-models. Xinyi et al. used machine-learning models (MLR, SVR, and ANN) to predict the heating and cooling loads for a residential building in Chongqing, China [80]. The independent variables included the exterior wall U-value, exterior window U-value, infiltration rate, occupant use, and heating and cooling setpoints. The model output was the annual heating or cooling load. The results indicated that the Gaussian radial basis function kernel SVR performed best. Furthermore, meta-models have been used to predict building energy use at the district level. Mauricio et al. developed a model based on ANNs to predict cooling energy consumption in Brazilian office buildings [81]. The required sample size and the best architecture for ANN models have also been studied. Ngoc-Tri proposed a model to predict cooling loads in 243 office buildings in Taiwan, using ANNs, regression trees, SVR, and linear regression [82]. The model demonstrated a good level of accuracy compared to the physics-based whole-building energy simulation.

2.3 Summary and thesis work introduction

Previous studies have focused on individual buildings as case studies. This means that a meta-model can only be used for a specific building. Few studies have predicted energy consumption

by coupling machine-learning models and building-energy models at a district scale. Among these, only specific or limited parameter combinations have been examined. None have simultaneously considered the building envelope, climate, and internal gain parameters at a district scale. Due to a lack of building data, a comprehensive evaluation of data-driven methods is insufficient in residential buildings [80]. Building energy prediction at the district level is limited. Moreover, meta-models analyzing building energy at the apartment-level are unavailable. A apartment-level meta-model could optimize energy use and aid retrofit analysis. Moreover, a model with an acceptable level of accuracy could help determine the cost and energy consumption charge at the apartment-level.

This thesis uses four machine-learning approaches to develop a meta-model that predicts monthly cooling load at the building level. A apartment-level meta-model is also developed. The thesis is outlined as follows: Chapter 3 presents the thesis methodology, Chapter 4 proposes a cooling energy meta-model at the building level, Chapter 5 introduces a cooling energy meta-model at the apartment-level, and Chapter 6 summarizes the conclusion , the limitations and recommendations for future work.

3 Methodology

3.1 Research framework

This section introduces the research methodology, which is presented in a process diagram (**Error! Reference source not found.**). Building-level and apartment-level meta-models were developed following a similar process:

(1) For building-level meta-model, 18 variant building energy models with different building shape typology are created in EnergyPlus to represent the building stock. OpenStudio SketchUp Plug-in is used to help quickly create building geometry. For the 18 variant building energy models, every floor is a thermal zone. EnergyPlus is selected as the modeling tool because it is the most authoritative software among all the physics-based software, widely used and validated. Next, sensitivity analysis was conducted using an RStudio script. Some parameters such as floor-to-floor height, building orientation are given with a typical value due to the characteristics of the building stock. Unknown parameters like building envelope parameters and their variations are defined by ASHARE or Qatar local standards. Latin Hypercube Sampling (LHS) method [81], using R "lhs" package, is applied to obtain 650 different combinations of the parameters as the inputs. An R package named "eplusr" developed by Jia [83] is used to perform the parametric simulation and collect input and output dataset automatically. SA is conducted on the obtained dataset from the selected buidling to identify significant parameters. By selecting first several important variables, we can exclusively focus on the essential parameters and reduce the simulation runs for the 18 building energy models. Then SA is conducted on all the building models. The third step is to develop the meta-models using the input-output dataset generated from parametric simulation. The dataset was divided into training and test data. The training data were normalized and then imported to train the four machine learning models with Python software [83]. Test data were used

to evaluate the models' performance as a part of the training process. The last step is meta-model verification. The new input data were entered into the EnergyPlus models and the meta-models. The output was compared to see the adaptability of the meta-models.

(2) The steps of apartment-level meta-model development are similar to the building-level meta-model. There are several differences between apartment- and building-level meta-model. First, the baseline model for the apartment-level meta-model is the actual slected building. It is modeled in detail. Each apartment is one thermal zone. Total 138 thermal zones are created. The parameters influencing apartment-level cooling loads are considered as independent variables of meta-model. Because of the complexity of the building, a limited number of parameters variation is applied to represent uncertainty.

3.2   Baseline model creation

First, to build the energy model, building information from audits, site-visits, surveys, and design documents is collected. Then the building model was created in SketchUp, in combination with OpenStudio, and based on the building floor plan. Next, the window-to-wall ratio, which is a measure of the percentage area (calculated by dividing the building's glazed area by its wall area), was established for different floors and façades. Space types and thermal zones were assigned to different space after the building geometry was completed. Space types contained information related to construction, building activity, internal loads, and schedules. Finally, the simulation was conducted using EnergyPlus. In this study, typical meteorological year (TMY) weather data in Doha is used. For all the building energy models, ideal air loads were used to calculate cooling loads. The ideal loads air system is modeled as an ideal VAV terminal unit with variable supply temperature and humidity. The supply air flow rate is varied between zero and the maximum in

21

order to satisfy the zone heating or cooling load, zone humidity controls, outdoor air requirements, and other constraints [84].

3.3   Sensitivity analysis

Sensitivity analysis (SA) plays an important role in building energy performance analysis. The SA methods used for building energy analysis can be divided into local and global approaches [85]. Local SA is focused on the effects of uncertain inputs around a base case, while global SA is more focused on the influences of uncertain inputs over the whole input space. The global SA includes regression methods, screening-based, variance-based, and meta-modeling approaches [85]. For example, the standardized regression coefficient (SRC) and T-value used in this study are regression methods.

SA is a valuable tool for its capability to identify the most influential parameters [86]. Tian [87] summarize typical steps for SA: determine input variations; create building energy models; run energy models; collect simulation results; run sensitivity analysis; presentation of sensitivity analysis results. SA is widely used in building energy analysis. Lam used DOE-2 to investigate an office building in Hong Kong [88]. The annual energy consumption and maximum design load were influenced by the internal load, window system, setpoint, and air conditioning system's efficiency. Rasouli used TRNSYS to study the effects of building character and air conditioning on the peak load, annual energy consumption, and operating costs of an air conditioning system in a Chicago office building [89]. The results indicated that the ventilation rate had the greatest impact on the air conditioning system's energy performance. Kavgic used sensitivity analysis to study the effects of different design parameters on energy consumption and CO_2 emissions in existing buildings [90]. The results demonstrated that the average indoor temperature, efficiency of space

heating systems, outdoor air temperature, and windows significantly impacted building energy consumption and CO_2 emissions.

In this study, some parameters that influence building cooling loads, such as floor-to-floor height and building orientation, are given a typical value due to the characteristics of the building stock. Unknown parameters like building envelope parameters and their variations are defined by ASHARE or Qatar local standards. Next, Latin hypercube sampling was used as the sampling method. Latin hypercube sampling is a statistical method typically used to generate a near-random sample of parameter values [91]. Assuming there are N variables (dimensions), each variable may be divided into M intervals with the same probability. At this time, M sample points that satisfy the Latin hypercube condition may be selected. Therefore, the sample size may be reduced, and the results are more robust compared with random sampling. A parametric simulation was conducted using EnergyPlus to generate the monthly cooling load using RStudio script. Finally, sensitivity analysis was performed to identify the key parameters that would subsequently be used as the meta-model independent variables. This study applied a sensitivity analysis method, Sensitivity Value Index (SVI), to compensate the differences in sensitivity analysis methods and target outputs [92]. Three sensitivity analysis methods including standardized regression coefficient (SRC), random forest variable importance, and T-values are used. More detailed information can be found in Ref. [85]. SVI is calculated using the following equation:

$$\sum_{l=1}^{m} \frac{\frac{\sum_{j=1}^{k}\left(\frac{V_{i,j}}{\sum_{i=1}^{n}|V_{i,j}|}\right)}{k}}{m \cdot k} \times 100 = Sensitivity\ Value\ Index\ (SVI)\ (\%) \qquad (3-1)$$

Where V is the value of a sensitivity analysis method, i is a parameter, j is a sensitivity method, n is the total number of parameters, k is the total number of sensitivity methods, m is the total number of target outputs, and l is the target output.

3.4   Meta-model development

Several steps were undertaken to develop the meta-model (

Figure 6). From the sensitivity analysis, we defined the key parameters as independent variables of the meta-model. We generated an input-output dataset from the baseline model's parametric simulation. The data was separated into training data and test data. After data normalization, the training data were imported to the four machine-learning models (SVR, MLR, ANN, and extreme gradient boosting [XGBoost]). Next, the meta-model's performance was evaluated using the test data as part of the training process. The trained model was then applied to new building models. The predicted results were compared with the simulation results to examine the meta-model performance on the new cases. Data normalization and the four machine learning approaches are introduced in more detail.
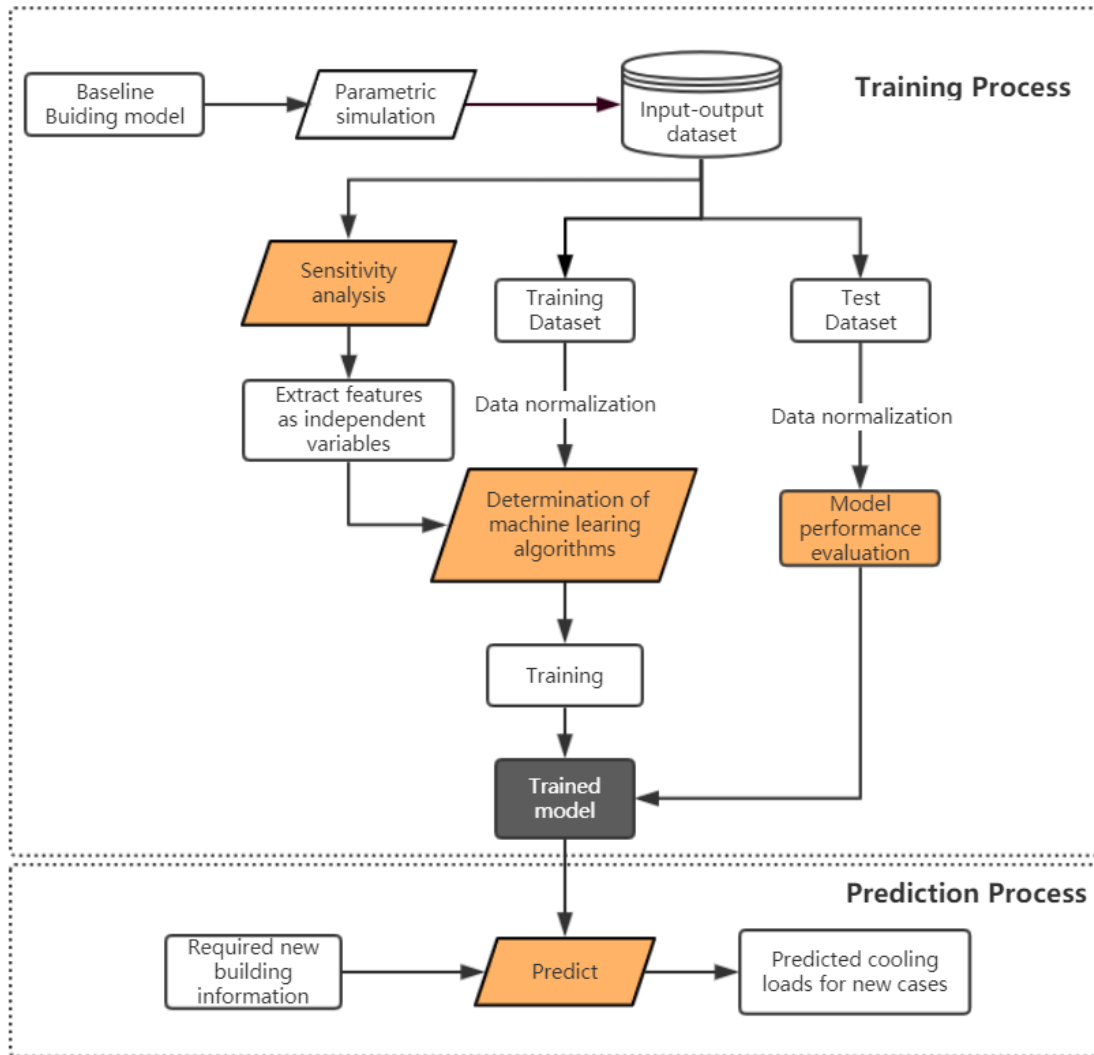
Figure 6. The training and prediction process to develop the meta-model.

3.4.1 Data normalization

Data normalization is used to scale the data proportionally so that it falls into a specific interval. It may remove the unit limit and convert the data into a pure dimensionless value so that indexes of different units or magnitudes may be compared and weighted. This step is essential in cases where the input data varies substantially. Zero-mean (Eq. $(3-2)$), is a standard method of normalization. The data was vertically slid so that the average was zero:

$$x' = \frac{x - \mu}{\sigma} \qquad (3-2)$$

where x' is the new value of the input feature, x is the original value, μ is the mean value, and σ is the standard deviation.

3.4.2 Multiple linear regression

Multiple linear regression is a statistical model capable of establishing a relationship between different variables connected to linear equations [93]. The MLR model used in this study was ordinary least squares linear regression, which is a mathematical optimization method for finding a suitable data fit by minimizing the squared sum of errors. The objective of ordinary least squares using one feature is described in the following equation:

$$\varepsilon = \min \sum_{i=1}^{n} (y_i - w_i x_i)^2 \qquad (3-3)$$

Where ε is the objective, y_i is the target, w_i is the coefficient, and x_i is the variable (feature). Multiple linear regression is widely used in energy prediction. Aranda introduced multiple regression models to predict annual energy consumption in Spain [94]. Fan analyzed prediction performance using MLR with three additional models to aid on-site cooling energy prediction [95]. Multiple linear regression may be presented in the following equation [96]:

$$y_i = a_0 + a_1 x_{i1} + a_2 x_{i2} + \cdots + a_j x_{ij} + e_i \qquad (3-4)$$

where y_i is the numeric response for the ith sample, a_0 is the estimated intercept, a_j is the estimated coefficient for the jth predictor, x_{ij} is the value of the jth predictor for the ith sample, and e_i represents random error. The advantages of MLR modeling are its simplicity and minimal risk of overfitting. Furthermore, many building parameters follow linear correlations.

3.4.3 Support vector regression
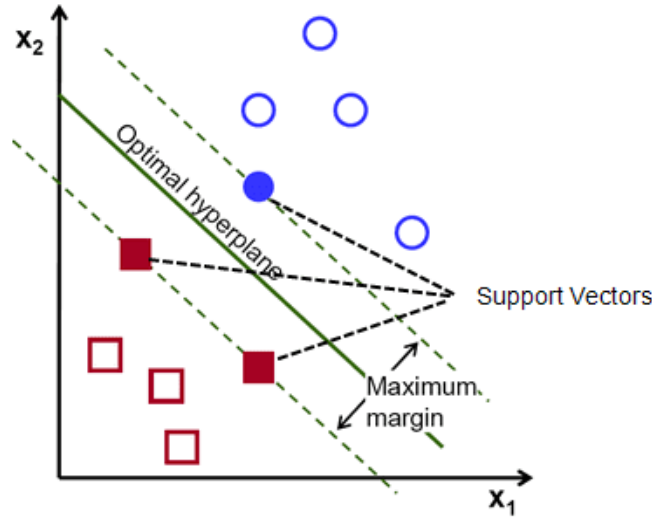
Figure 7. The principles behind support vector machines [97].

Support vector machines were initially developed for classification. A support vector machine algorithm finds a hyperplane in an N-dimensional space. This process distinctly classifies the data points, where N stands for the number of features or independent variables. We used the hyperplane and best fitting margin to differentiate the data. The hyperplane was plotted at equal distances from the extreme ends. The SVM application has been extended to regression (i.e., support vector regression) [98]. The kernel functions used in SVM may transform the data to the required form. Kernel functions include linear, polynomial, and radial basis functions (RBFs). Support vector regression follows a similar principle to SVM; it finds a regression plane, ensuring that all the data is nearest to that plane. Assuming that x refers to the input parameters and y is the output, the SVR equation is $y = f(x)$. Traditional regression methods consider a prediction to be correct if the regression $f(x)$ is precisely equal to y. In linear regression, for example, $(f(x) - y)^2$ is commonly used to calculate the model's loss. Conversely, SVR assumes that if $f(x)$ does not deviate too far from y, the prediction may be considered correct without calculating the loss. In the SVR model, we set a threshold value of ε. Only the loss for data points that met

27

$|f(x) - y| > \varepsilon$ was calculated (Figure 8). The data points located in the gap between the two grey lines are considered to have been predicted accurately, and only the loss for the out-of-gap data points was counted. More detailed information regarding SVR is described in citation [99]. Yan Ding studied two different SVR models (GA-SVR and GA-WD-SVR) to predict short-term and ultra-short-term cooling loads in office buildings [100].
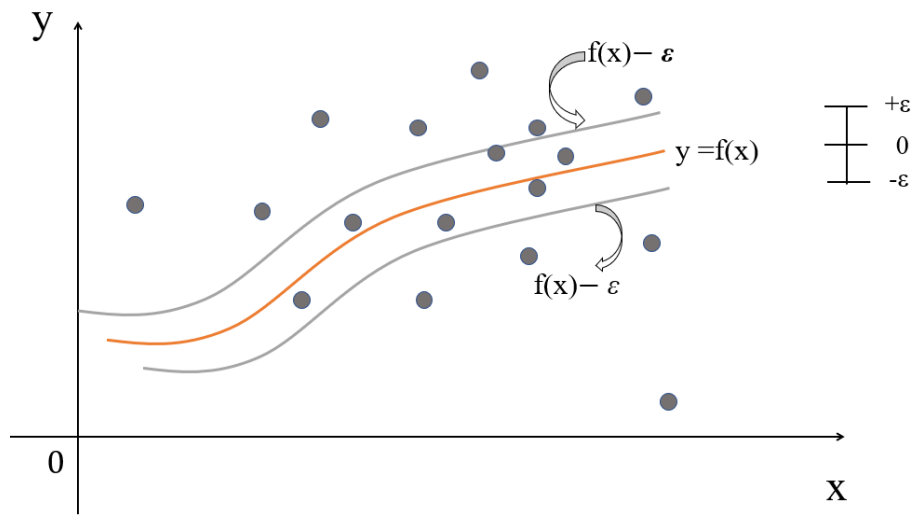
Figure 8. The support vector regression principle.

3.4.4 Artificial neural networks

The basic component of a neural network is the neuron; a mathematical neuron corresponds to a biological nerve cell. Hence, artificial neural network theory uses the abstract mathematical concept of the neuron to describe biological cells in the objective world. Artificial neural networks (Figure 9) consist of simple and highly interconnected processors termed neurons. The input value is fed into each neuron of the input layer. The neurons in one layer are connected to the neurons in the next layer via channels. Each channel is given a numerical value known as a weight. The input values are multiplied by the weights. Their sum is input in the hidden layer. Bias is then

added to the sum, and this value is passed through the activation function. The activation function determines whether this neuron will be activated:

$$y_{ij} = \sum x_i w_{ij} + b_i \qquad (3-5)$$

where y_{ij} represents the values that are sent from node i in the input layer to node j in the hidden layer, x_i is the input to the input layer, and w_{ij} is the weight given to the channel connected nodes i and j. During the training process, the weight w_{ij} is adjusted, and this is the network's learning process. The mean square error (MSE) between the actual and predicted values is minimized through iteration:

$$MSE = \frac{1}{n} \sum_{i}^{n} (y_i - \hat{y}_i) \qquad (3-6)$$

where y_i is the actual value, $\hat{y}_i$ is the predicted value.
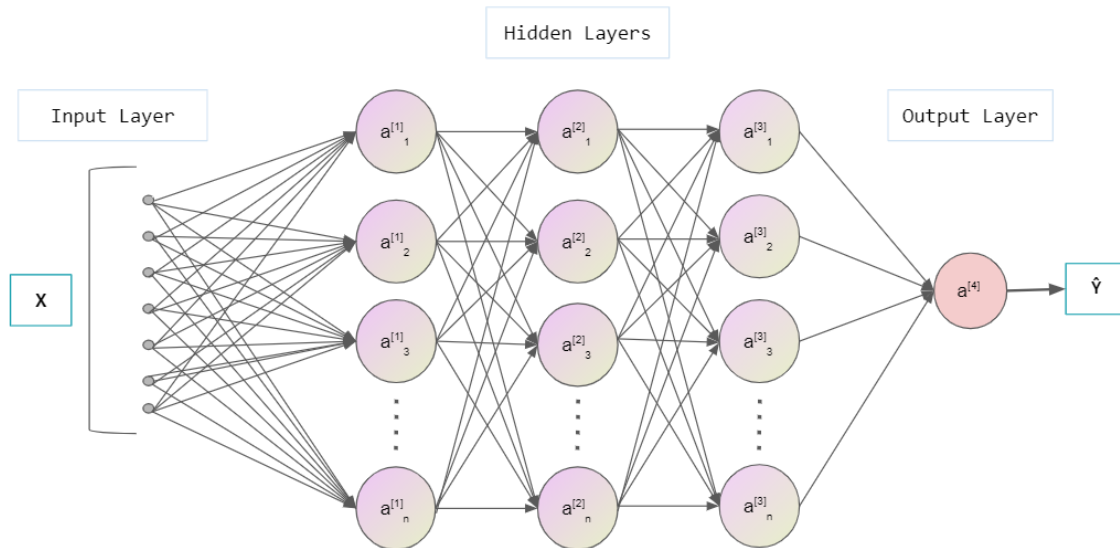
Figure 9. Artificial neural network model structures[101].

Artificial neural networks have three basic characteristics:

- Non-linear. Artificial neurons exist in a state of either activation or inhibition, and this behavior is mathematically represented as a nonlinear relationship. Neurons with thresholds form networks with superior performance, which can improve fault tolerance and storage capacity.

- Non-limiting. A neural network usually consists of multiple neurons that are extensively connected. The overall behavior depends not only on an individual neuron's characteristics but also on the interactions and connections between units. Many connections between units simulate the non-limiting nature of the brain. Associative memory is a classic example of non-limitation.

- Very qualitative. Artificial neural networks have adaptive, self-organizing, and self-learning capabilities. The information processed by a neural network varies in several ways. However, the nonlinear dynamic system is changed continuously as it processes the data.

3.4.5 Extreme gradient boosting

Extreme gradient boosting is a machine-learning system based on a gradient boosting decision tree and is a commonly used ensemble method. The tree ensemble model consists of classification and regression trees (CARTs) that categorize features into different leaves and assign them a score on the corresponding leaf. Each CART node receives a predicted value. When the tree branches, each feature threshold is exhaustively searched to find a better segmentation point. However, the measurement standard is no longer greater entropy but the MSE. Usually, a single tree is not sufficiently robust. Therefore, the ensemble model, which sums the predictions of multiple trees, is used. The ensemble tree model may be described in the following equation:

$$\hat{y}_i = \sum_{j=1}^{j} f_j(x_i), f_j \epsilon F \qquad (3-7)$$

where j is the number of trees, f_j is a function in the functional space F, and F is the set of all possible CARTs [102]. Extreme gradient boosting adds a regularization term to control the model complexity and avoid overfitting [103]. This is an advantage of XGBoost over traditional gradient boosting decision trees.

3.5   Meta-model verification

To verify the meta-models, new building energy models were created. The EnergyPlus simulation results and trained model prediction results were compared to evaluate the meta-models' performance. The prediction accuracy for the four regression models was evaluated using the normalized mean bias error (NMBE), the coefficient of variation of the root mean squared error CV(RMSE), and R-squared (R^2). The CV(RMSE) and NMBE quantify the data's variance while R^2 estimates the model's fitting accuracy.

$$NMBE(\%) = \frac{1}{\bar{y}_{predicted}} \frac{\sum_{k=1}^{n}(y_{predicted\,k} - y_{simulation\,k})}{n} \times 100 \qquad (3-8)$$

$$CV(RMSE)(\%) = \frac{1}{\bar{y}_{predicted}} \sqrt{\frac{\sum_{k=1}^{n}(y_{predicted\,k} - y_{simulation\,k})^2}{n}} \times 100 \qquad (3-9)$$

$$R^2 = 1 - \frac{\sum_{k=1}^{n}(y_{predicted\,k} - y_{simulation\,k})^2}{\sum_{k=1}^{n}(\bar{y}_{predicted} - y_{simulation\,k})^2} \qquad (3-10)$$

Where $y_{predicted}$ is the meta-model prediction results, $y_{simulation}$ is the simulation results from EnergyPlus.

31

Germán Ramos Ruiz summarizes three primary document calibration criteria for monthly and hourly data (Table 2) [104].

Table 2 The calibration criteria [104]

Data Type	Criteria	FEMP [105]	ASHRAE [106]	IPMVP [107]
Monthly	NMBE (%)	±5	±5	±20
	CV(RMSE) (%)	15	15	-
Hourly	NMBE (%)	±10	±10	±5
	CV(RMSE) (%)	30	30	20
	R^2	-	≥0.75	≥0.75

4 Predicting Monthly Building-Level Cooling Load Using Machine-Learning Approaches

This chapter describes a meta-model to predict the monthly cooling load of residential units at the building level. Four machine-learning algorithms are used: MLR, SVR, ANNs, and XGBoost. The critical parameters identified by the sensitivity analysis are the independent variables, which simultaneously consider the building envelope, climate, and internal gain parameters at a district scale. New cases are applied to the meta-models to test their performance. The results show that all four machine learning models got a good R^2, the ANN exhibited the best performance among the models with R^2=0.9991, while MLR, SVR, and XGBoost with R^2= 0.9742, 0.9730, 0.9949, respectively. Regarding CV(RMSE), ANN also showed the best performance (1.9%). In contrast, CV(RMSE) of MLR, SVR, and XGBoost is 10.4%, 10.8%, and 4.7%, respectively. Although ANN performs best, the development of the ANN model is time-consuming. The sample size of training data and the number of neurons in the hidden layer are studied to reduce the computing time. The results show that with a 25% sample size and 30 neurons in the hidden layer, the processing time of ANN can be reduced to 40.6% of the original processing time while maintaining an excellent performance (R^2=0.9992, CV(RMSE)=1.9%).

4.1 Baseline model creation

4.1.1 A typical residential building - based model

Detailed information of a residential building in the Lusial city was obtained. It is a multi-apartment building with 19 stories (including two basements and a ground floor) as presented in Figure 10. Its floor-to-floor height is 3.8 m. The total floor area is 26,147.72 m². The building is constructed at an orientation of 341.57° from north. The two basements are not cooled as they are used for parking. A summary of the building specifications is provided in Table 3. The building's

cooling energy are provided through a district cooling system. It is important to note, however, that due to the building's complexity and the nature of the study, the HVAC of the building was not modeled. Instead, the ideal cooling zone method was used to estimate cooling loads.
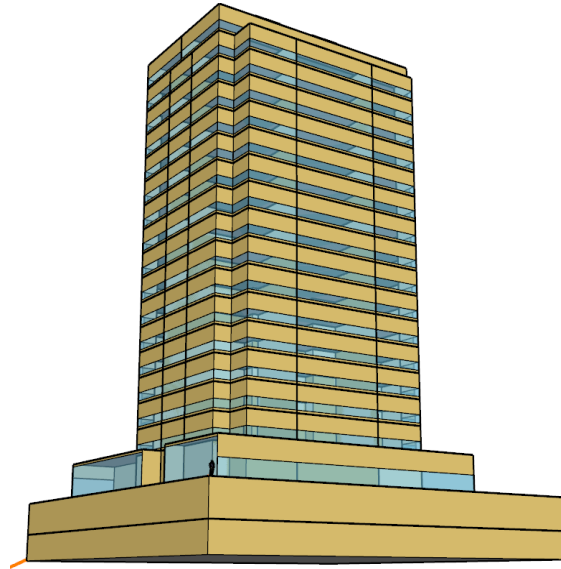
Figure 10. A 3D rendering model in EnergyPlus for the residential building

Table 3 Floor plan summary

Floor	Dimension (m×m)	Floor Height (m)	Function	WWR			
				Front	Rear	Left	Right
2nd Basement	60.70×58.33	3.9	Parking	/	/	/	/
1st Basement	60.70×58.33	4.7	Parking	/	/	/	/
Ground Floor	46.86×44.50	6.08	Lobby	46%	59%	87%	87%
Typical Floor(1st-15th)	35.80×31.50	3.8	Residential	31%	31%	32%	32%
16th Floor	35.80×23.00	4.06	Residential	31%	31%	32%	32%
Roof	21.48×11.46	3.8	Pump room & lift lobby	/	/	/	/

The building consists of 138 apartments. Each apartment is modeled as one thermal zone. The ground floor is modeled as one thermal zone. The 1st to 15th floors typically have eight apartments (zones S, N, W, E, SW, SE, NW, and NE) and one core corridor (zone C). The 16th floor comprises two four-bedroom apartments (zones N and S) and a core corridor (zone C) as

presented in Figure 11. Detailed information is presented in Table 4 and Table 5 .The daily

occupancy, equipment, and lighting power density fractions are given in Figure 12.
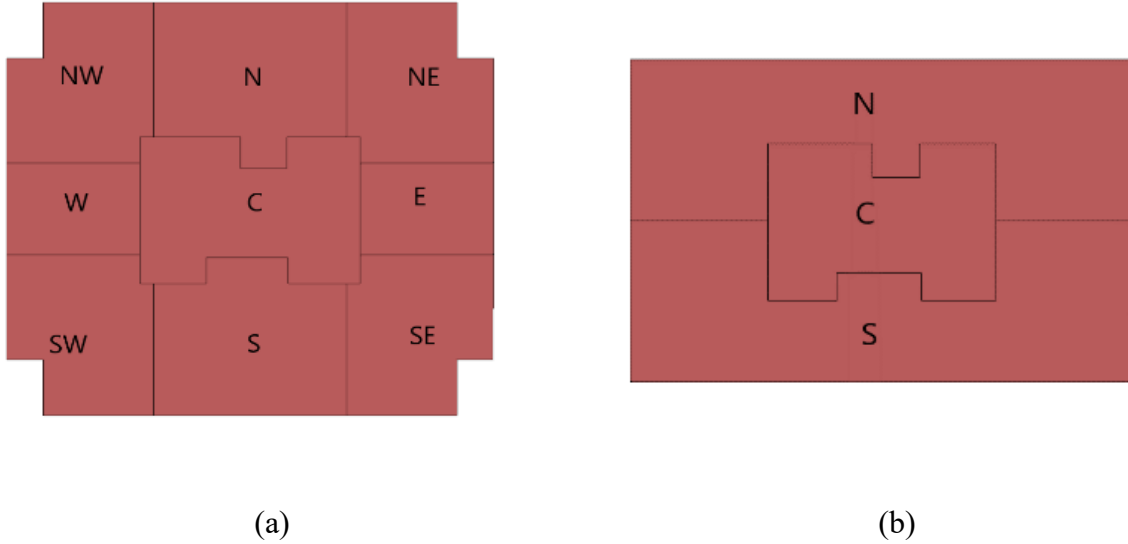
(a)   (b)

Figure 11. Floor plans: (a) floors 1–15, (b) floor 16.

Table 4 Basic Features of the Residential Building Model

Parameter	Description of the Base Case
Location	Doha, Qatar
Floor area	26147.72 m^2
Number of floors	Total:19 (plus two basement)
Thermal zoning	1st -15th floor: 9 thermal zones including eight perimeter zones of apartments and one core thermal zone of the lobby; 16th floor: 3 thermal zones including two perimeter zones of apartments and one core thermal zone of the lobby; Basement, ground floor, and roof: every floor is a thermal zone.
Total number of thermal zones	142 (plus basement)
Window locations	Even distribution among all four sides
Shading Geometry	None
HVAC system	Ideal air loads system
Thermostat Setting	Apartments: 23 °C for cooling (No heating) Ground floor: 18 °C for cooling (No heating)

Table 5 Information of thermal zones

Floor number	Thermal zone	Area (m²)	Space type
Basement 1st, 2nd	BA1, BA2	3540.63	Corridor

35

Ground floor	G	1840.55	Corridor
	C	161.28	Corridor
	W, E	68.6	1-bedroom apartment
1st -15th floor	SW, SE, NW, NE	118.99	2-bedroom apartment
	S, N	153.85, 154.85	3-bedroom apartment
16th floor	C	161.28	Corridor
	S, N	331.36, 330.76	4-bedroom apartment
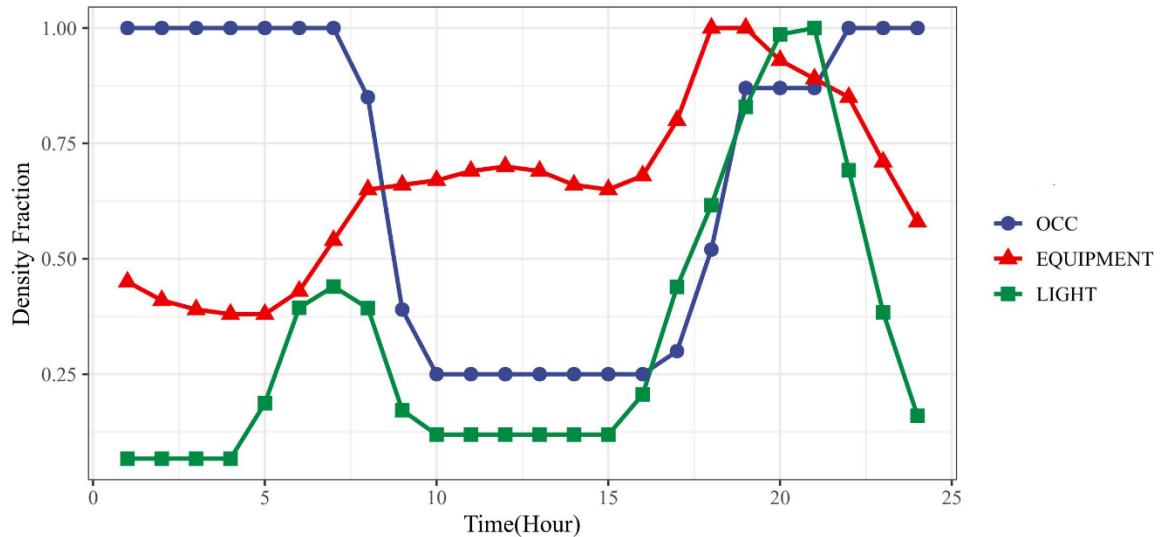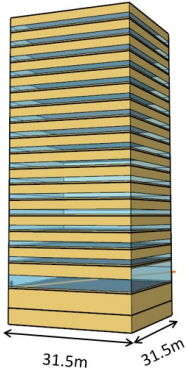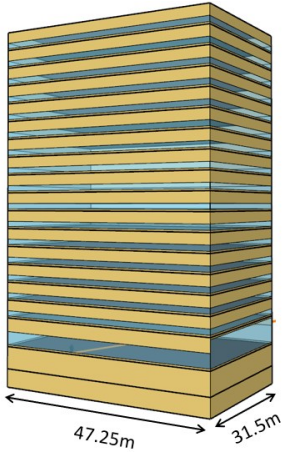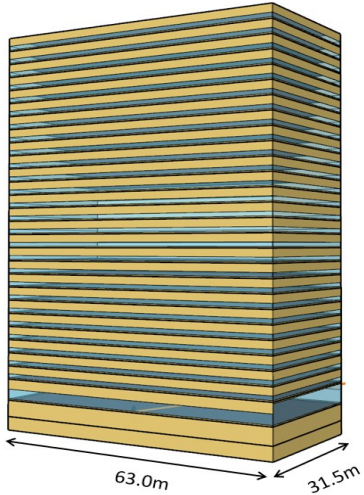
Figure 12. Daily occupancy, lighting, and equipment density fractions.

4.1.2 Base model variant models

We developed 18 variant building models with different aspect ratios and story numbers to represent the building stock in Lusail city, based on the building. The buildings were modeled using rectangular geometry. Each building had two basement levels and a ground floor, each having the same floor height and window-to-wall ratio as the building. The height of a typical story is 3.8m, which is the same in the building and the standard floor height in high-rise residential buildings in Doha [108]. The window-to-wall ratio was set as 30%, a typical value in high-rise residential buildings following the ASHRAE Standard 90.1[109], which is also remarkably close to the building. According to GSAS codes [110], Qatar's optimum building

36

orientation, which is close to but slightly east of due south, is centered at 172.5° clockwise from north. Since the optimum orientation range is small, and the building orientation is within the range, the building models' direction was set to match the building. The geometric variables were aspect ratio and floor numbers. The aspect ratio was defined as 1.0–2.0, obtained from a GIS file of a selected building in Lusail City. According to Emporis standards [111], a high-rise building is defined as having 12–39 floors. Uniform distribution was used to sample the two parameters. Finally, 18 building models with different building shapes were created using EnergyPlus, as shown in Table 6. The input and output data of these 18 models were used as train data to develop the meta-model.

Table 6 Characteristics of the 18 building energy models

EnergyPlus model			
Aspect ratio	1.0	1.5	2.0
Floor number of case study		14, 19, 24, 29, 34, 39	

4.2 Sensitivity analysis

4.2.1 Input factors

A building energy model requires many input parameters influencing building cooling load. These variables include climate, building thermal-physical and internal gain parameters. This study used typical meteorological year data from Doha to simulate the climate condition. Afshari et al. demonstrated that two weather indicators, temperature, and relative humidity, are sufficient to describe the climate in hot and humid areas [11]. This study uses the monthly average outdoor dry bulb temperature and relative humidity as climate factors. Building thermal-physical include building geometry and building envelope materials. The building geometry variables were floor numbers and aspect ratios for the 18 baseline buildings. Building envelope materials comprised the following variables: roof insulation U-value, wall U-value, floor U-value, window U-value, window solar heat gain coefficient (SHGC), window solar transmittance, and the solar reflectance of interior diffusing roll blinds. The ranges for the variables were defined using ASHARE 189.1 201 standards (90.1-2019) [112] and Lusail City GSAS 2 Star Rating Guidelines [113]. The range of internal gain parameters is described as follows. The cooling setpoint (CSP) range was set from 21°C to 26°C, based on Lusail City's GSAS 2 Star Rating Guidelines, in which the default occupied internal setpoint value for cooling in Qatar is 23°C [113]. The occupancy (OCC) range was set at 38–90 m² per person, based on a calculation of ASHARE 189.1 2010 standards [112]. The input value for lighting power density (LPD) was selected as 3–6 W/m². According to Lusail City's GSAS 2 Star Rating Guidelines [113], the peak power intensity in an installed lighting system should be below 6 W/m² [113]. For equipment power density (EPD), we selected 2–8 W/m² as the input value. The ASHRAE Standards (90.1-2004) [112] Building Energy Analysis suggests a value for electrical equipment power densities of 0.75 W/ft² (8.01 W/m²) [109]. Autodesk Sustainable Building Design [114] suggests energy use of 0.5 W/ft² (5.38 W/m²) for a single family and 0.7 W/ft² (7.53 W/m²) for multiple families. For the solar reflectance of interior diffusing roll

38

blinds (SR), we choose 0.4–0.8 as the value range. In Qatar, solar radiation is a significant factor influencing building cooling load. In Ref. [115], 0.53 is a typical SR value for inside shading. According to EN 13363-2:2005 [116] , values of 0.3, 0.7, and 0.6 are recommended for different materials. The infiltration and ventilation ranges were based on ASHRAE-Fundamentals (Chapters 16.15 and 16.29) and ASHARE 62.1-2010 [112]. Table 7 provides detailed information concerning the input parameters and the range of values.

Table 7 The input parameters and range of values.

Number	Input parameters	Range of values	Unit	Reference
1	Aspect ratio	1-2	/	GIS file of a selected building in Lusail City
2	Number of stories	12-39 (do not include two basements)	/	Emporis standards [111]
3	Roof insulation U-value	≤0.25	W/m²·K	ASHARE 189.1 201 standards (90.1-2019) [111]
4	Wall U-value	≤0.3	W/m²·K	ASHARE 189.1 201 standards (90.1-2019) [111]
5	Floor U-value	≤0.332	W/m²·K	ASHARE 189.1 201 standards (90.1-2019) [111]
6	Window U-value	≤1.8	W/m²·K	ASHARE 189.1 201 standards (90.1-2019) [111]
7	Window SHGC	≤0.21	W/m²·K	ASHARE 189.1 201 standards (90.1-2019) [111]
8	Window solar transmittance	≤0.25	/	ASHARE 189.1 201 standards (90.1-2019) [111]
9	Solar reflectance of interior diffusing blinds roll	0.4–0.8	/	Solar protection [114], EN 13363-2:2005 [115]
10	Cooling setpoint	21–26	°C	Lusail City GSAS 2 Star Rating Guidelines [112]
11	Occupancy density	38–90	m²/person	ASHARE 189.1 2010 standards [111]
12	Lighting power density	3–6	W/m²	Lusail City's GSAS 2 Star Rating Guidelines [112]
13	Equipment power density	2–8	W/m²	ASHRAE Standards (90.1-2004) [111]
14	Infiltration	0.1–2	ACH	ASHRAE-Fundamentals (Chapters 16.15 and 16.29)
15	Ventilation	0.0003–0.0006	m³/s· m²	ASHARE 62.1-2010 [111]
16	Monthly average outdoor dry bulb temperature	18.04,19.30,21.44,27.17,31.81,34.56,35.	°C	TMY weather data for Doha

17	Monthly average relative humidity	98,35.29,33.36,29.8 5,24.95,19.46 68.46%,65.44%,58. 88%,49.98%,41.01 %,39.99%,46.39%,5 3.96%,58.73%,61.9 2%,63.19%,68.12%	/	TMY weather data for Doha

4.2.2 Sampling method

There are two sampling methods for all parameters in Table 7. For aspect ratio and floor numbers, as mentioned in Section 4.1.2, uniform distribution was used. To run parametric simulation, the LHS method was performed to generate 650 [117] samples of the remain uncertain input parameters. The parametric simulation was performed using EnergyPlus with RStudio to generate the annual and monthly cooling loads for the 650 cases. The parametric simulation was conducted for all the buildings. In total, 11,700 cases were created.

4.2.3 Sensitivity analysis results

First, we conducted a parametric simulation and sensitivity analysis for the building to identify the ten parameters most likely to influence annual energy use intensity (EUI). Hence, we were able to relieve computing time for subsequent parametric simulations for all the buildings. The results are presented in Table 8. The cooling setpoint appears to be the dominant parameter. Floor U-value, Solar reflectance of interior diffusing blinds roll, and window solar transmittance are the least influential parameters and were excluded from the further simulation.

Table 8 The sensitivity analysis results for the annual energy use intensity in the typical building.

Parameter	SRC	Random Forest	T-Value	SVI	Rank
Cooling setpoint	0.70	165.80	168.74	31.07	1
Equipment power density	0.39	102.19	94.47	18.05	2
Ventilation	0.36	97.07	85.95	16.75	3

Window SHGC	0.28	49.55	65.36	11.09	4
Lighting power density	0.20	24.05	46.66	7.13	5
Infiltration	0.14	15.71	32.42	4.88	6
Window U-value	0.10	15.57	22.83	3.74	7
Occupancy density	0.09	7.54	20.99	2.98	8
Wall U-value	0.09	3.17	20.62	2.63	9
Roof Insulation U-value	0.02	2.13	3.90	0.60	10
Floor U-value	0.02	0.99	3.94	0.53	11
Solar reflectance of interior diffusing blinds roll	0.01	0.32	3.22	0.40	12
Window Solar Transmittance	0.01	0.23	1.23	0.16	13

Subsequently, a sensitivity analysis was conducted based on all the independent variables for the building stock (presented in Table 7). At this step, floor numbers and aspect ratio are added as independent variables. The output was the monthly EUI. Table 9 demonstrates that the two climatic factors had the most significant influence on monthly EUI. The aspect ratio and the number of stories ranked highly, suggesting that building geometry significantly impacts monthly EUI. The CSP and EPD were also significant parameters. All building material parameters ranked as low, indicating that Qatar building envelope standards have played a perfect role in building energy efficiency.

Table 9 The sensitivity analysis results for the monthly energy use intensity for the eighteen buildings.

Parameters	SRC	Random Forest	T-Value	SVI	Rank
Outdoor air drybulb temperature	0.69	253.14	16.55	32.15	1
Outdoor air relative humidity	0.53	130.96	12.59	21.77	2
Cooling setpoint	0.20	47.29	7.54	9.83	3
Aspect ratio	0.03	188.11	1.20	9.46	4
Equipment power density	0.12	19.16	4.31	5.27	5
Floor number	0.03	79.31	1.09	4.59	6
Window SHGC	0.11	3.90	4.01	4.30	7
Ventilation	0.08	24.30	3.06	4.22	8
Infiltration	0.06	4.11	2.20	2.47	9
Occupancy density	0.05	0.83	1.87	1.96	10

Window U-value	0.04	2.75	1.50	1.66	11
Lighting power density	0.02	4.78	0.85	1.08	12
Wall U-value	0.02	2.37	0.85	0.98	13
Roof insulation U-value	0.01	0.70	0.21	0.25	14

4.3 Meta-model development

The sensitivity analysis identified the most significant 14 parameters. These were used as independent variables to develop the meta-model. The output was the monthly EUI. First, the dataset generated from the parametric simulation was imported. The data obtained from the 37-story building with an aspect ratio of 1.0 was not included since it would be used as an unseen case to test the meta-model. Data normalization was performed on the independent variables. The dataset was randomly separated training and test data. 80% of the data was used for training; the remaining 20% was used for testing. The model was subsequently developed using the training data. Finally, the test data was used to evaluate the meta-model performance.

The MLR and SVR models were obtained from scikit-learn, a third-party machine-learning library for Python, which integrates a large number of commonly used machine-learning methods [118]. Four SVR models were used in this study: SVR with linear kernel, poly kernel, and RBF kernel, and LinearSVR. The latter is similar to SVR with linear kernel, although implemented using LIBLINEAR rather than LIBSVM, and can be used when a dataset is exceptionally large. The ANN model was built by Keras, a high-level neural network application programming interface written using Python [119]. To determine the number of neurons in the hidden layer, we used the rule of thumb, which states that the number of hidden neurons should be two-thirds of the input layer size, plus the size of the output layer [120]. In this case, our model had 14 inputs and one output, providing 13 neurons in the hidden layer. The XGBoost model was built from the Python package [121].

The Figure 13 and Table 10 demonstrate the performance of the machine-learning models. The results of the SVR linear kernel, poly kernel, and RBF kernel are not presented because the training times of these models exceeded thirty minutes. The ANN model was trained to five epochs. The relative errors in the test data's predictions met the required standards in the four models. The R^2 of the MLR, SVR, ANN, and XGBoost models was 0.9742, 0.9730, 0.9991, and 0.9949, respectively, demonstrating that the models accurately described the relationship between the monthly cooling load and the independent variables. The processing time for the MLR, SVR, and XGBoost models was shorter than that of the ANN. The CV(RMSE) of the MLR and SVR was 10.4% and 10.8%, respectively, much higher than ANN (1.9%) and XGBoost model (4.7%). To better understand the performance of these models, we tested them on cases that were not included in the training and test datasets.

(a)   (b)

(c)   (d)
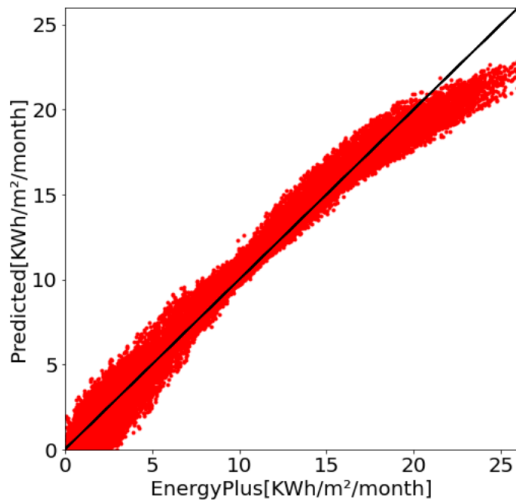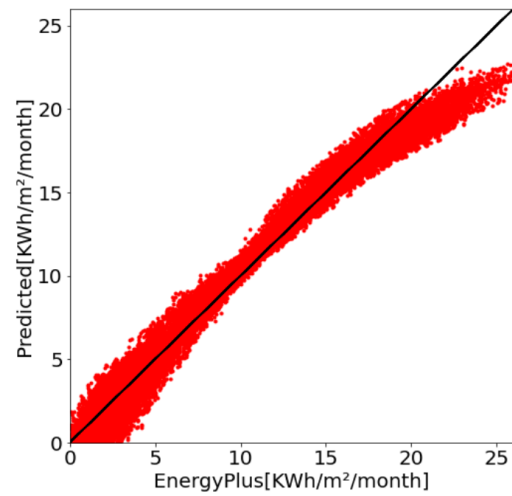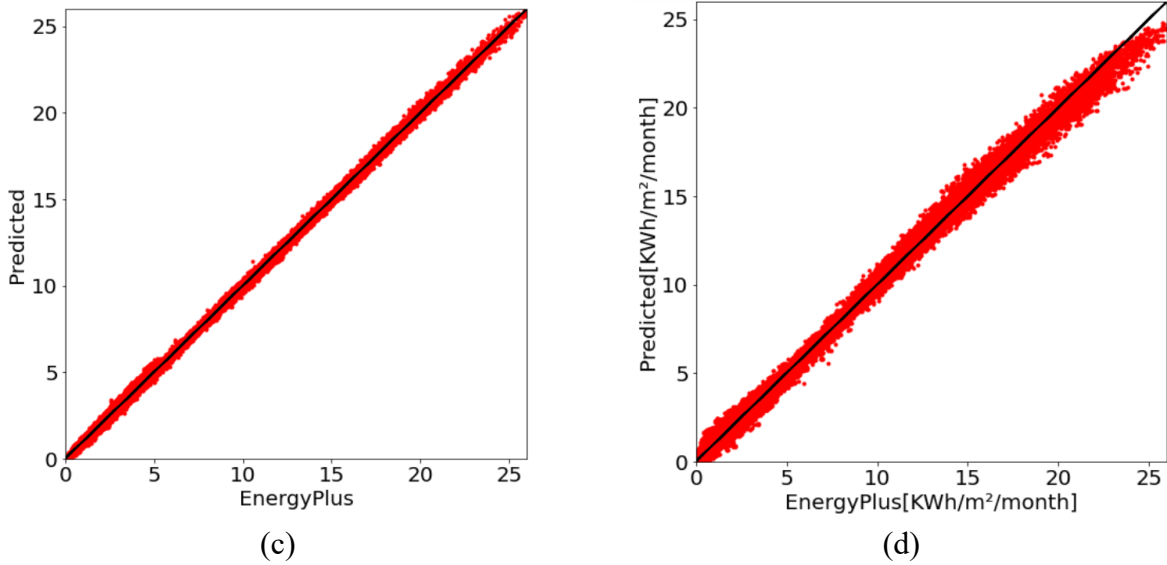
Figure 13. Comparison of monthly cooling load generated from EnergyPlus and developed meta-

models: (a) MLR, (b) LinearSVR, (c) ANN, and (d) XGBoost.

Table 10 A comparison of the evaluation index of the test data for the four models

Criteria	MLR	SVR	ANN	XGBoost	Standards
R^2	0.9742	0.9730	0.9991	0.9949	$\geqslant 0.75$
NMBE %	0	1.5	0	0	± 5
CV(RMSE) %	10.4	10.8	1.9	4.7	15
Process time (s)	1	1	138	6	/

4.4   Meta-model verification

To test the meta-models' flexibility and generalization ability, we applied them to two unseen

cases. The dataset generated from these unseen cases are not included in the data to train the meta-

models.

4.4.1   Case 1: A thirty-seven story rectangular building

This first case is a rectangular building with 37 floors (aspect ratio = 1.0), one of the baseline

models which was not included in the training and test cases. EnergyPlus simulation results and

the four meta-models prediction results deviation for one case are shown in Figure 14. Comparison

of the performance of the four meta-models to predict the 12 monthly cooling load are shown in

Table 11. We can see that ANN has the lowest monthly cooling load deviation compared with the

other three meta-models, with the highest R²=0.9996 and lowest CV(RMSE)=1.2%.
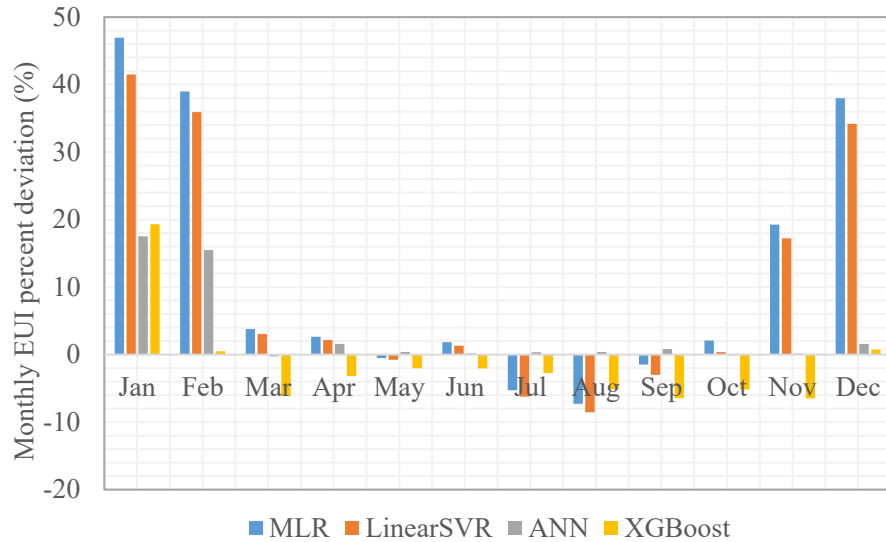
Figure 14. Monthly cooling load deviation between the four meta-model prediction results and

EnergyPlus simulation results for one case.

Table 11 Meta-model verification performance for one case

Criteria	MLR	SVR	ANN	XGBoost	Standards
R^2	0.9864	0.9854	0.9996	0.9931	≥ 0.75
NMBE %	-1.5	7.9	1.2	5.4	± 5
CV(RMSE) %	7.6	-0.3	-0.9	3.8	15

To further compare the performance of the meta-models, the building envelope's physical and

internal gain properties were parameterized to provide a more extensive validation. The

parameterization changed the roof insulation U-value, wall U-value, window U-value, window

SHGC, CSP, OCC, LPD, EPD, infiltration, and ventilation rates into the ranges indicated in

Section 4.2.1. Forty-eight random samples were generated, which is shown in Appendix 3. 48

cases randomly generated for meta-model verification. The simulation results were compared with

the prediction results of the four meta-models, and the findings are displayed in Figure 15 and

Table 12. The comparison shows perfect matching, particularly for the ANN and XGBoost models. The R^2 of the four models is above 0.9.

It takes 900 seconds to run the 50 cases using EnergyPlus. The prediction time for all the models is one second, which significantly saves computing time compared to the EnergyPlus simulation. However, the CV(RMSE) of the MLR and SVR reached 15%, indicating a higher relative error value. In summary, the ANN and XGBoost models indicated a better fit between the prediction and simulation results.
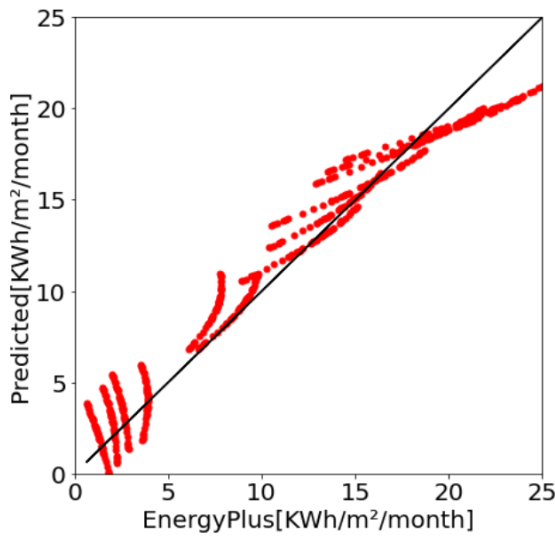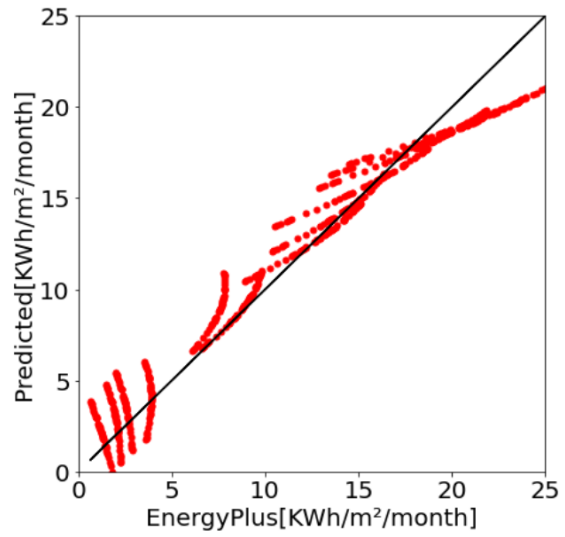
(a)   (b)
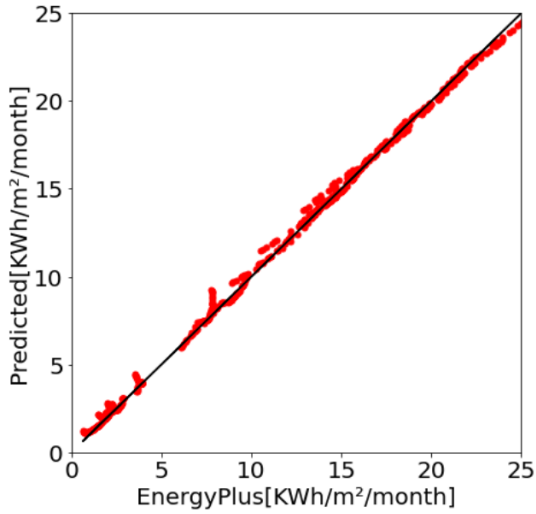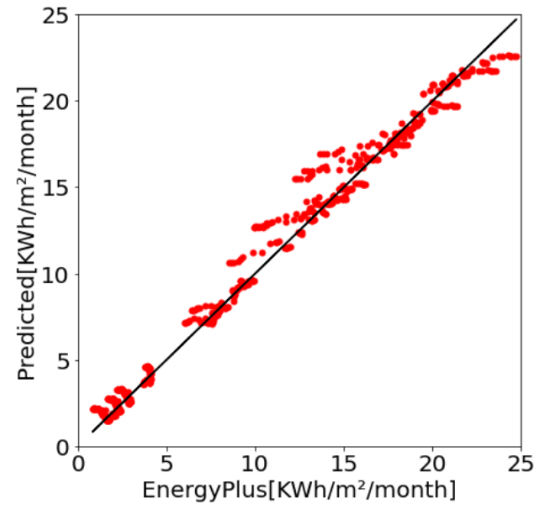
(c)   (d)

Figure 15. Monthly cooling load comparison between EnergyPlus and the four meta-models

prediction results for 48 cases: (a) MLR, (b) LinearSVR, (c) ANN, and (d) XGBoost.

Table 12 Meta-model verification performance averaged criteria

Criteria	MLR	SVR	ANN	XGBoost	Standards
R^2	0.9548	0.9548	0.9982	0.9852	≥0.75
NMBE %	3.0	-1.8	-3.0	-3.0	±5
CV(RMSE) %	14.4	14.4	2.9	8.2	15

4.4.2 Case 2: Base Model Tower

The second test case used the typical residential building, comprising one ground floor, sixteen

intermediate stories, and a rooftop (Figure 10). There are several differences between the selected

building and the buildings used as baseline models to obtain the meta-models. Firstly, the floors

of the selected building are not rectangular, and the sixteenth floor has a configuration that is

different from the typical floors. Secondly, the building's ground floor has a complex configuration,

and its area is much larger than the typical floor area. Conversely, in the baseline models, the

ground floor is rectangular and retains the typical floor area. As in the first test case, first, one case

is compared, and then the same parameterization was applied. EnergyPlus simulation results and

the four meta-models prediction results deviation for one case are shown in Figure 16. Comparison of the performance of the four meta-models to predict the 12 monthly cooling load are shown in Table 13. Figure 17 demonstrate the monthly EUI predictions of the meta-models for 48 cases. A trend similar to that in Case 1 is observed. The R^2 of all the models is remarkably high. However, the CV(RMSE) of the MLR and SVR are much higher than those of the ANN and XGBoost models. In summary, the ANN model has the highest R^2 and the lowest CV(RMSE).
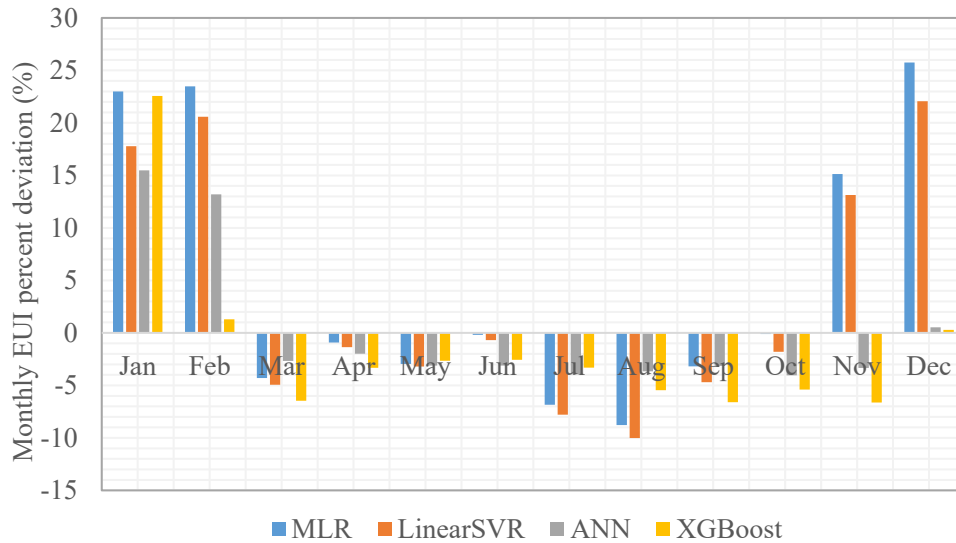
Figure 16. Monthly cooling load deviation between the four meta-model prediction results and EnergyPlus simulation results for one case.

Table 13 Meta-model verification performance for one case

Criteria	MLR	SVR	ANN	XGBoost	Standards
R^2	0.9924	0.9912	0.9991	0.9969	≥0.75
NMBE %	0.1	1.3	1.5	2.8	±5
CV(RMSE) %	5.5	5.9	1.9	3.5	15

(a)

(b)

(c)

(d)
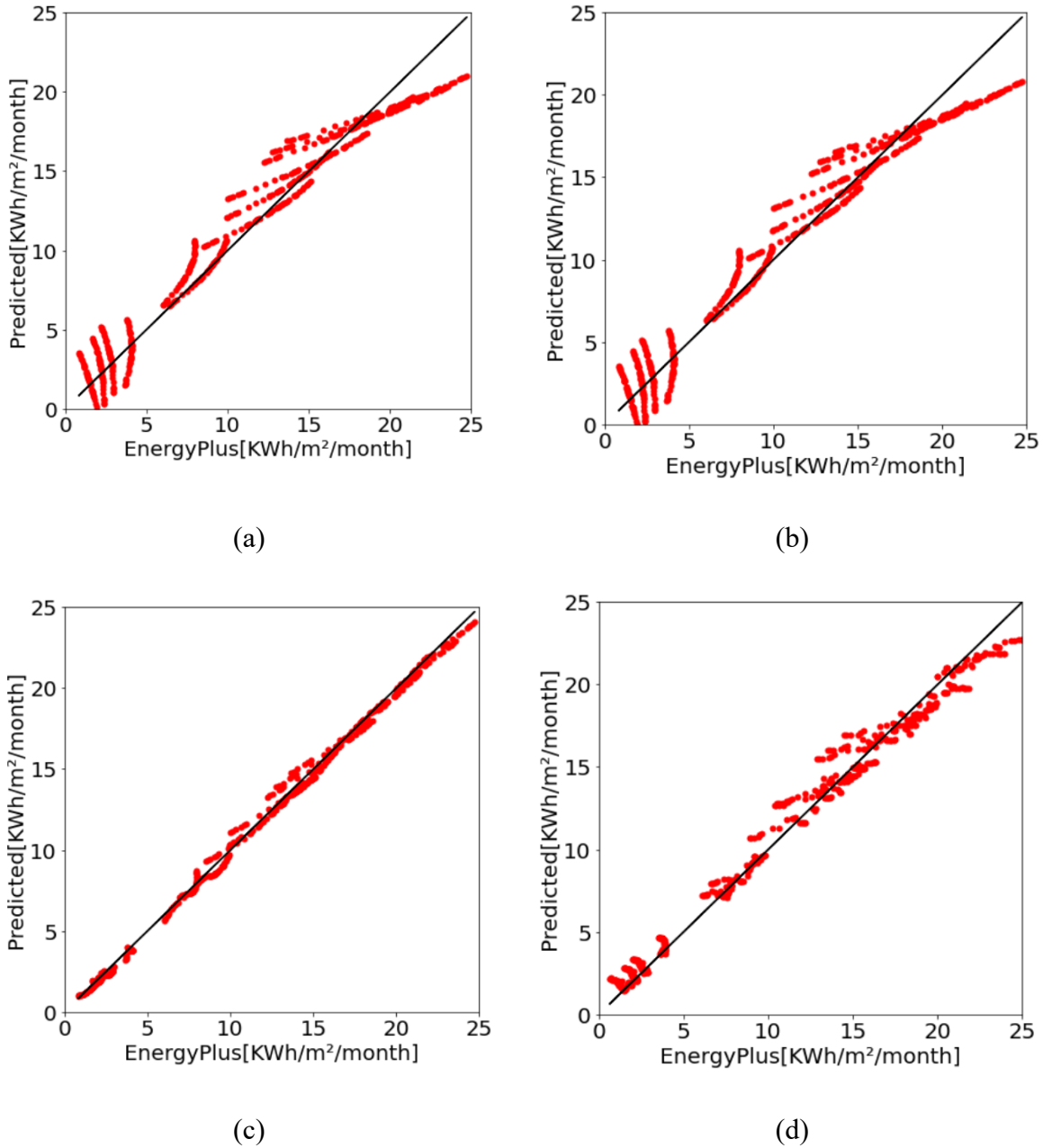
Figure 17. Comparison of monthly cooling load generated from EnergyPlus and developed meta-

models: (a) MLR, (b) LinearSVR, (c) ANN, and (d) XGBoost.

Table 14 Meta-model verification performance averaged criteria

Criteria	MLR	SVR	ANN	XGBoost	Standards
R^2	0.9576	0.9576	0.9976	0.9824	≥ 0.75
NMBE %	-1.3	-0.2	1.2	-1.4	± 5
CV(RMSE) %	13.58	13.58	3.3	8.7	15

4.5   ANN model optimization

We observed that using the entire dataset (11,700 cases) during the training process resulted in a long processing time for the ANN (Table 10). It was necessary to determine how the training data sample size and the number of neurons in the hidden layer would affect the meta-model's performance. Thus the meta-model can have good accuracy with lower processing time.

4.5.1   Sample size

The ANN was selected as the meta-model in this study due to its high level of accuracy. First, the number of neurons remained at 13, as in Section 4.3. We chose to test the use of samples comprising 5%, 15%, 25%, 50%, and 75% of the dataset. The selected building was used as the test case.

Figure 18 demonstrates a linear relationship between the processing time and the training data sample size. The ANN's performance improves as the sample size increases. The growth rate is greater in the first 20% of the increments. It is also evident that when 5% of data is used to train the ANN model, the R^2 is 0.9800, higher than the R^2 of the MLR and SVR models when trained using the full dataset (Table 10). The result confirms that the ANN model accurately describes the relationship between the independent variables and monthly EUI using a small dataset. When the sample size is increased to about 20%, the line of CV(RMSE) and processing time intersect, which means at this point, the ANN model can have a good performance while remaining an acceptable processing time. Thus, a 25% sample size is a good choice, which is the closest to the intersect.

Table 15 The artificial neural network performance with different sample sizes and epoch numbers.

Sample size	Epochs	R^2	CV(RMSE)	NMBE	Processing time(s)

5%	8	0.9816	8.9%	0.1%	9
15%	8	0.9942	5.0%	0.7%	32
25%	8	0.9970	3.6%	0.7%	56
50%	8	0.9990	2.0%	0.4%	112
75%	8	0.9986	2.5%	0.3%	168
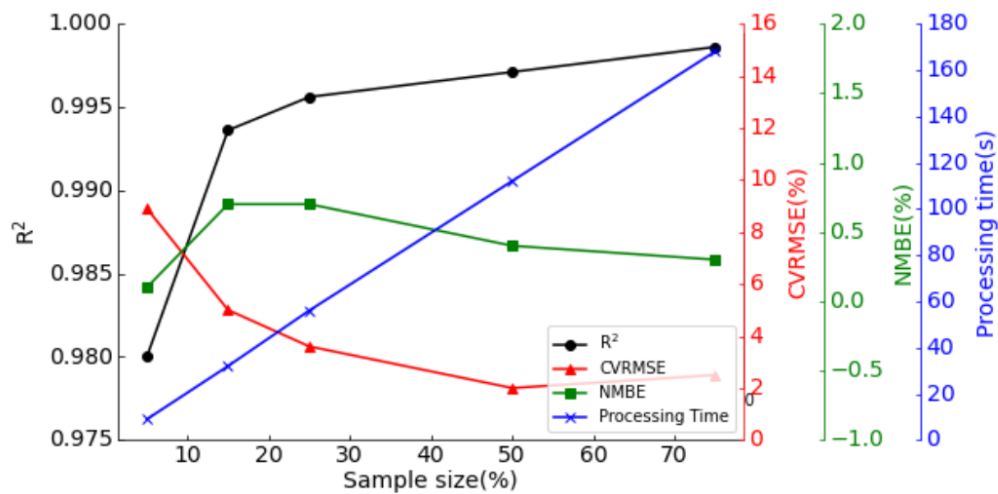
Figure 18. The artificial neural network performance versus the training data sample size.

4.5.2 The number of neurons in the hidden layer

From the previous discussion, it may be observed that using a 25% sample size, the ANN demonstrates superior prediction ability within an acceptable processing time. To determine the effect of the number of neurons in the hidden layer on the model's performance, new ANNs were created using hidden layer containing neurons proportional to 0.5, 1.0, 1.5, 2.0 times the sum of the input and outputs neurons (i.e., 8, 15, 23, and 30). It is evident that the higher the number of neurons, the more accurate the result. The ANN model shows the greatest prediction ability when the hidden layer contains 30 neurons.

Table 16 The artificial neural network performance with different numbers of neurons in the hidden layer

51

Number of neurons	Sample size	Epochs	R^2	CV(RMSE)	NMBE	Processing time(s)
8	25%	8	0.9986	2.5%	0	55
13	25%	8	0.9968	3.3%	0	56
15	25%	8	0.9982	2.7%	-0.1%	56
23	25%	8	0.9985	2.5%	0.4%	56
30	25%	8	0.9992	1.9%	0	56

4.6 Summary

This chapter has investigated the application of machine learning to predict the monthly EUI in residential buildings at the district scale. The climate parameters (outdoor dry bulb temperature and relative humidity), building thermal-physical characteristics (floor numbers, aspect ratio, wall U-value, and window U-value), and building operation parameters (occupancy, lighting, and equipment density) were all considered as input parameters. Sensitivity analysis was conducted to identify the key parameters influencing the monthly EUI. The most significant parameters were used as independent variables to develop the meta-models. Four machine-learning models (MLR, SVR, ANN, and XGBoost) were evaluated for their prediction performance. The applicability of different machine-learning models in predicting monthly cooling loads was validated and compared. The results indicated that the four models could predict monthly EUI. Their performance using test data was acceptable, with R^2 values greater than 0.9. The four meta-models were also applied to new building energy models for evaluation. The results revealed that the ANN and XGBoost performed better than MLR and SVR. The CV(RMSE) values of the MLR and SVR models were close to evaluation standards. Finally, the ANN was chosen as the meta-model with the best performance in predicting building-level energy, having the highest R^2 and lowest CV(RMSE) values.

To run the same 50 cases, EnergyPlus requires 900 seconds, whereas the meta-model takes just one second. Therefore, using the meta-model to predict cooling loads in many buildings will save a considerable amount of time.

The linear kernel SVR, polynomial kernel SVR, and Gaussian radial basis function kernel SVR poorly handle large datasets. The ANN model exhibited the best performance amongst the models when predicting monthly cooling loads; it also predicted the monthly cooling load accurately using a small dataset. The meta-model with 14 neurons in the input layer, 30 neurons in the hidden layer, and 1 neuron in the outer layer, performed best as the test case, using 50% of the sample data and eight epochs ($R^2 = 0.9992$ and CV(RMSE) = 1.9%).

5   Predicting Monthly Apartment-Level Cooling Load Using Machine-Learning Approaches

This chapter develops a machine-learning model to predict the monthly cooling load of residential buildings at the apartment-level, using the selected building, which has 138 apartments, as a case study. First, we analyzed apartment cooling-load variation by height and orientation. Five parameters (CSP, OCC, LPD, EPD, and interior SR) were selected as independent variables to create ninety-six different scenarios. Four machine-learning models were used as meta-models to generalize the relationships between cooling energy and the model parameters. The meta-models' prediction accuracies were evaluated using the NMBE, CV(RMSE), and R^2. The results indicated that the ANN model performed best. A generic building energy model was subsequently established to validate the meta-model. The results indicated that the proposed ANN model with five hidden layers trained 250 times was accurate and efficient in predicting cooling load during the summer and transition months in a building with similar floor configurations, with $R^2 = 0.89$.

5.1   Baseline model

The selected residential building is a multi-apartment block comprising 19 stories (including two basements), as displayed before in Figure 10. The building simulation results can be seen in Figure 19. According to the information provided by the stakeholders, 60% of the building is occupied. For the 60% occupancy of the building energy model, monthly cooling load results of August and September are near 10 to 15% of the actual measured data provided by the stakeholders.
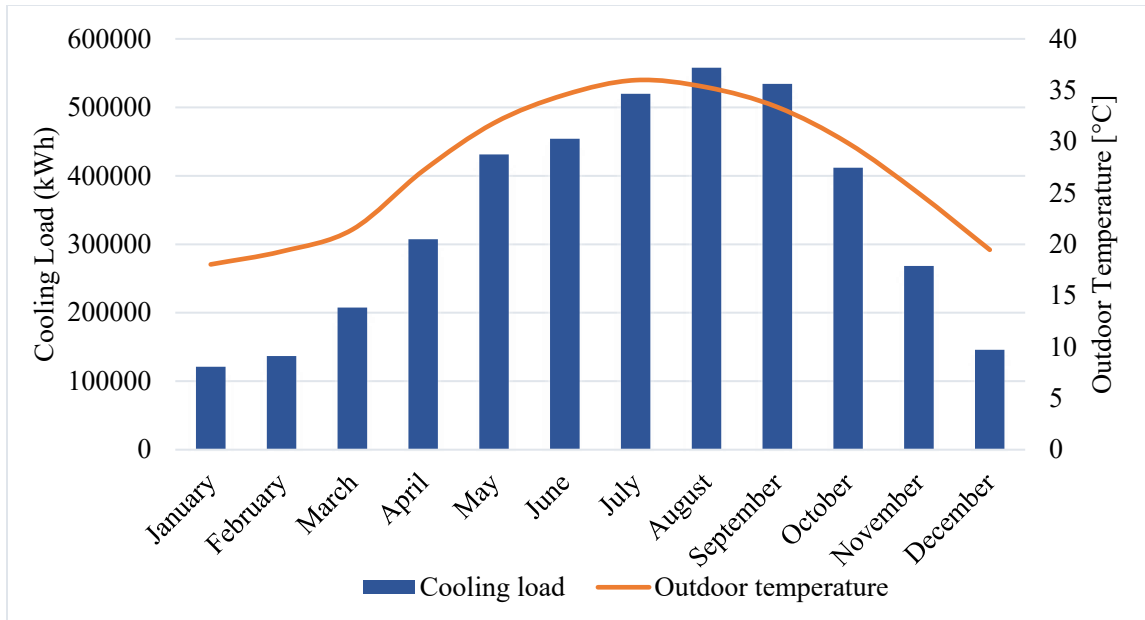
Figure 19. The building monthly cooling load (100% occupancy).

5.2 Apartment-level cooling-load analysis

As Figure 20 demonstrates, on January 21, the outdoor temperature remained between 15°C and 20°C. From 23:00 to 09:00 hours, the LPD and EPD were extremely low. Therefore, the cooling load remained close to zero. From 18:00 to 22:00 hours, the cooling load gradually increased as the internal load grows. The load increased to a maximum of 60,000 W at 20:00 hours. On July 21, the outdoor temperature was highest at 11:00 hours (it can reach 40°C). The maximum daily cooling load occurred later, at 15:00 hours, due to thermal mass. Throughout the day, the load fluctuated between 40,000 W and 70,000 W.
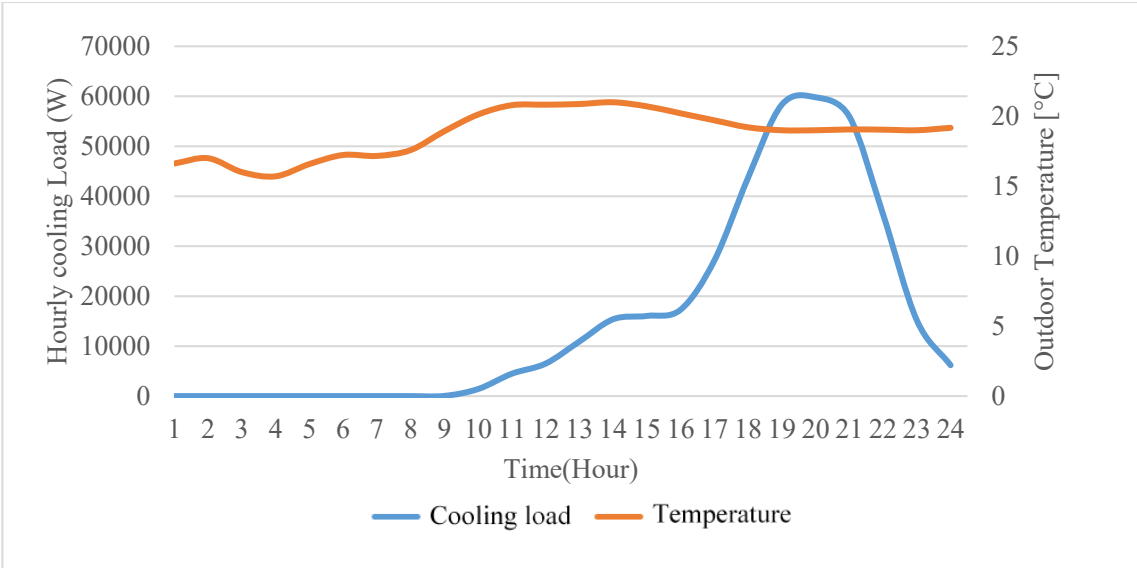
(a)
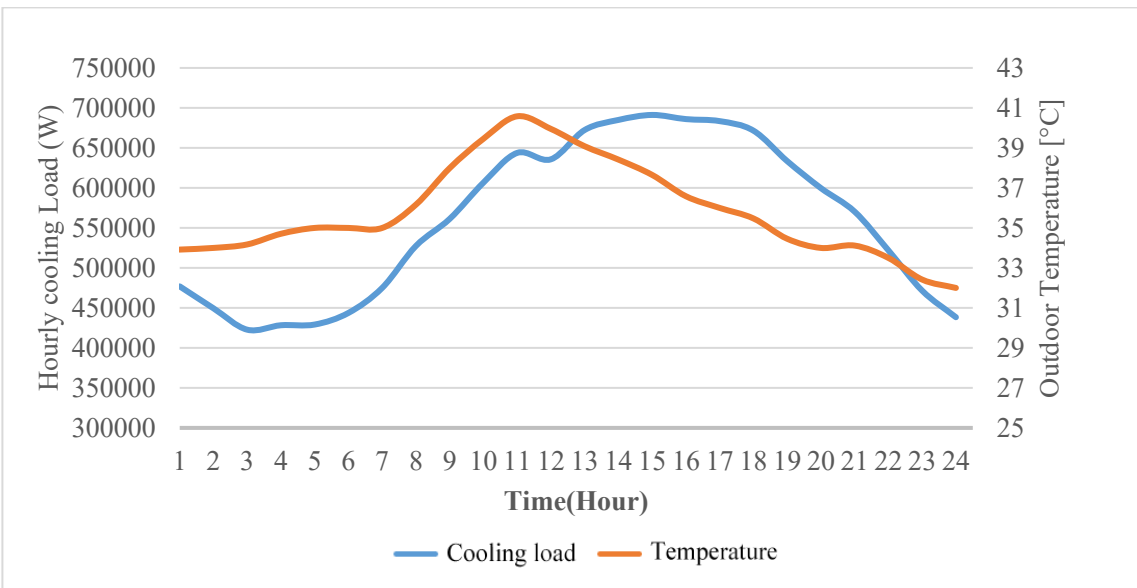
(b)

Figure 20. Daily cooling-load profile on design day: (a) winter design day January 21,(b)

summer design day July 21.

In the EnergyPlus simulation, the wind distribution is estimated along with the height and the rate of air temperature drop by elevation [122]. Local wind speed is modified from the measured meteorological wind speed [122]:

$$V_z = V_{met} \left(\frac{\delta_{met}}{z_{met}}\right)^{a_{met}} \left(\frac{z}{\delta}\right)^{a} \qquad (5-1)$$

where z is the height of the centroid of the system, z_{met} is the height of the standard meteorological wind speed measurement, and a and δ are terrain-dependent coefficients. δ is the boundary layer thickness for the given terrain type. The value of a, δ, a_{met}, and δ_{met} depend on the roughness characteristics of the surrounding terrain.

Local outdoor air temperature calculations are done through the following equation [122]:

$$T_z = T_b + L\,(H_z - H_b) \qquad (5-2)$$

where T_z is air temperature at altitude z, T_b is air temperature at the base of the layer, i.e., ground level for the troposphere, L is air temperature gradient, equal to –0.0065 K/m in the troposphere, H_b is offset equal to zero for the troposphere, H_z is geopotential altitude.

The variable H_z is defined by [122]:

$$H_z = \frac{E_z}{(E+z)} \qquad (5-3)$$

where $E = 6{,}356$ km, the radius of the Earth, $z =$ altitude. To modeling buildings in the troposphere, altitude z refers to the height above ground level, not the height above sea level. The height above ground is calculated as the height of the centroid, or area-weighted center point, for each zone and surface.

From the TMY weather data, we know that the outdoor air temperature decreases in a linear curve as the floor level increase. The difference between the top floor and ground floor is about 0.5°C for each month, as shown in Figure 21. For zones located on the same floor, the outdoor air temperature is the same. Figure 21 shows the monthly EUI variation between different floors. While there is little evidence of variation between floor levels, major increase can be found on the 15th floor. This is because part of its roof is exposed to the sun. In previous research [123], a

building with a height of 1,000 meters was studied to assess the impact of height on cooling and heating loads. The author observed that the cooling load decreased as the height increased. In Dalian, China, the hourly cooling-load gradient with height was -2 W·m^{-2}· 100 m $^{-1}$ in apartments located in the south and north of a building. In this study, the building height is 71 meters. As such, the change in annual EUI due to height is less apparent. From Figure 22, we can find that apartments facing northeast, northwest, southeast, and southwest directions in all the representative floors had higher annual EUI. These apartments all have two external walls, which receive more sunlight during the year.
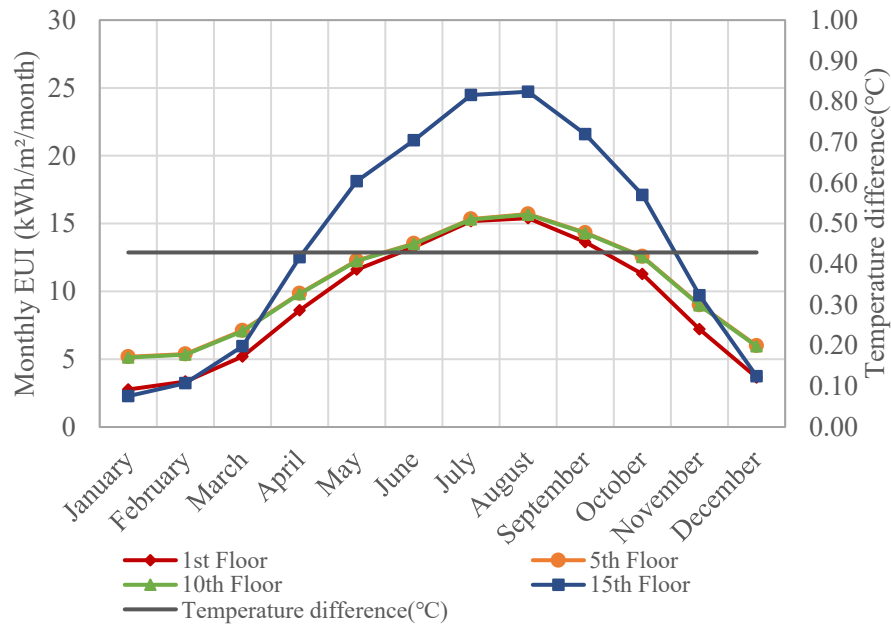
Figure 21. Monthly EUI and average monthly temperature variations with floors
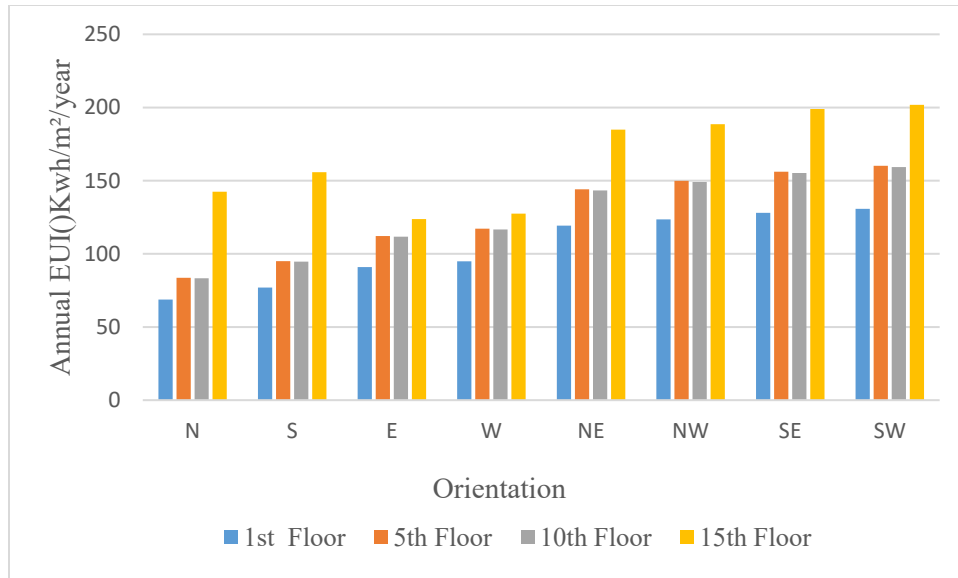
Figure 22. Annual EUI variations with orientation in representative floors.

Figure 23 is a dendrogram presenting the monthly mean outdoor air temperature for different floors. The temperature difference between different floors is relatively small, so there is no significant classification on the Y-axis. The color change from black to yellow indicates an increase in the monthly mean outdoor air temperature. In the dendrogram, distinct seasonal patterns may be observed: winter, summer, and transition months. The winter season includes January, February, March, and December. The summer months are May, June, July, August, and September. The transition months are April, October, and November.
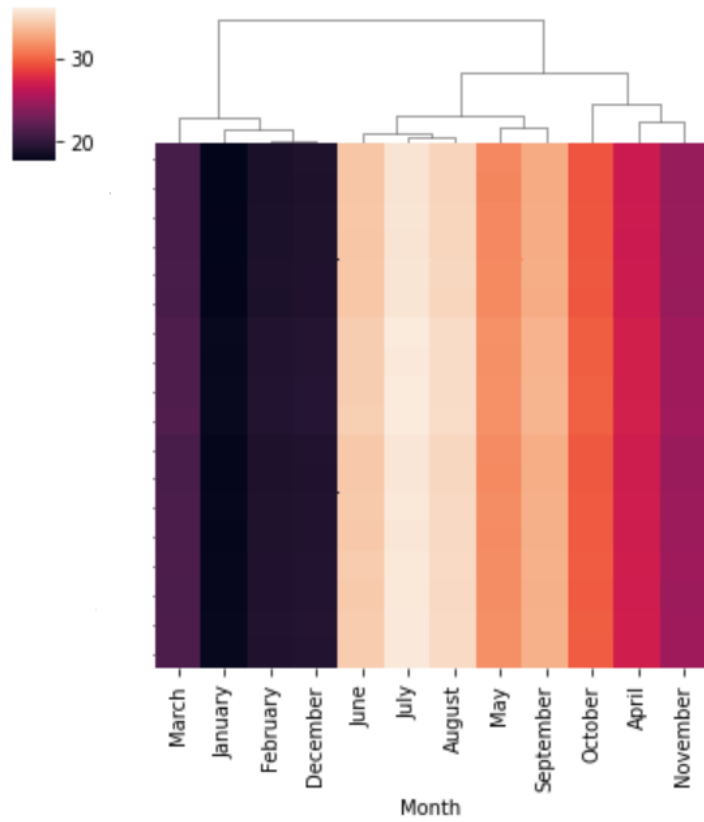
Figure 23. A dendrogram indicating monthly mean outdoor temperature for different floors.

To better understand the monthly EUI variation in different seasons, we plot Figure 24. Different patterns for monthly EUI variation with floors in different seasons can be observed. Throughout the year, we can see that apartments on 5th and 10th floor in the same directions have equal monthly EUI. For 15th floor, monthly EUI varies greatly with the season. During the summer and transition months, the monthly EUI of all apartments on the 15th floor is higher than other floors, while in winter, the EUI value of these apartments is the lowest. This phenomenon indicates that the roof, which is directly exposed to the sun, significantly impacts apartments' cooling load. In summer and transition months, apartments facing northeast, northwest, southeast, and southwest directions in all the representative floors have the highest monthly EUI compared with apartments in other directions. In winter, this pattern no longer applies. The monthly EUI of south, west, and east apartments exceed northwest and northeast apartment in winter. The sun's direction causes this. Figure 25 is the plan view of the sun's path through the sky, showing altitude and azimuth. Table 17 shows sun angle at different times in summer and winter. From the figure and the table, we can see that the sun is almost directly overhead during the summer, especially at noon, so apartments in all direction will receive a large amount of solar radiation. Thus the roof area and the exterior wall area are crucial for the apartment-level cooling load in summer. In winter, the sun path remains in the southern sky and the sun angle is low the entire day. In this way, the apartments on the north could barely be exposed to the sun. Thus the north, northwest, and northeast apartments have the lowest monthly EUI in winter.
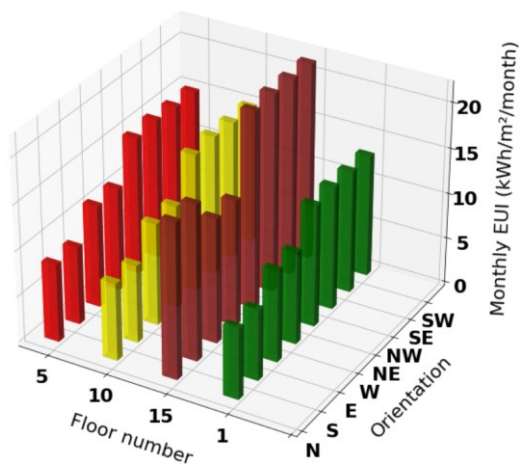
(a) -(1): May
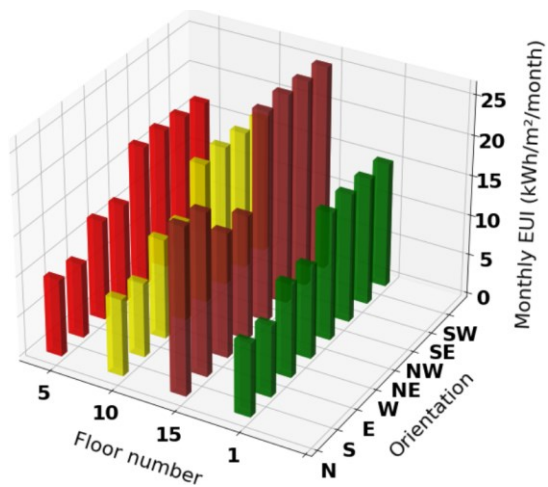
(a) -(2): June
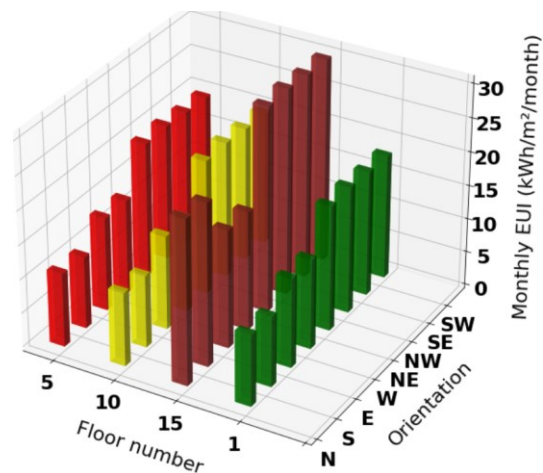
(a) -(3): July
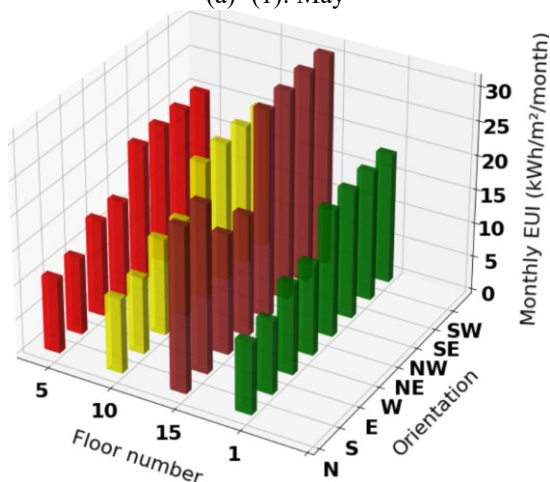
(a) -(4): August
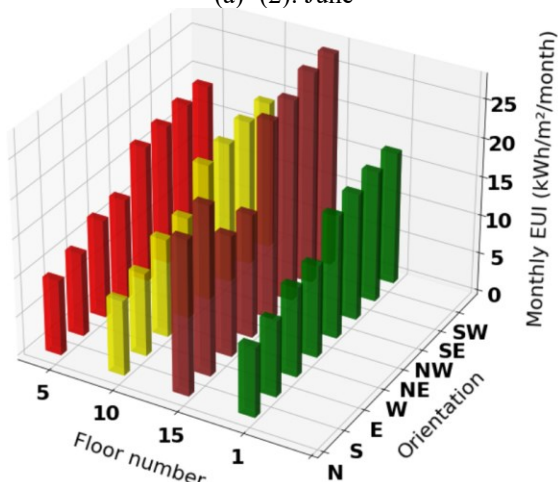
(a) -(5): September
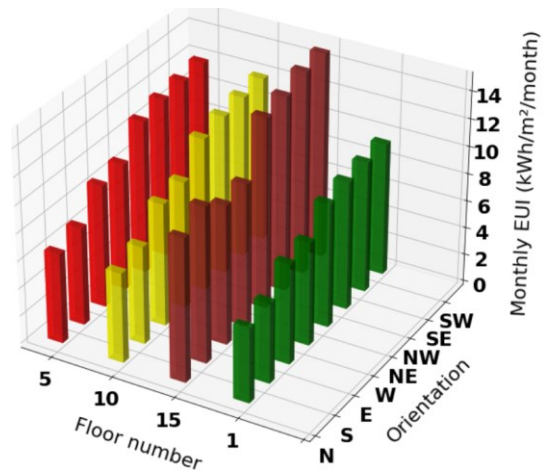
(b) -(1): April
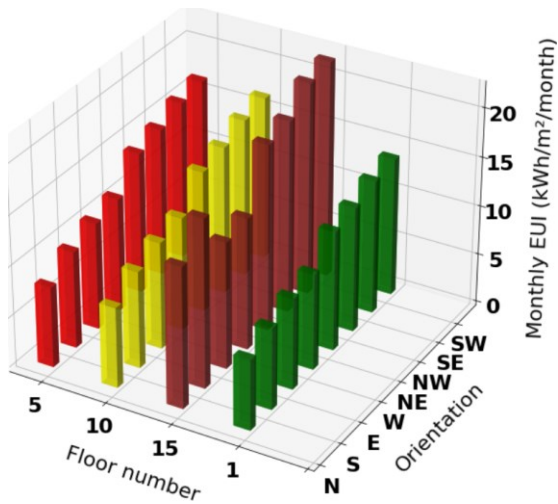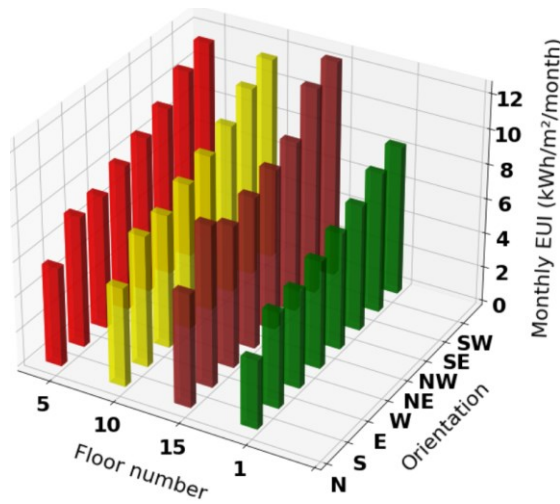
(b) -(2): October   (b) -(3): November   (c) -(1): December
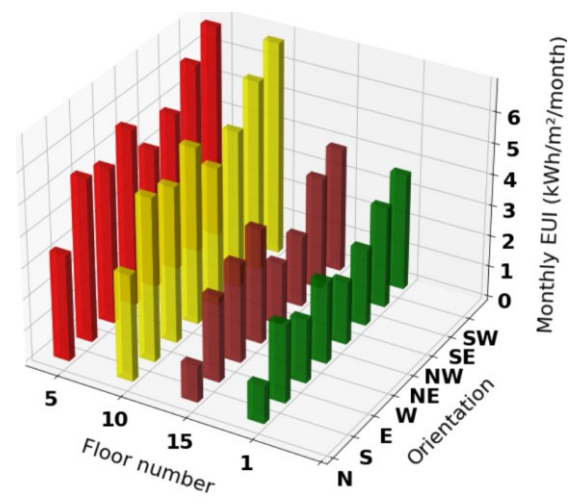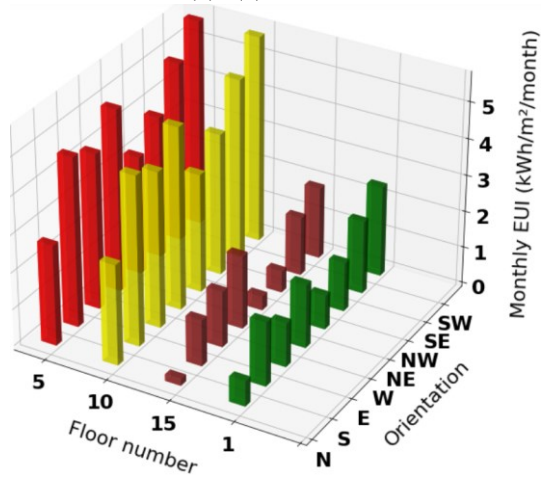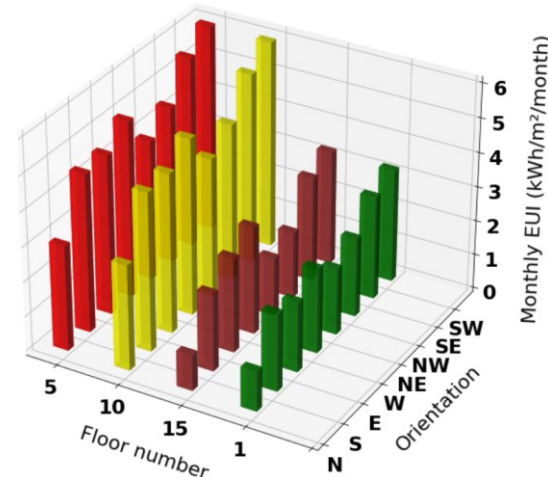
(c) -(2): January   (c) -(3): February   (c) -(4): March
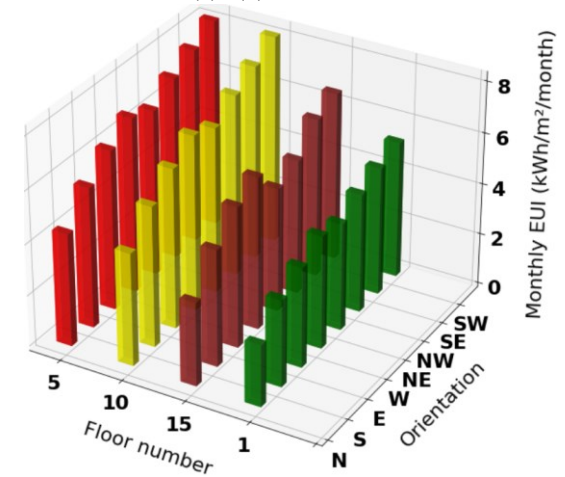
Figure 24. The monthly EUI of apartments located on representative floors in all orientations:

(a) Summer, (b)Transition months, (c) Winter
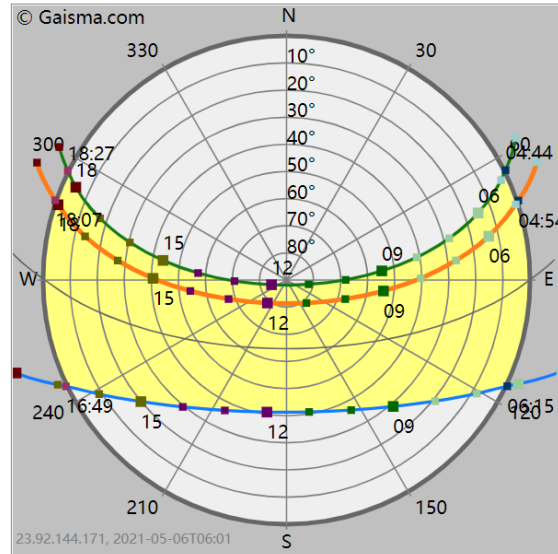
Figure 25. Doha, Qatar - Sun path diagram [124].

Table 17 Sun angle at the different time [125]

Time	Sun angle
Jun.21, 9 am	48°
Jun.21, noon	88°
Jun.21, 4 pm	37°
Dec.21, 9 am	25°
Dec.21, noon	42°
Dec.21, 4 pm	15°

The hourly apartment cooling load on a summer day (July 21) is plotted in Figure 26, which illustrates that apartments with two external walls (located in the northwest, northeast, southwest, and southeast) have larger cooling loads. The cooling loads per area in flats located in the northwest, southwest, and west follow a familiar trend over time. The maximum value occurs at 18:00 hours. However, the maximum cooling load in northeast, southeast, and east apartments is at 14:00 hours. In south and north apartments, the peak cooling load occurs at 19:00 hours. Such differences are in accordance with the maximum

solar radiation received by apartments with different orientations. Cao and Liu observed a similar variation in cooling loads among apartments in different locations [123].
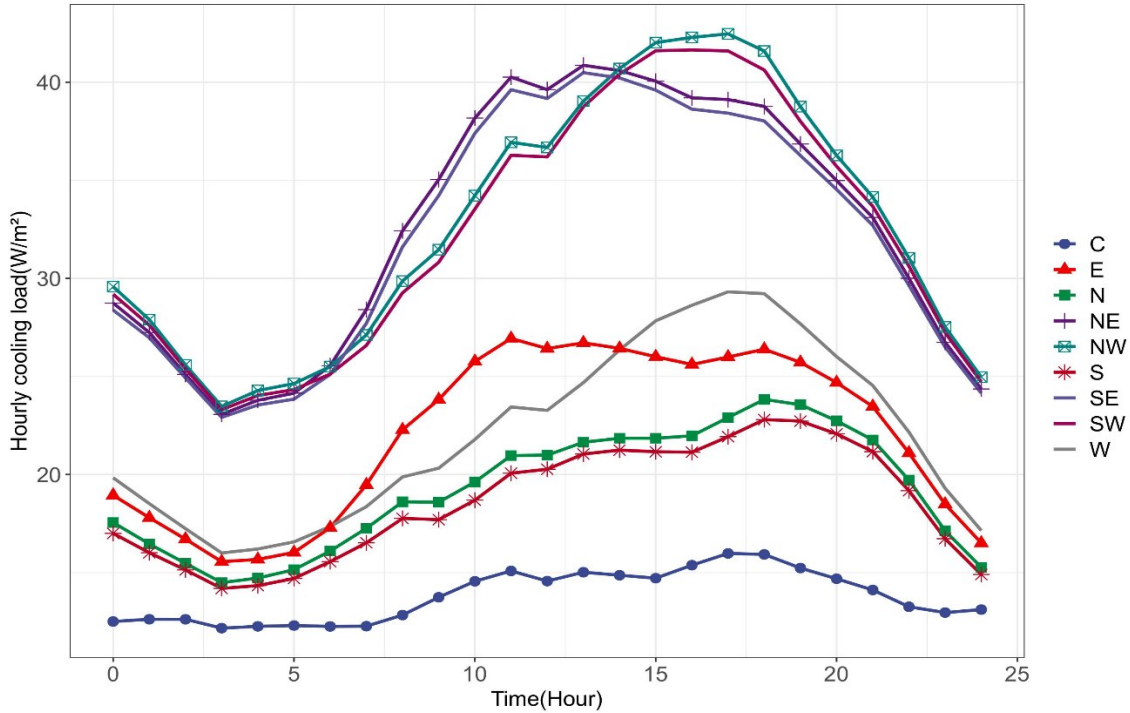
Figure 26. The daily variation in the cooling load of 10th-floor apartments with different orientations.

5.3 Sensitivity analysis

5.3.1 Input factors

In our model, the building envelope was created using a prototypical midrise apartment template, following ASHRAE 189.1-2009 building construction guidelines. For a single building in a specific climate, the parameters for the building envelope (including wall U-value and floor U-value) and outdoor conditions (dry bulb temperature, relative humidity, solar radiation, and wind conditions) remain constant between simulations. The CSP, OCC, LPD, EPD, and SR, which significantly influence apartment-level cooling loads, were

selected as input parameters. Input parameter values were selected to represent different conditions in the apartments. According to Lusail City's GSAS 2 Star Rating Guidelines [113], for example, the default value for an occupied internal cooling setpoint in Qatar is 23℃. Occupants in some apartments may prefer a lower setpoint of 21℃, some apartments may not be occupied, or the setpoint may be higher, such as 26℃. To create the dataset for the sensitivity analysis and meta-model development, the input parameters (CSP, OCC, LPD, EPD, and SR) were changed to generate monthly cooling loads at the apartment level. All combinations were considered to create 96 (3×4×2×2×2) scenarios. The parametric simulation was performed using EnergyPlus with RStudio. For apartments located at different orientations, apartment configuration parameters such as volume, wall area, and window area, were different. For apartments located on different floors, the height above ground was different. The month of the year was also a significant variable. The EnergyPlus parameters (CSP, OCC, LPD, EPD, and SR), combined with apartment configuration (e.g., apartment height above ground), and the month of the year were used as input parameters to create the dataset. Table 18 summarizes the independent variables used in the meta-model development.

Table 18 A summary of the input parameters

Input parameters	Values	Variations
Cooling setpoint	21,23,26	3
Solar Reflectance of Interior Diffusing Blinds Roll	0,0.4,0.6,0.8	4
Lighting power density(W/m^2)	3,6	2
Equipment power density(W/m^2)	2,8	2
Occupancy (person/zone)	One-bedroom:1,2 Two-bedroom:2,4 Three-bedroom:3,6 Four-bedroom:4,8	8
Apartment orientation	S, N, W, E, SW, SE, NW, NE	8

Apartment volume(m^3)	260.68, 451.41, 452.17, 584.64, 588.44, 612.86	6
South wall area(m²)	0, 41.04, 53.96, 61.56, 145.35	5
North wall area(m²)	0, 41.04, 53.96, 61.56, 145.35	5
West wall area(m²)	0, 26.6, 42.56, 46.69	4
East wall area(m²)	0, 26.6, 42.56, 46.69	4
South window area(m²)	0,12.72, 16.70, 45.06	4
North window area(m²)	0,12.72, 16.70, 45.06	4
West window area(m²)	0, 8.27,14.91,14.94	4
East window area(m²)	0, 8.27,14.91,14.94	4
Roof area(m²)	0,34.59,60.49,161.28,331.36	5
Apartment height above ground(m)	7.98, 11.78, 15.58, 19.38, 23.18, 16.98, 30.78,34.58, 38.38, 42.18,45.98, 49.78, 53.58,57.38, 61.18, 65.11, 69.04	16

5.3.2 Sensitivity analysis results

We conducted the sensitivity analysis in three steps. First, we randomly selected thirty-six apartments on different floors and orientations to see how the apartment configuration parameters influence the cooling load. Table 19 demonstrates that month, apartment volume, and roof area are the most significant parameters. The cooling load varies significantly during different months of the year due to changes in outdoor air temperature. The greater the apartment volume, the higher the cooling demand. The roof will receive more solar radiation due to direct exposure to the sun. Hence, the roof area is a key parameter. A lower setpoint also produces a higher cooling demand. The south wall area is another critical parameter that influences the amount of solar radiation received.

Table 19 The sensitivity analysis for thirty-six apartments according to floor location and orientation

Parameter	SRC	Random Forest	T-Value	SVI	Rank
Month	0.34	633.67	23.84	35.18	1
Apartment volume	46.98	44.48	1.25	20.57	2
Roof area	0.76	22.91	15.48	10.82	3
Setpoint	0.06	226.53	0.48	7.46	4
S wall area	9.17	13.84	1.78	5.15	5

Parameter				
N wall area	8.32	19.16	1.72	4.95	6
E wall area	7.82	7.05	1.75	4.39	7
W wall area	6.99	0.09	1.49	3.68	8
S window area	2.76	17.84	1.84	2.81	9
Height above ground	1.22	45.97	0.70	2.37	10
N window area	0.79	15.77	0.49	1.12	11
W window area	0.01	3.71	1.29	0.94	12
E window area	0.00	7.91	0.49	0.56	13

Then, the nine apartments located on the 10th floor were randomly selected to conduct a sensitivity analysis. Building operation parameters such as occupancy, lighting power density, and equipment power density were considered at this stage. The critical parameters were observed to be the month, setpoint, south wall area, south window area, and apartment volume. The results were similar to those in the first step. Among building operation factors, equipment power density ranked much higher than the remaining parameters.

Table 20 The sensitivity analysis for nine apartments located on the same floor

Parameter	SRC	Random Forest	T-Value	SVI	Rank
Month	0.27	506.68	17.06	21.97	1
Setpoint	-0.22	437.83	-13.82	18.49	2
S wall area	1.76	19.96	0.07	11.70	3
S window area	-1.71	20.31	-0.07	11.38	4
Apartment volume	0.37	185.85	9.95	11.38	5
Equipment	0.20	92.98	10.91	8.38	6
E wall area	0.29	1.19	9.10	5.83	7
W wall area	0.29	1.52	9.00	5.80	8
Occupants	0.09	12.93	3.45	2.43	9
Lighting	0.05	11.56	2.72	1.78	10
N wall area	0.01	20.10	0.13	0.60	11
Orientation	0.00	10.05	0.00	0.25	12

At last, a typical apartment is chosen to study the building operation parameters. For a single apartment, configuration parameters such as the volume, wall area, and window area are fixed. Six input parameters, including setpoint, occupancy, and equipment power

density, were changed during the simulation. The east apartment on the 10th floor was used to conduct the sensitivity analysis. Since the month of the year was the main parameter in the first and second steps, it was decided to conduct the sensitivity analysis for every month, rather than group them, at this stage. The variables for each month are ranked in order of importance in Table 21. As Table 21 indicates, equipment power density ranked highest throughout the year. The influence of solar reflectance varies according to different months. In the winter months, solar radiation is low, which results in a lower rank for solar reflectance and vice versa in summer and transition months.

Table 21 The sensitivity analysis for one apartment during different months

Month	Parameters	Rank
1,2,3,12 (winter)	Equipment power density	1
	Setpoint	2
	Lighting power density	3
	Occupants	4
	Solar reflectance	5
4,5,6,7,8,9,10,11 (summer and transition months)	Equipment power density	1
	Setpoint	2
	Solar reflectance	3
	Occupants	4
	Lighting power density	5

5.4 Meta-model development

We used the independent variables in Table 18 to develop the meta-models. First, we determined which machine-learning model best predicted the apartment-level cooling load. The MLR, SVR, ANN, and XGBoost models were used to develop the meta-model. Eighty percent of the data was used for training, and the model performance was evaluated using the remaining 20% as test data. The predicted and EnergyPlus results are displayed in the Figure 27. Two ANN models, with one and five hidden layers, respectively, were used. The model with one hidden layer was the same ANN used to develop the building-level

meta-model (termed ANN1). The ANN model with five hidden layers (ANN5) had 64, 64, 128, 64, and 64 neurons in each layer. Both ANN models were trained to 50 and 250 epochs to compare the difference. The prediction relative errors for the test data under MLR, SVR, and ANN1 were high, whereas the ANN5 and XGBoost models predicted the monthly cooling load correctly.

Table 22 indicates that the R^2 of the MLR and SVR models is 0.41 and 0.36, respectively, demonstrating that the models cannot describe the relationship between the apartment-level cooling load and the independent variables. Moreover, the CV(RMSE) for the MLR and SVR models is 64.97% and 66.90%, respectively, much higher than the criteria described in Table 2. However, the NMBEs for the two models are low. This is because the sum of positive and negative values could reduce the NMBEs. The ANN1 models with 50 and 250 epochs also performed poorly, although these models demonstrated reasonable ability in predicting building-level cooling loads. The results of the ANN5 and XGBoost models demonstrate a good fit between simulation and prediction results. The ANN5 model trained to 250 epochs performed best (R^2 = 0.99, CV[RMSE] = 2.5).
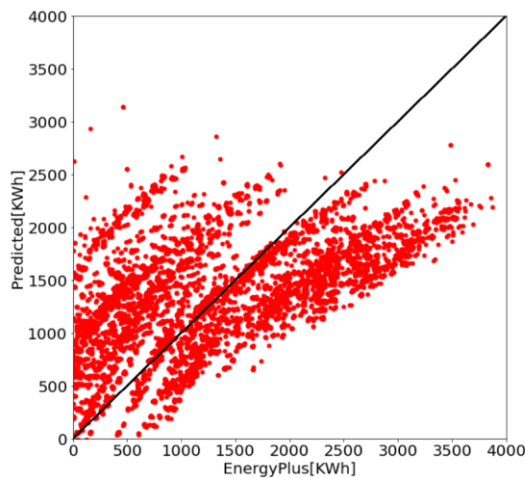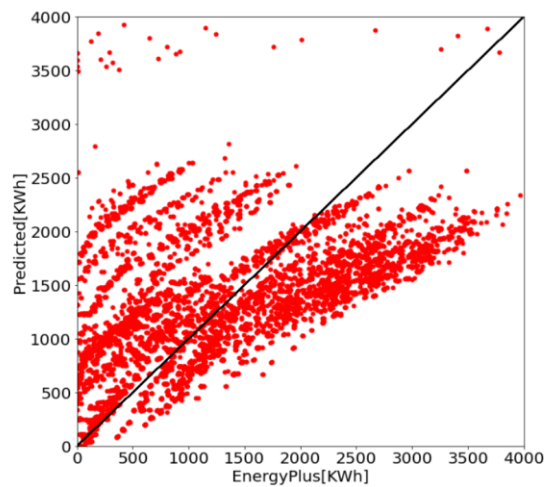
(a)   (b)
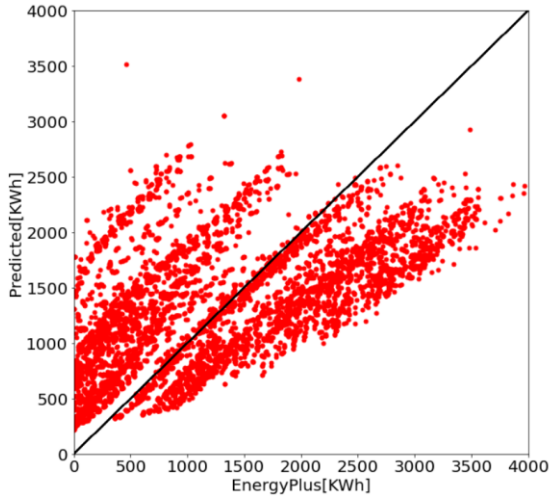
(c)
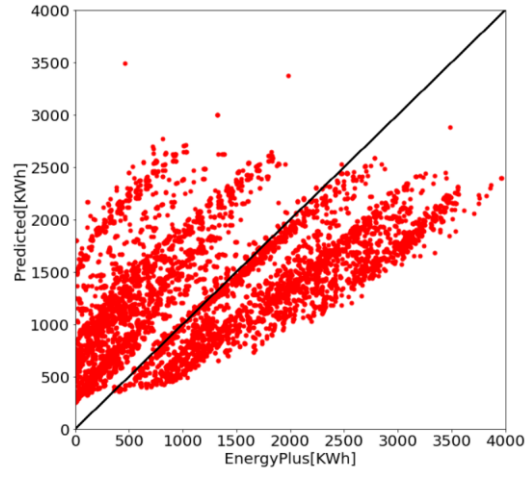
(d)
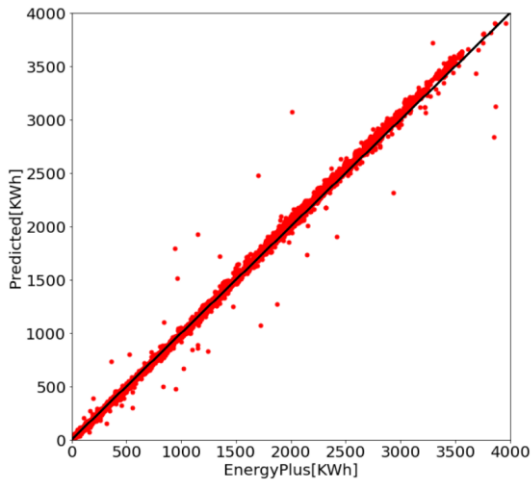
(e)
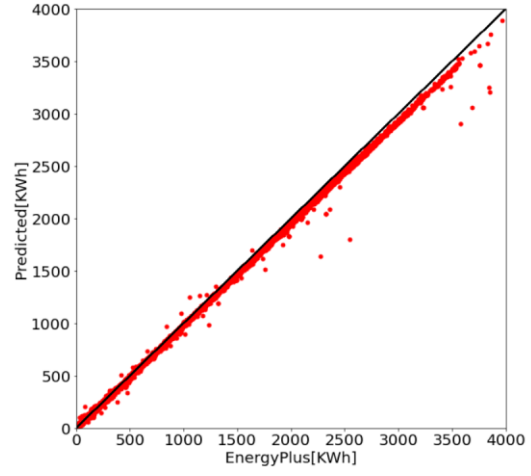
(f)
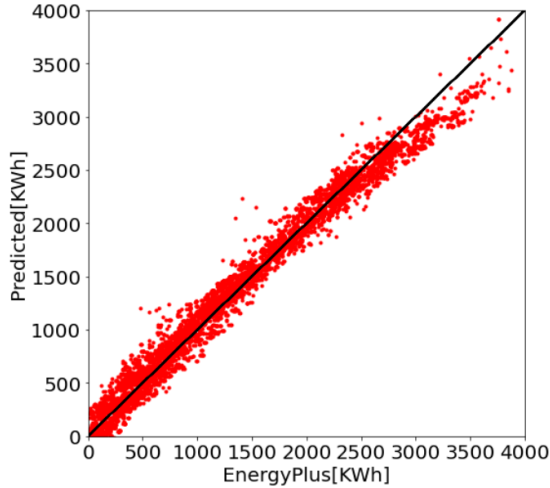
(g)

Figure 27. Comparison of monthly cooling load generated from EnergyPlus and developed meta-models: (a) MLR, (b) LinearSVR, (c) ANN1(50 epochs), (d) ANN1(250 epochs), (e) ANN5(50 epochs), (f) ANN5(250 epochs), and (g) XGBoost.

Table 22 A comparison of the evaluation indexes for the meta-models

Criteria	MLR	SVR	ANN1 (50 epochs)	ANN1 (250 epochs)	ANN5 (50 epochs)	ANN5 (250 epochs)	XGBoost	Standards
R^2	0.41	0.36	0.40	0.40	0.99	0.99	0.98	≥0.75
NMBE %	-0.65	-1.42	0	0	0	1.65	0	±5
CV(RMSE) %	64.97	66.90	64.51	64.39	5.03	2.50	11	15
Training time (s)	3	9	500	2500	500	2500	3	/

5.5 Meta-model verification

The ANN5 model (trained to 250 epochs) was selected as the meta-model in this study since it had the highest level of accuracy. To validate the meta-model, we created a generic building energy model by reducing the baseline model from 15 to 12 floors. The floor height was adjusted from 3.8 m to 4.5 m. The window-to-wall ratio was changed from 31% to 26%. The plan for floors 1–11 remained the same as that in the baseline model. The top floor configuration was altered to test the meta-model's adaptability. The meta-model

generated a monthly apartment-level cooling load from the new input data. The results were compared with the simulation outcomes from EnergyPlus (Figure 28). The R^2 was 0.89, indicating a good fit between the prediction and simulation results. It was established via the sensitivity analysis that the month has the most significant influence on apartment cooling load. Distinct seasonal patterns were observed during the winter, summer, and transition months.

To better analyze the meta-model's performance, we plotted a heat map of the CV(RMSE) for the monthly apartment-level cooling load in different apartments during different seasons (Figure 29). In summer, the CV(RMSE) remained between 1% and 4.5%. During the transition months, the CV(RMSE) indicated a slight increase, although most of the values remained below 7.5%, indicating a good level of accuracy for the meta-model. Only the CV(RMSE) for the apartments located on the top floor, which has a different configuration to the baseline model, was higher than the standards (Table 2). This was due to the influence of solar heat gain from the roof. Conversely, in the baseline model, only two apartments on the 16th floor are exposed to the sun, which reduces the meta-model's accuracy. The meta-model had difficulty predicting apartment cooling load in winter, which has a small magnitude and is prone to uncertainties.
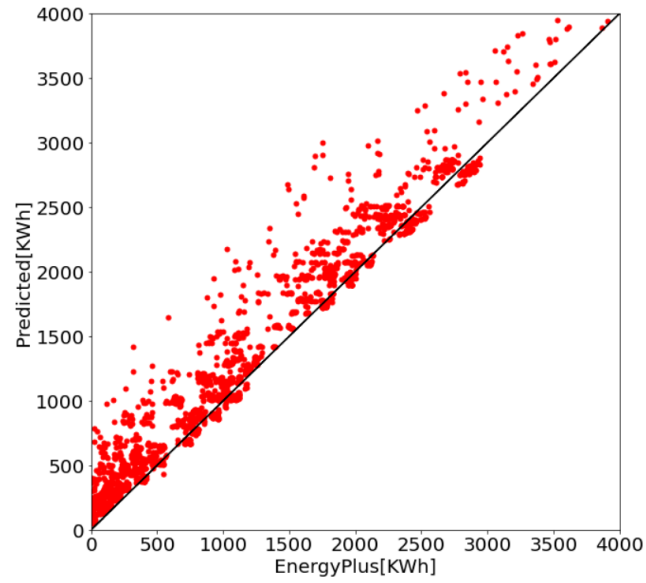
Figure 28. Comparison of monthly cooling energy for each apartment generated from EnergyPlus and meta-model.

(a)
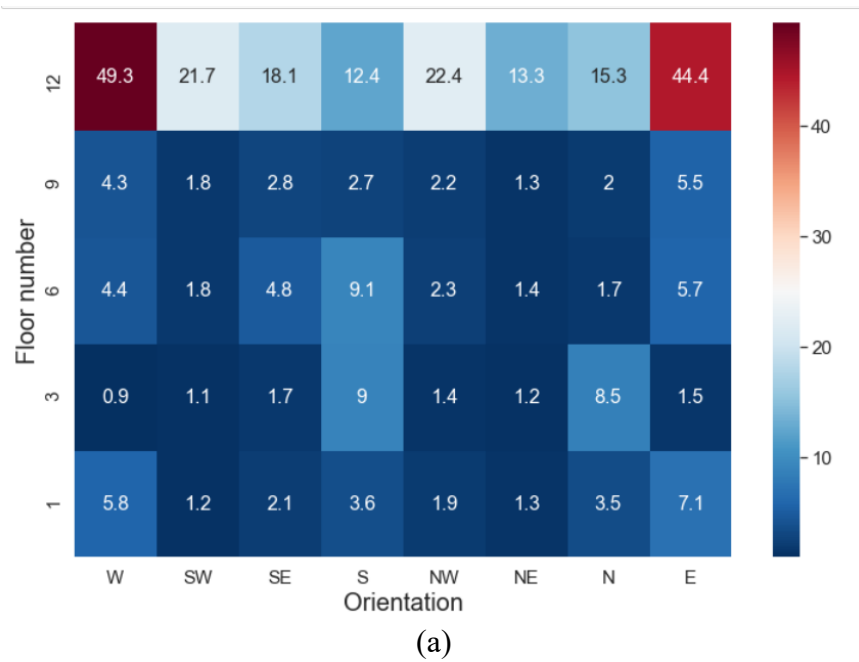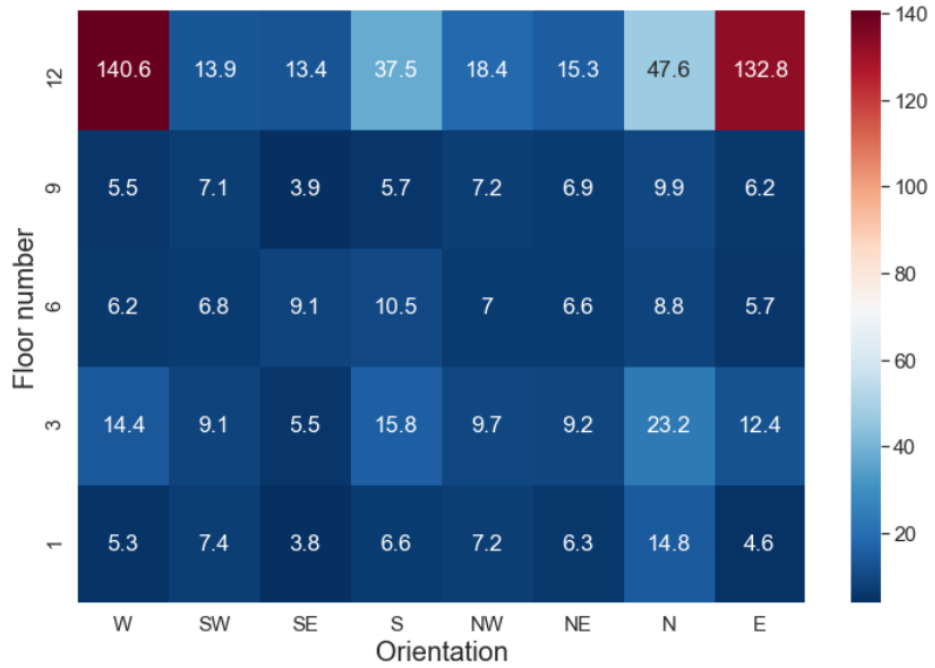
(b)
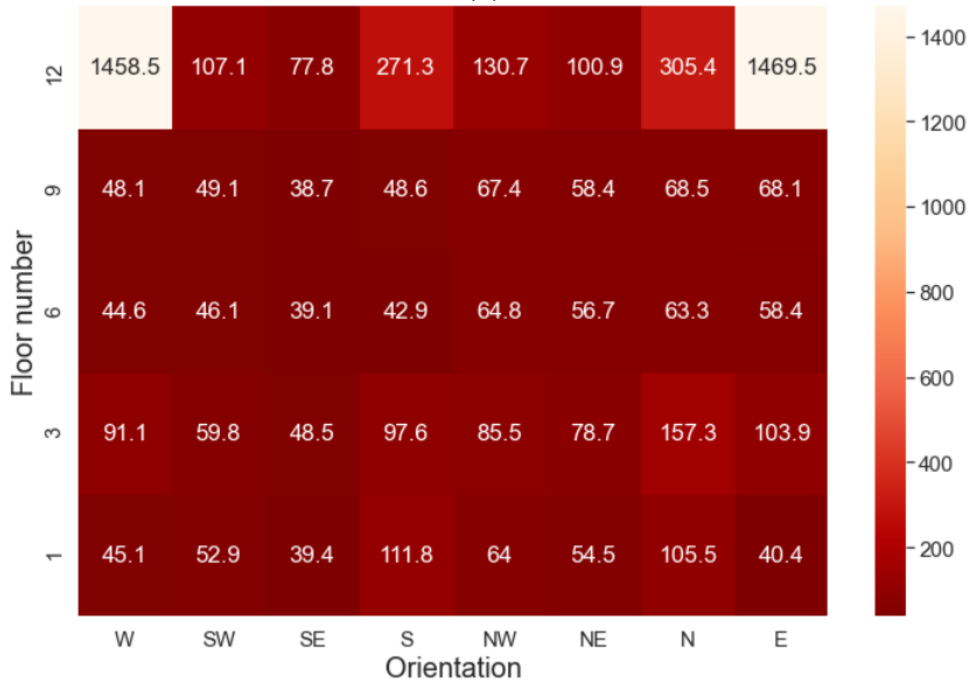
(c)

Figure 29. The CV(RMSE) in different seasons: (a) summer months, (b) transition

months, and (c) winter months.

5.6   Summary

In this chapter, we used a typical high-rise residential building with 138 apartments as a baseline. Detailed building energy models were created using EnergyPlus with each apartment considered to be one thermal zone. Cooling-load variations were observed in different apartments. The annual EUI of the upper-level floors was higher than that of the middle floors due to sun exposure. The apartments with two exterior walls, located in the southwest, southeast, northwest, and northeast, had higher annual EUIs. During the winter months, however, the monthly EUI was highest in the south apartments.

Sensitivity analysis was conducted in different stages to examine parameter significance. Among the operation parameters, equipment power density had a key role in influencing cooling load at the apartment level. Four machine-learning approaches (MLR, SVR, ANN, and XGBoost) were applied to develop a meta-model of apartment cooling load. The results indicated that the MLR, SVR, and ANN1 models had difficulty generalizing the relationship between input parameters and cooling load. In terms of the ANN model's performance, the number of hidden layers was more significant than the number of epochs. The ANN5 model trained 250 times was selected as the apartment-level meta-model due to its superior accuracy.

The proposed meta-model is accurate and efficient in predicting cooling energy during summer and transition months for a building with similar floor configurations. The prediction error of the cooling load during the winter months is high. The adaptability of the meta-model to buildings with different configurations remains a challenge.

6 Conclusion and Future Work

6.1 Conclusion

This study developed two meta-models to predict cooling loads at different levels. One meta-model predicted building-level cooling load at the district level and used the building envelope, climate, and internal gain parameters as independent variables. The building-level cooling load meta-model demonstrated a remarkable ability when applied to new buildings ($R^2 = 0.9992$ and CV[RMSE] = 1.9%). The second model predicted apartment-level cooling load, using a typical high-rise residential building as a case study. The independent variables used in the meta-model included the EnergyPlus input parameters (CSP, OCC, LPD, EPD, and SR) combined with apartment configuration parameters (apartment volume, wall area, window area, apartment height above ground) and the month of the year. The meta-model demonstrated a good level of prediction accuracy ($R^2 = 0.89$) for a building with a similar configuration. It was essential to study the apartment-level cooling load as we observed a significant difference between apartments located at different orientations and different floors. The difference between the annual EUI of apartments facing different directions may be as much as 60 kWh/m^2.

From the results, we observed that MLR and SVR could be used to predict building-level cooling loads, although their prediction accuracy was suboptimal. Moreover, their ability to predict apartment-level cooling load was poor. The ANN model, with one hidden layer, predicted the building-level cooling load well, although it produced unsatisfactory results in apartment-level cooling-load prediction. More hidden layers could significantly improve the ANN model's ability.

From the sensitivity analysis results, we observed that climate parameters were the most significant factors influencing both building-level and apartment-level cooling load. The setpoint and equipment power density were also crucial for improving building energy efficiency.

The primary contributions of this work are as follows:

- An overall methodology to develop a building- and apartment-level building energy meta-model is demonstrated.

- Four machine learning-based residential energy prediction meta-models, at both a building- and apartment-level, are developed. ANN was found to perform best among all the meta-models, while the number of hidden layers can significantly influence the ability of ANN, like the ANN with one hidden layer showed bad performance for apartment-level cooling load prediction.

- Climate, building thermal-physic characteristics, and operation parameters are simultaneously considered as independent variables to develop the whole building energy meta-model at a district level. Apartment operation parameters and apartment configuration parameters are considered to develop apartment-level energy meta-model.

- The applicability of machine learning in monthly apartment-level residential building energy prediction was validated.

- Sensitivity analyses for both building- and apartment-level cooling loads are conducted to show the importance of different parameters, which can contribute to the decision-making of energy savings.

6.2   Limitations

There exist several limitations of this study:

- Building shape variation is limited: In the building-level meta-model, only rectangular geometry energy models are developed, non-rectangular geometries are not considered. Several parameters are defined as typical values, including floor height and building orientation.

- Apartment-level meta-model performance for winter: The proposed apartment-level meta-model is only accurate and efficient when predicting cooling load during the summer and transition months. The prediction results for winter are not good. The meta-model is only applied to a building with a similar floor plan (Figure 11). Its applicability to buildings with different floor plan remains a challenge.

- Limited measurement data validated the building energy model: The building energy model was validated only with two monthly measurement data.

- The building is a typical residential high-rise residential building in the selected district in Lusail city. However, it cannot be used as a reference building energy model for the whole country.

- A detailed HVAC system is not modeled for the building energy models, and occupancy schedules are assumed based on engineering experience.

- The urban microclimate is not considered in this study.

6.3 Recommendations for future work

This study demonstrated a method for predicting building-level and apartment-level cooling loads. There are several recommendations for future work:

- If statistical data for the buildings in Qatar were available, different building shapes and more parameter values could be added to develop the building level meta-model.

- In developing the apartment-level meta-model, the choice of predictors affects the model performance significantly. In the future, more suitable parameter choices could lead to innovations in apartment-level meta-model development. Although we have included as many parameters as possible in this study, they could not reflect heat transfer between adjacent apartments. This may be the reason for the meta-model's limited adaptability.

- With more measurement data available in the future, the building energy model can be calibrated, which would improve the accuracy of the cooling load simulation results.

- With statistical data for the buildings in Qatar available in the future, a reference building energy model can be developed to expand the proposed building-level meta-model into an urban scale.

- Actual occupancy schedules can be obtained through the survey, which will help improve the accuracy of the building energy models.

- The urban microclimate can be added as independent variables to improve the meta-model's performance in the future.

7 REFERENCES

[1] W. Feng *et al.*, "A review of net zero energy buildings in hot and humid climates: Experience learned from 34 case study buildings," *Renew. Sustain. Energy Rev.*, vol. 114, no. November 2018, p. 109303, 2019, doi: 10.1016/j.rser.2019.109303.

[2] "Qatar Economy." https://en.wikipedia.org/wiki/Qatar#Economy.

[3] KAHRAMAA, "Annual Statistics Report," pp. 68–70, 2019.

[4] The Peninsula, "Qatar leads region in district cooling regulation." https://www.thepeninsulaqatar.com/article/05/04/2020/Qatar-leads-region-in-district-cooling-regulation#:~:text="District cooling is a solution,manner%2C" said Al Sada.&text="District Cooling (DC) consists,through a water piping network. (accessed Apr. 10, 2020).

[5] F. Saffouri, I. S. Bayram, and M. Koc, "Quantifying the Cost of Cooling in Qatar," no. February, pp. 1–9, 2018, doi: 10.1109/ieeegcc.2017.8448269.

[6] "Lusail city," 2020. https://www.lusail.com/the-project/the-city-today/.

[7] General Secretarian For Development Planning, "July 2008 General Secretariat For Development Planning," no. July, 2008, [Online]. Available: www.planning.gov.qa.

[8] L. Canale, M. Dell'Isola, G. Ficco, T. Cholewa, S. Siggelsten, and I. Balen, "A comprehensive review on heat accounting and cost allocation in residential buildings in EU," *Energy and Buildings*, vol. 202. Elsevier Ltd, Nov. 01, 2019, doi: 10.1016/j.enbuild.2019.109398.

[9] H. Radhi, "A comparison of the accuracy of building energy analysis in Bahrain using data from different weather periods," *Renew. Energy*, vol. 34, no. 3, pp. 869–875, 2009, doi: 10.1016/j.renene.2008.06.008.

[10] K. M. H. Swhli, S. Jovic, N. Arsic, and P. Spalevic, "Detection and evaluation of

heating load of building by machine learning," *Sens. Rev.*, vol. 38, no. 1, pp. 99–101, 2018, doi: 10.1108/SR-07-2017-0139.

[11]   A. Afshari, C. Nikolopoulou, and M. Martin, "Life-cycle analysis of building retrofits at the urban scale-a case study in United Arab Emirates," *Sustain.*, vol. 6, no. 1, pp. 453–473, 2014, doi: 10.3390/su6010453.

[12]   A. Gastli, Y. Charabi, R. A. Alammari, and A. M. Al-Ali, "Correlation between climate data and maximum electricity demand in Qatar," *2013 7th IEEE GCC Conf. Exhib. GCC 2013*, no. November, pp. 565–570, 2013, doi: 10.1109/IEEEGCC.2013.6705841.

[13]   "Building envelope." https://zhishi.xkyn.net/jingyan-nvbbvvsma.htm.

[14]   R. Ourghi, A. Al-Anzi, and M. Krarti, "A simplified analysis method to predict the impact of shape on annual energy use for office buildings," *Energy Convers. Manag.*, vol. 48, no. 1, pp. 300–305, 2007, doi: 10.1016/j.enconman.2006.04.011.

[15]   A. AlAnzi, D. Seo, and M. Krarti, "Impact of building shape on thermal performance of office buildings in Kuwait," *Energy Convers. Manag.*, vol. 50, no. 3, pp. 822–828, 2009, doi: 10.1016/j.enconman.2008.09.033.

[16]   B. Andersson, W. Place, R. Kammerud, and M. P. Scofield, "The impact of building orientation on residential heating and cooling," *Energy Build.*, vol. 8, no. 3, pp. 205–224, 1985, doi: 10.1016/0378-7788(85)90005-2.

[17]   F. Chi, J. Zhang, G. Li, Z. Zhu, and D. Bart, "An investigation of the impact of Building Azimuth on energy consumption in sizhai traditional dwellings," *Energy*, vol. 180, pp. 594–614, 2019, doi: 10.1016/j.energy.2019.05.114.

[18]   "Building orientation." http://news.syjiancai.com/n_280034.html.

[19]   G. Tibi and A. Mokhtar, "Glass selection for high-rise residential buildings in the United Arab Emirates based on life cycle cost analysis," *Energy Procedia*, vol. 62, pp. 270–279, 2014, doi: 10.1016/j.egypro.2014.12.388.

[20]   Y. Huang and J. lei Niu, "Application of super-insulating translucent silica aerogel glazing system on commercial building envelope of humid subtropical climates - Impact on space cooling load," *Energy*, vol. 83, pp. 316–325, 2015, doi: 10.1016/j.energy.2015.02.027.

[21]   E. O. Assem and A. A. Al-Mumin, "Code compliance of fully glazed tall office buildings in hot climate," *Energy Build.*, vol. 42, no. 7, pp. 1100–1105, 2010, doi: 10.1016/j.enbuild.2010.02.001.

[22]   J. B. M.Bojic, F.Yik, K, Wan, "Investigations of cooling loads in high-rise residential buildings in Hong Kong," pp. 1–21.

[23]   M. Bojic, F. Yik, K. Wan, and J. Burnett, "Influence of envelope and partition characteristics on the space cooling of high-rise residential buildings in Hong Kong," *Build. Environ.*, vol. 37, no. 4, pp. 347–355, 2002, doi: 10.1016/S0360-1323(01)00045-2.

[24]   E. Solgi, R. Fayaz, and B. M. Kari, "Cooling load reduction in office buildings of hot-arid climate, combining phase change materials and night purge ventilation," *Renew. Energy*, vol. 85, pp. 725–731, 2016, doi: 10.1016/j.renene.2015.07.028.

[25]   J. H. Park, B. Y. Yun, S. J. Chang, S. Wi, J. Jeon, and S. Kim, "Impact of a passive retrofit shading system on educational building to improve thermal comfort and energy consumption," *Energy Build.*, vol. 216, 2020, doi: 10.1016/j.enbuild.2020.109930.

[26] Z. Wu, M. Qin, and M. Zhang, "Phase change humidity control material and its impact on building energy consumption," *Energy Build.*, vol. 174, pp. 254–261, 2018, doi: 10.1016/j.enbuild.2018.06.036.

[27] L. Yang and Y. Li, "Cooling load reduction by using thermal mass and night ventilation," *Energy Build.*, vol. 40, no. 11, pp. 2052–2058, 2008, doi: 10.1016/j.enbuild.2008.05.014.

[28] R. Qiao and T. Liu, "Impact of building greening on building energy consumption: A quantitative computational approach," *J. Clean. Prod.*, vol. 246, p. 119020, 2020, doi: 10.1016/j.jclepro.2019.119020.

[29] S. Schiavon, K. H. Lee, F. Bauman, and T. Webster, "Influence of raised floor on zone design cooling load in commercial buildings," *Energy Build.*, vol. 42, no. 8, pp. 1182–1191, 2010, doi: 10.1016/j.enbuild.2010.02.009.

[30] J. Du and W. Pan, "Impact Of Window Opening Behaviors On Cooling Load Of High-Rise Residential Buildings In Hong Kong," *Proc. Build. Simul. 2019 16th Conf. IBPSA*, vol. 16, no. September, pp. 2403–2410, 2020, doi: 10.26868/25222708.2019.211418.

[31] W. A. Friess, K. Rakhshan, T. A. Hendawi, and S. Tajerzadeh, "Wall insulation measures for residential villas in Dubai: A case study in energy efficiency," *Energy Build.*, vol. 44, no. 1, pp. 26–32, 2012, doi: 10.1016/j.enbuild.2011.10.005.

[32] S. S. K. Kwok and E. W. M. Lee, "A study of the importance of occupancy to building cooling load in prediction by intelligent approach," *Energy Convers. Manag.*, vol. 52, no. 7, pp. 2555–2564, 2011, doi: 10.1016/j.enconman.2011.02.002.

[33] S. S. K. Kwok, R. K. K. Yuen, and E. W. M. Lee, "An intelligent approach to

assessing the effect of building occupancy on building cooling load prediction," *Build. Environ.*, vol. 46, no. 8, pp. 1681–1690, 2011, doi: 10.1016/j.buildenv.2011.02.008.

[34] J. C. Lam, C. L. Tsang, and L. Yang, "Impacts of lighting density on heating and cooling loads in different climates in China," *Energy Convers. Manag.*, vol. 47, no. 13–14, pp. 1942–1953, 2006, doi: 10.1016/j.enconman.2005.09.008.

[35] H. M. Taleb, "Natural ventilation as energy efficient solution for achieving low-energy houses in Dubai," *Energy Build.*, vol. 99, pp. 284–291, 2015, doi: 10.1016/j.enbuild.2015.04.019.

[36] J. Deng, S. He, Q. Wei, M. Liang, Z. Hao, and H. Zhang, "Research on systematic optimization methods for chilled water systems in a high-rise office building," *Energy Build.*, vol. 209, p. 109695, 2020, doi: 10.1016/j.enbuild.2019.109695.

[37] A. Foucquier, S. Robert, F. Suard, L. Stéphan, and A. Jay, "State of the art in building modelling and energy performances prediction: A review," *Renew. Sustain. Energy Rev.*, vol. 23, pp. 272–288, 2013, doi: 10.1016/j.rser.2013.03.004.

[38] K. Amasyali and N. M. El-Gohary, "A review of data-driven building energy consumption prediction studies," *Renew. Sustain. Energy Rev.*, vol. 81, no. April 2017, pp. 1192–1205, 2018, doi: 10.1016/j.rser.2017.04.095.

[39] X. Li and J. Wen, "Review of building energy modeling for control and operation," *Renew. Sustain. Energy Rev.*, vol. 37, pp. 517–537, 2014, doi: 10.1016/j.rser.2014.05.056.

[40] "Heat transfer." https://www.azom.com/article.aspx?ArticleID=15386.

[41] "BSim." https://sbi.dk/bsim/Pages/Start.aspx.

[42] F. C. Winkelmann *et al.*, "DOE-2 supplement: Version 2.1E," United States, 1993.

[43] "ESP-r." http://www.esru.strath.ac.uk/Courseware/ESP-r/tour/.

[44] "IDA ICE." https://www.equa.se/en/ida-ice.

[45] "IES VE." https://www.iesve.com/.

[46] "eQUEST." https://www.doe2.com/equest/.

[47] D. B. Crawley *et al.*, "EnergyPlus: Creating a new-generation building energy simulation program," *Energy Build.*, 2001, doi: 10.1016/S0378-7788(00)00114-6.

[48] S. A. Klein, "TRNSYS-A transient system simulation program," *Univ. Wisconsin-Madison, Eng. Exp. Stn. Rep.*, pp. 38--12, 1988.

[49] D. B. Crawley, J. W. Hand, M. Kummert, and B. T. Griffith, "Contrasting the capabilities of building energy performance simulation programs," *Build. Environ.*, vol. 43, no. 4, pp. 661–673, 2008, doi: 10.1016/j.buildenv.2006.10.027.

[50] "DeST." http://elearning-southzeb.eu/mod/page/view.php?id=106.

[51] J. Ma, J. Qin, T. Salsbury, and P. Xu, "Demand reduction in building energy systems based on economic model predictive control," *Chem. Eng. Sci.*, vol. 67, no. 1, pp. 92–100, 2012, doi: 10.1016/j.ces.2011.07.052.

[52] K. Yun, R. Luck, P. J. Mago, and H. Cho, "Building hourly thermal load prediction using an indexed ARX model," *Energy Build.*, vol. 54, pp. 225–233, 2012, doi: 10.1016/j.enbuild.2012.08.007.

[53] J. W. Moon and J. J. Kim, "ANN-based thermal control models for residential buildings," *Build. Environ.*, vol. 45, no. 7, pp. 1612–1625, 2010, doi: 10.1016/j.buildenv.2010.01.009.

[54] J. Yang, H. Rivard, and R. Zmeureanu, "On-line building energy prediction using

adaptive artificial neural networks," *Energy Build.*, vol. 37, no. 12, pp. 1250–1259, 2005, doi: 10.1016/j.enbuild.2005.02.005.

[55]   Z. Hou, Z. Lian, Y. Yao, and X. Yuan, "Cooling-load prediction by the combination of rough set theory and an artificial neural-network based on data-fusion technique," *Appl. Energy*, vol. 83, no. 9, pp. 1033–1046, 2006, doi: 10.1016/j.apenergy.2005.08.006.

[56]   L. Zhang *et al.*, "A review of machine learning in building load prediction," *Appl. Energy*, vol. 285, no. December 2020, p. 116452, 2021, doi: 10.1016/j.apenergy.2021.116452.

[57]   "Machine learning." https://towardsdatascience.com/what-is-machine-learning-and-types-of-machine-learning-andrews-machine-learning-part-1-9cd9755bc647#:~:text=Tom Mitchell provides a more,%2C improves with experience E.".

[58]   B. Yildiz, J. I. Bilbao, and A. B. Sproul, "A review and analysis of regression and machine learning models on commercial building electricity load forecasting," *Renew. Sustain. Energy Rev.*, vol. 73, no. March 2016, pp. 1104–1122, 2017, doi: 10.1016/j.rser.2017.02.023.

[59]   N. D. Roman, F. Bre, V. D. Fachinotti, and R. Lamberts, "Application and characterization of metamodels based on artificial neural networks for building performance simulation: A systematic review," *Energy Build.*, vol. 217, 2020, doi: 10.1016/j.enbuild.2020.109972.

[60]   Y. Sun, F. Haghighat, and B. C. M. Fung, "A review of the-state-of-the-art in data-driven approaches for building energy prediction," *Energy Build.*, vol. 221, p.

110022, 2020, doi: 10.1016/j.enbuild.2020.110022.

[61] S. R. Mohandes, X. Zhang, and A. Mahdiyar, "A comprehensive review on the application of artificial neural networks in building energy analysis," *Neurocomputing*, vol. 340, pp. 55–75, 2019, doi: 10.1016/j.neucom.2019.02.040.

[62] M. Bourdeau, X. qiang Zhai, E. Nefzaoui, X. Guo, and P. Chatellier, "Modeling and forecasting building energy consumption: A review of data-driven techniques," *Sustain. Cities Soc.*, vol. 48, no. April, p. 101533, 2019, doi: 10.1016/j.scs.2019.101533.

[63] N. Wei, C. Li, X. Peng, F. Zeng, and X. Lu, "Conventional models and artificial intelligence-based models for energy consumption forecasting: A review," *J. Pet. Sci. Eng.*, vol. 181, no. June, p. 106187, 2019, doi: 10.1016/j.petrol.2019.106187.

[64] J. S. Hygh, J. F. DeCarolis, D. B. Hill, and S. Ranji Ranjithan, "Multivariate regression as an energy assessment tool in early building design," *Build. Environ.*, vol. 57, pp. 165–175, 2012, doi: 10.1016/j.buildenv.2012.04.021.

[65] M. Al Gharably, J. F. DeCarolis, and S. R. Ranjithan, "An enhanced linear regression-based building energy model (LRBEM+) for early design," *J. Build. Perform. Simul.*, vol. 9, no. 2, pp. 115–133, 2016, doi: 10.1080/19401493.2015.1004108.

[66] P. Geyer and S. Singaravel, "Component-based machine learning for performance prediction in building design," *Appl. Energy*, vol. 228, no. April, pp. 1439–1453, 2018, doi: 10.1016/j.apenergy.2018.07.011.

[67] Q. Li, L. Gu, G. Augenbroe, C. F. Jeff Wu, and J. Brown, "Calibration of dynamic building energy models with multiple responses using Bayesian inference and linear

regression models," *Energy Procedia*, vol. 78, pp. 979–984, 2015, doi: 10.1016/j.egypro.2015.11.037.

[68]   M. Manfren, N. Aste, and R. Moshksar, "Calibration and uncertainty analysis for computer models - A meta-model based approach for integrated building energy simulation," *Appl. Energy*, vol. 103, pp. 627–641, 2013, doi: 10.1016/j.apenergy.2012.10.031.

[69]   F. Zhao, S. H. Lee, and G. Augenbroe, "Reconstructing building stock to replicate energy consumption data," *Energy Build.*, vol. 117, pp. 301–312, 2016, doi: 10.1016/j.enbuild.2015.10.001.

[70]   B. Eisenhower, Z. O'Neill, S. Narayanan, V. A. Fonoberov, and I. Mezić, "A methodology for meta-model based optimization in building energy models," *Energy Build.*, 2012, doi: 10.1016/j.enbuild.2011.12.001.

[71]   J. Yang, H. Rivard, and R. Zmeureanu, "Building energy prediction with adaptive artificial neural networks," *IBPSA 2005 - Int. Build. Perform. Simul. Assoc. 2005*, pp. 1401–1408, 2005.

[72]   S. A. Kalogirou and M. Bojic, "Artificial neural networks for the prediction of the energy consumption of a passive solar building," *Energy*, 2000, doi: 10.1016/S0360-5442(99)00086-9.

[73]   M. Aydinalp, V. I. Ugursal, and A. S. Fung, "Modeling of the space and domestic hot-water heating energy-consumption in the residential sector using neural networks," *Appl. Energy*, 2004, doi: 10.1016/j.apenergy.2003.12.006.

[74]   W. Tian, J. Song, Z. Li, and P. de Wilde, "Bootstrap techniques for sensitivity analysis and model selection in building thermal performance analysis," *Appl.*

Energy, 2014, doi: 10.1016/j.apenergy.2014.08.110.

[75]   Y. J. N. Kim, K. U. Aim, C. S. Park, and I. H. Kim, "Gaussian emulator for stochastic optimal design of a double glazing system," *Proc. BS 2013 13th Conf. Int. Build. Perform. Simul. Assoc.*, pp. 2217–2224, 2013.

[76]   M. Riddle and R. T. Muehleisen, "A guide to Bayesian calibration of building energy models," *2014 ASHRAE/IBPSA-USA Build. Simul. Conf.*, no. January, pp. 276–283, 2014, doi: 10.13140/2.1.1674.9127.

[77]   F. Bre, N. Roman, and V. D. Fachinotti, "An efficient metamodel-based method to carry out multi-objective building performance optimizations," *Energy Build.*, vol. 206, p. 109576, 2020, doi: 10.1016/j.enbuild.2019.109576.

[78]   S. A. Sharif and A. Hammad, "Developing surrogate ANN for selecting near-optimal building energy renovation methods considering energy consumption, LCC and LCA," *J. Build. Eng.*, vol. 25, no. October 2018, p. 100790, 2019, doi: 10.1016/j.jobe.2019.100790.

[79]   Z. Romani, A. Draoui, and F. Allard, "Metamodeling the heating and cooling energy needs and simultaneous building envelope optimization for low energy building design in Morocco," *Energy Build.*, vol. 102, pp. 139–148, 2015, doi: 10.1016/j.enbuild.2015.04.014.

[80]   X. Li and R. Yao, "A machine-learning-based approach to predict residential annual space heating and cooling loads considering occupant behaviour," *Energy*, vol. 212, p. 118676, 2020, doi: 10.1016/j.energy.2020.118676.

[81]   M. N. Lopes and R. Lamberts, "Development of a metamodel to predict cooling energy consumption of HVAC systems in office buildings in different climates,"

Sustain., vol. 10, no. 12, 2018, doi: 10.3390/su10124718.

[82] N. T. Ngo, "Early predicting cooling loads for energy-efficient design in office buildings by machine learning," *Energy Build.*, vol. 182, pp. 264–273, 2019, doi: 10.1016/j.enbuild.2018.10.004.

[83] "Python." https://www.python.org/.

[84] "Ideal air loads." https://bigladdersoftware.com/epx/docs/8-0/engineering-reference/page-092.html.

[85] T. Wei, "A review of sensitivity analysis methods in building energy analysis," *Renew. Sustain. Energy Rev.*, vol. 20, pp. 411–419, 2013, doi: 10.1016/j.rser.2012.12.014.

[86] F. Feng, Z. Li, Y. Ruan, and P. Xu, "An Empirical Study of Influencing Factors on Residential Building Energy Consumption in Qingdao City, China," *Energy Procedia*, vol. 104, pp. 245–250, 2016, doi: 10.1016/j.egypro.2016.12.042.

[87] Z. Pang, Z. O'Neill, Y. Li, and F. Niu, "The role of sensitivity analysis in the building performance analysis: A critical review," *Energy Build.*, vol. 209, p. 109659, 2020, doi: 10.1016/j.enbuild.2019.109659.

[88] J. C. Lam, K. K. W. Wan, and L. Yang, "Sensitivity analysis and energy conservation measures implications," *Energy Convers. Manag.*, vol. 49, no. 11, pp. 3170–3177, 2008, doi: 10.1016/j.enconman.2008.05.022.

[89] M. Rasouli, G. Ge, C. J. Simonson, and R. W. Besant, "Uncertainties in energy and economic performance of HVAC systems and energy recovery ventilators due to uncertainties in building and HVAC parameters," *Appl. Therm. Eng.*, vol. 50, no. 1, pp. 732–742, 2013, doi: 10.1016/j.applthermaleng.2012.08.021.

[90] M. Kavgic, D. Mumovic, A. Summerfield, Z. Stevanovic, and O. Ecim-Djuric, "Uncertainty and modeling energy consumption: Sensitivity analysis for a city-scale domestic energy model," *Energy Build.*, vol. 60, pp. 1–11, 2013, doi: 10.1016/j.enbuild.2013.01.005.

[91] Q. Li, G. Augenbroe, and J. Brown, "Assessment of linear emulators in lightweight Bayesian calibration of dynamic building energy models for parameter estimation and performance prediction," *Energy Build.*, vol. 124, pp. 194–202, 2016, doi: 10.1016/j.enbuild.2016.04.025.

[92] H. Lim and Z. J. Zhai, "Comprehensive evaluation of the influence of meta-models on Bayesian calibration," *Energy Build.*, vol. 155, pp. 66–75, 2017, doi: 10.1016/j.enbuild.2017.09.009.

[93] K. N. Çerçi and E. Hürdoğan, "Comparative study of multiple linear regression (MLR) and artificial neural network (ANN) techniques to model a solid desiccant wheel," *Int. Commun. Heat Mass Transf.*, vol. 116, no. June, 2020, doi: 10.1016/j.icheatmasstransfer.2020.104713.

[94] A. Aranda, G. Ferreira, M. D. Mainar-Toledo, S. Scarpellini, and E. Llera Sastresa, "Multiple regression models to predict the annual energy consumption in the Spanish banking sector," *Energy Build.*, vol. 49, pp. 380–387, 2012, doi: 10.1016/j.enbuild.2012.02.040.

[95] C. Fan, Y. Ding, and Y. Liao, "Analysis of hourly cooling load prediction accuracy with data-mining approaches on different training time scales," *Sustain. Cities Soc.*, vol. 51, no. February, p. 101717, 2019, doi: 10.1016/j.scs.2019.101717.

[96] M. Kuhn and K. Johnson, *Applied predictive modeling*. 2013.

[97] "SVM." https://www.listendata.com/2017/01/support-vector-machine-in-r-tutorial.html.

[98] N. Parveen, S. Zaidi, and M. Danish, "Development of SVR-based model and comparative analysis with MLR and ANN models for predicting the sorption capacity of Cr(VI)," *Process Saf. Environ. Prot.*, vol. 107, pp. 428–437, 2017, doi: 10.1016/j.psep.2017.03.007.

[99] S. Zaidi, "Novel application of support vector machines to model the two phase boiling heat transfer coefficient in a vertical tube thermosiphon reboiler," *Chem. Eng. Res. Des.*, vol. 98, pp. 44–58, 2015, doi: 10.1016/j.cherd.2015.04.002.

[100] Y. Ding, Q. Zhang, and T. Yuan, "Research on short-term and ultra-short-term cooling load prediction models for office buildings," *Energy Build.*, vol. 154, pp. 254–267, 2017, doi: 10.1016/j.enbuild.2017.08.077.

[101] D. a. Community, "ML Visuals." https://github.com/dair-ai/ml-visuals.

[102] "XGBoost." https://xgboost.readthedocs.io/en/latest/tutorials/model.html.

[103] "XGBoost Documentation." https://xgboost.readthedocs.io/en/latest/tutorials/model.html.

[104] G. R. Ruiz and C. F. Bandera, "Validation of calibrated energy models: Common errors," *Energies*, vol. 10, no. 10, 2017, doi: 10.3390/en10101587.

[105] "M&V Guidelines: Measurement and Verification for Performance-Based Contracts Version 4.0." https://www.energy.gov/sites/prod/files/2016/01/f28/mv_guide_4_0.pdf.

[106] "ASHRAE Guideline 14-2014." https://webstore.ansi.org/standards/ashrae/ashraeguideline142014.

[107] "International Performance Measurement & Verification Protocol." https://www.nrel.gov/docs/fy01osti/29564.pdf.

[108] Qatar national master plan, "Residential (R6) – Residential Tower Zone." [Online]. Available: http://www.mme.gov.qa/QatarMasterPlan/Downloads-qnmp/Regulation/English/01-Residential Zones/06-Residential 6 August 2017.pdf.

[109] E. Shearer, "Ashrae standard 90.1 - 2004 building energy analysis _____ _____," pp. 1–33, 2004.

[110] Y. M. Alhorr, "GSAS Building Typologies Manual: Design Guidelines - v2.1," 2015, [Online]. Available: http://www.gord.qa/admin/Content/Link232201723143.pdf.

[111] "Emporis standards." https://www.emporis.com/building/standards#:~:text=Emporis Standards is an information,all systems connected to Emporis.

[112] "ASHRAE Standards." https://www.ashrae.org/technical-resources/standards-and-guidelines/read-only-versions-of-ashrae-standards.

[113] Lusail City, "Lusail City GSAS 2 Star Rating Guidelines," 2016. [Online]. Available: http://www.qataridiar.com/English/OurProjects/Pages/Lusail-City.aspx.

[114] "AUTODESK." https://knowledge.autodesk.com/search-result/caas/simplecontent/content/equipment-and-lighting-loads.html.

[115] T. I. Wa-, "Solar protection," *Nano Mater.*, no. February, pp. 144–145, 2008, doi: 10.1007/978-3-7643-8321-3_45.

[116] "EN 13363-2:2005." https://standards.iteh.ai/catalog/standards/cen/ff3aa145-4f04-

44d3-921a-929a1b88e549/en-13363-2-2005.

[117] A. Matala, "Sample Size Requirement for Monte Carlo simulations using Latin Hypercube Sampling," *Indep. Res. Proj. Appl. Math.*, pp. 1–24, 2008, [Online]. Available: http://www.sal.tkk.fi/vanhat_sivut/Opinnot/Mat-2.4108/pdf-files/emat08.pdf.

[118] G. Varoquaux, L. Buitinck, G. Louppe, O. Grisel, F. Pedregosa, and A. Mueller, "Scikit-learn," *GetMobile Mob. Comput. Commun.*, vol. 19, no. 1, pp. 29–33, 2015, doi: 10.1145/2786984.2786995.

[119] C. Study, "3 Case Study with Keras."

[120] G. Panchal, A. Ganatra, Y. P. Kosta, and D. Panchal, "328-L318-3," vol. 3, no. 2, pp. 332–337, 2011.

[121] "XGBoost Python Package." https://xgboost.readthedocs.io/en/latest/python/index.html.

[122] "EnergyPlus Engineering Reference," 2020. https://energyplus.net/sites/all/modules/custom/nrel_custom/pdfs/pdfs_v9.3.0/EngineeringReference.pdf.

[123] J. Cao, J. Liu, and X. Man, "A united WRF/TRNSYS method for estimating the heating/cooling load for the thousand-meter scale megatall buildings," *Appl. Therm. Eng.*, vol. 114, pp. 196–210, 2017, doi: 10.1016/j.applthermaleng.2016.11.195.

[124] "Sun path." https://www.gaisma.com/en/location/doha-qa.html.

[125] "Qatar climate." https://urbanizedadaptation.files.wordpress.com/2012/09/qatar_int_climate.pdf.

8 APPENDIX

Appendix 1. 650 parameters combination generated by Latin hypercube sampling method

Number	Roof Insulation U Value	Wall U Value	Floor U Value	Window U Value	Window SHGC	Window Solar Transmittance	Solar Reflectance	EPD	LPD	OCC	Infiltration	Ventilation	Setpoint
1	0.25	0.19	0.15	0.37	0.19	0.21	0.61	7.46	4.95	65.32	0.15	0.00060	23.27
2	0.00	0.24	0.02	0.99	0.09	0.14	0.47	7.27	5.63	74.51	0.17	0.00033	22.69
3	0.23	0.04	0.17	0.55	0.18	0.20	0.64	5.44	3.35	63.51	0.13	0.00059	21.54
4	0.10	0.10	0.13	1.51	0.06	0.04	0.65	4.07	4.09	68.72	0.10	0.00032	24.90
5	0.23	0.09	0.08	0.41	0.05	0.00	0.58	7.59	3.38	77.56	0.13	0.00046	22.93
6	0.07	0.26	0.14	1.54	0.17	0.19	0.73	4.65	5.92	80.65	0.11	0.00046	25.05
7	0.16	0.15	0.09	1.17	0.03	0.11	0.71	3.66	5.70	75.86	0.17	0.00042	25.72
8	0.09	0.07	0.25	0.19	0.18	0.09	0.73	4.28	3.02	38.93	0.11	0.00036	21.88
9	0.19	0.15	0.23	1.27	0.00	0.01	0.40	6.32	4.56	68.09	0.17	0.00053	25.03
10	0.22	0.07	0.33	1.48	0.07	0.04	0.62	6.06	3.23	71.07	0.11	0.00055	22.47
11	0.06	0.04	0.27	0.05	0.11	0.05	0.43	3.80	4.84	63.35	0.13	0.00033	25.29
12	0.02	0.27	0.19	0.48	0.13	0.16	0.57	6.24	5.78	71.44	0.15	0.00049	22.47
13	0.23	0.11	0.24	1.75	0.14	0.24	0.54	5.60	5.69	52.76	0.19	0.00057	21.95
14	0.12	0.23	0.04	1.58	0.21	0.12	0.75	3.10	4.67	89.03	0.18	0.00046	24.73
15	0.14	0.26	0.13	1.11	0.00	0.09	0.42	2.13	3.20	64.68	0.18	0.00039	24.59
16	0.15	0.23	0.08	1.42	0.18	0.15	0.58	6.84	5.33	69.91	0.12	0.00032	21.90
17	0.10	0.18	0.01	1.01	0.20	0.01	0.70	3.98	3.24	71.01	0.13	0.00057	23.99
18	0.19	0.21	0.14	1.09	0.05	0.12	0.78	2.31	4.02	49.80	0.19	0.00050	21.55
19	0.16	0.03	0.01	1.37	0.09	0.23	0.49	4.93	4.04	89.79	0.12	0.00058	23.43
20	0.23	0.04	0.06	1.65	0.01	0.23	0.70	5.04	5.83	70.90	0.18	0.00040	21.94
21	0.01	0.22	0.01	0.79	0.21	0.13	0.52	7.25	5.81	46.54	0.19	0.00047	24.17
22	0.09	0.24	0.18	1.33	0.01	0.14	0.56	7.60	3.70	59.13	0.14	0.00054	24.27

23	0.01	0.16	0.24	0.88	0.21	0.05	0.80	3.77	3.04	79.07	0.10	0.00037	23.35
24	0.09	0.11	0.11	0.45	0.06	0.17	0.67	7.24	5.88	67.26	0.16	0.00039	23.43
25	0.20	0.21	0.25	1.20	0.13	0.21	0.43	6.34	5.24	85.90	0.16	0.00040	22.57
26	0.07	0.08	0.07	0.77	0.14	0.21	0.56	4.15	4.03	69.23	0.14	0.00043	22.30
27	0.13	0.24	0.10	1.40	0.08	0.13	0.53	3.82	3.87	60.99	0.17	0.00047	22.49
28	0.04	0.30	0.11	1.58	0.07	0.03	0.42	6.20	3.46	69.37	0.17	0.00046	21.92
29	0.07	0.23	0.14	1.47	0.19	0.12	0.56	7.45	4.06	65.24	0.17	0.00035	25.49
30	0.10	0.26	0.07	0.93	0.10	0.21	0.55	2.63	4.04	78.63	0.11	0.00058	21.35
31	0.21	0.16	0.18	0.80	0.03	0.24	0.43	5.60	3.46	72.75	0.18	0.00041	25.18
32	0.08	0.10	0.08	1.01	0.17	0.11	0.66	6.74	5.12	59.95	0.11	0.00052	22.41
33	0.14	0.28	0.32	0.58	0.12	0.06	0.52	5.74	5.24	72.66	0.14	0.00038	22.04
34	0.22	0.14	0.16	1.59	0.11	0.03	0.63	2.67	5.30	43.97	0.11	0.00054	24.08
35	0.03	0.25	0.18	0.64	0.10	0.19	0.53	4.34	3.38	61.55	0.15	0.00033	25.59
36	0.22	0.20	0.22	0.24	0.06	0.02	0.59	3.20	4.72	69.35	0.16	0.00055	24.95
37	0.17	0.27	0.19	1.48	0.19	0.16	0.74	2.81	4.12	68.38	0.10	0.00059	25.21
38	0.24	0.17	0.04	1.52	0.04	0.10	0.42	4.01	4.70	72.92	0.12	0.00039	22.38
39	0.01	0.03	0.26	0.03	0.21	0.05	0.62	5.03	3.27	58.48	0.14	0.00037	24.65
40	0.19	0.25	0.22	0.29	0.07	0.20	0.51	7.99	3.01	39.76	0.12	0.00053	24.45
41	0.22	0.04	0.13	1.29	0.20	0.01	0.76	5.30	5.85	67.52	0.16	0.00058	24.52
42	0.04	0.02	0.33	1.12	0.07	0.14	0.59	6.37	5.52	45.38	0.12	0.00047	22.05
43	0.07	0.25	0.05	1.03	0.12	0.12	0.54	6.22	3.46	72.38	0.17	0.00059	22.73
44	0.23	0.24	0.10	1.18	0.09	0.19	0.58	4.32	4.83	56.95	0.18	0.00056	21.04
45	0.15	0.26	0.17	0.89	0.15	0.04	0.48	4.55	4.24	84.63	0.14	0.00039	21.27
46	0.13	0.17	0.14	0.96	0.15	0.08	0.73	7.55	4.50	60.46	0.12	0.00050	21.51
47	0.20	0.20	0.21	0.68	0.10	0.02	0.53	4.64	5.83	56.56	0.14	0.00036	23.80
48	0.21	0.19	0.04	0.06	0.12	0.25	0.58	7.77	5.32	72.13	0.14	0.00048	23.57
49	0.03	0.12	0.16	0.36	0.14	0.01	0.49	7.68	3.96	64.80	0.14	0.00053	25.55
50	0.09	0.01	0.07	1.73	0.08	0.04	0.45	7.41	5.43	47.56	0.17	0.00048	21.29

51	0.18	0.05	0.03	1.08	0.02	0.15	0.48	7.70	4.24	74.03	0.15	0.00041	21.97
52	0.17	0.13	0.30	1.50	0.04	0.03	0.50	5.22	4.42	81.35	0.17	0.00042	21.28
53	0.23	0.14	0.29	0.61	0.06	0.17	0.70	5.75	3.99	75.03	0.11	0.00051	22.88
54	0.18	0.01	0.28	1.30	0.18	0.07	0.67	7.89	5.59	56.83	0.16	0.00056	23.13
55	0.16	0.10	0.16	1.26	0.09	0.12	0.70	3.52	4.11	81.21	0.10	0.00050	25.57
56	0.16	0.18	0.23	0.73	0.06	0.21	0.58	7.82	4.49	64.50	0.16	0.00053	21.19
57	0.12	0.03	0.21	1.24	0.19	0.25	0.60	7.16	4.68	81.08	0.18	0.00057	24.92
58	0.10	0.14	0.02	0.67	0.17	0.24	0.77	5.62	5.88	59.37	0.12	0.00037	23.80
59	0.20	0.29	0.14	0.28	0.12	0.02	0.77	4.95	5.30	77.04	0.19	0.00056	21.70
60	0.19	0.26	0.28	0.94	0.20	0.12	0.50	7.80	4.60	62.04	0.18	0.00052	22.13
61	0.09	0.25	0.20	0.28	0.07	0.03	0.75	7.71	5.36	48.37	0.15	0.00031	24.99
62	0.05	0.23	0.08	0.55	0.01	0.24	0.43	2.18	4.54	55.73	0.12	0.00057	22.42
63	0.24	0.08	0.25	0.99	0.16	0.24	0.77	2.08	5.55	82.80	0.18	0.00041	25.41
64	0.07	0.17	0.10	1.25	0.20	0.11	0.48	6.61	3.03	66.36	0.11	0.00035	21.47
65	0.06	0.10	0.09	0.83	0.12	0.03	0.50	2.29	5.74	64.94	0.12	0.00045	23.62
66	0.15	0.23	0.06	0.30	0.09	0.03	0.70	3.63	3.36	89.70	0.18	0.00045	22.67
67	0.04	0.09	0.08	0.20	0.17	0.13	0.79	5.27	4.74	43.24	0.12	0.00033	24.17
68	0.09	0.24	0.30	1.07	0.18	0.17	0.47	2.89	4.76	64.32	0.19	0.00039	22.83
69	0.12	0.13	0.18	1.32	0.12	0.24	0.60	7.05	3.88	43.87	0.12	0.00034	23.20
70	0.03	0.08	0.30	0.58	0.16	0.10	0.67	3.24	4.61	45.69	0.16	0.00040	21.06
71	0.21	0.15	0.03	0.86	0.03	0.09	0.59	2.36	4.20	67.29	0.18	0.00030	21.23
72	0.15	0.24	0.15	1.37	0.06	0.16	0.54	6.49	5.02	77.89	0.14	0.00052	24.03
73	0.13	0.05	0.17	0.78	0.16	0.09	0.40	7.07	4.07	55.77	0.18	0.00033	24.86
74	0.06	0.22	0.17	0.50	0.10	0.05	0.61	6.00	4.39	60.61	0.17	0.00044	22.91
75	0.03	0.29	0.13	0.03	0.10	0.12	0.67	6.55	3.82	78.03	0.14	0.00042	22.13
76	0.03	0.20	0.27	1.34	0.18	0.16	0.40	7.81	3.62	64.06	0.17	0.00050	22.83
77	0.22	0.23	0.23	1.59	0.05	0.24	0.49	3.31	3.65	87.57	0.20	0.00043	22.16
78	0.01	0.03	0.16	1.70	0.21	0.19	0.68	4.86	4.72	84.44	0.17	0.00038	23.70

79	0.04	0.19	0.00	0.21	0.09	0.14	0.58	6.76	3.34	89.56	0.15	0.00039	23.22
80	0.00	0.23	0.03	1.17	0.19	0.02	0.69	3.09	3.47	62.84	0.14	0.00059	22.21
81	0.12	0.29	0.20	1.13	0.02	0.21	0.54	7.40	5.86	84.82	0.16	0.00041	25.09
82	0.11	0.05	0.04	0.11	0.00	0.21	0.77	6.69	4.14	45.46	0.16	0.00040	21.36
83	0.03	0.07	0.12	0.72	0.14	0.05	0.49	5.48	3.25	63.26	0.10	0.00036	21.17
84	0.14	0.27	0.09	1.78	0.08	0.18	0.46	8.00	4.22	58.31	0.12	0.00039	21.81
85	0.25	0.16	0.32	1.72	0.09	0.08	0.45	2.61	3.52	64.97	0.11	0.00052	23.91
86	0.13	0.28	0.28	0.05	0.19	0.22	0.45	7.36	4.23	57.80	0.13	0.00057	22.09
87	0.05	0.12	0.32	0.62	0.03	0.18	0.58	4.73	3.11	70.23	0.12	0.00043	22.19
88	0.00	0.29	0.28	1.76	0.20	0.23	0.66	6.17	4.11	77.96	0.19	0.00037	24.93
89	0.18	0.22	0.25	1.00	0.20	0.05	0.50	2.27	3.80	56.09	0.19	0.00033	25.89
90	0.00	0.01	0.15	1.51	0.15	0.07	0.42	5.28	4.63	77.71	0.11	0.00051	24.30
91	0.13	0.04	0.25	0.35	0.13	0.04	0.53	4.90	3.05	79.20	0.14	0.00059	21.59
92	0.08	0.20	0.01	1.00	0.17	0.01	0.51	3.68	4.44	78.37	0.19	0.00051	25.76
93	0.11	0.11	0.22	1.08	0.07	0.11	0.75	6.56	5.15	47.25	0.11	0.00047	23.96
94	0.23	0.21	0.14	1.14	0.05	0.14	0.74	5.21	4.42	42.01	0.11	0.00038	25.80
95	0.10	0.08	0.14	0.55	0.15	0.01	0.79	6.82	5.32	82.12	0.20	0.00060	24.40
96	0.17	0.12	0.08	1.66	0.05	0.05	0.44	5.71	4.00	53.30	0.18	0.00053	23.46
97	0.18	0.02	0.07	0.51	0.04	0.08	0.73	6.45	3.32	39.96	0.17	0.00038	23.17
98	0.15	0.11	0.10	0.90	0.05	0.04	0.56	5.54	4.79	83.67	0.15	0.00056	22.08
99	0.09	0.24	0.27	1.05	0.18	0.03	0.61	4.06	5.17	57.66	0.18	0.00037	21.71
100	0.11	0.01	0.32	1.73	0.08	0.11	0.68	5.46	5.18	45.66	0.12	0.00053	25.04
101	0.01	0.17	0.29	1.38	0.12	0.00	0.72	7.22	3.94	58.81	0.17	0.00045	22.02
102	0.22	0.09	0.11	0.00	0.03	0.18	0.43	7.20	3.57	54.93	0.19	0.00043	24.79
103	0.16	0.29	0.19	0.14	0.20	0.10	0.53	7.29	4.67	76.93	0.14	0.00045	24.21
104	0.01	0.28	0.07	0.42	0.19	0.06	0.56	3.95	5.41	68.28	0.15	0.00031	25.79
105	0.01	0.10	0.12	0.61	0.17	0.19	0.76	3.92	4.82	80.41	0.11	0.00041	25.32
106	0.11	0.12	0.04	0.45	0.17	0.01	0.43	2.76	4.71	71.71	0.11	0.00035	25.01

107	0.24	0.18	0.22	0.20	0.01	0.19	0.62	5.05	3.94	75.96	0.16	0.00054	25.99
108	0.13	0.05	0.03	1.43	0.11	0.21	0.57	3.02	5.75	88.17	0.10	0.00049	25.58
109	0.16	0.20	0.18	0.47	0.04	0.08	0.65	5.81	4.85	55.56	0.14	0.00037	21.82
110	0.19	0.28	0.08	0.17	0.16	0.10	0.74	3.30	5.44	83.54	0.12	0.00046	23.14
111	0.22	0.18	0.21	0.66	0.17	0.17	0.49	7.43	4.93	75.60	0.12	0.00049	24.40
112	0.07	0.22	0.18	0.43	0.12	0.11	0.42	4.68	4.10	69.98	0.11	0.00037	21.48
113	0.12	0.20	0.14	0.45	0.02	0.24	0.46	7.33	5.65	42.90	0.18	0.00056	25.17
114	0.21	0.15	0.14	1.45	0.04	0.06	0.51	6.41	5.56	68.05	0.17	0.00036	22.79
115	0.08	0.09	0.29	1.30	0.14	0.14	0.45	2.03	3.12	67.97	0.16	0.00043	24.55
116	0.06	0.27	0.20	1.80	0.05	0.13	0.67	4.46	3.37	57.89	0.16	0.00044	24.11
117	0.16	0.03	0.31	0.45	0.01	0.15	0.50	5.69	3.30	63.71	0.18	0.00059	23.68
118	0.12	0.25	0.02	1.02	0.16	0.17	0.69	6.62	3.02	88.28	0.18	0.00054	22.36
119	0.04	0.13	0.15	0.16	0.07	0.06	0.46	3.22	3.16	54.75	0.17	0.00035	25.34
120	0.11	0.14	0.21	1.20	0.00	0.14	0.54	6.99	4.53	72.05	0.15	0.00048	22.17
121	0.15	0.05	0.33	0.40	0.16	0.18	0.79	4.22	4.52	51.69	0.14	0.00032	25.19
122	0.23	0.15	0.14	1.35	0.06	0.08	0.62	7.97	4.69	86.82	0.11	0.00033	21.12
123	0.08	0.14	0.04	0.53	0.03	0.08	0.67	4.19	3.18	39.25	0.19	0.00057	24.72
124	0.14	0.02	0.11	0.67	0.14	0.05	0.54	5.12	3.77	49.31	0.17	0.00039	21.62
125	0.16	0.01	0.20	0.58	0.05	0.09	0.69	3.30	3.76	41.57	0.11	0.00047	23.00
126	0.06	0.23	0.22	1.02	0.09	0.17	0.44	3.91	5.30	67.84	0.17	0.00041	23.97
127	0.11	0.24	0.25	1.48	0.17	0.13	0.58	4.76	3.78	44.91	0.11	0.00044	25.03
128	0.12	0.25	0.30	0.26	0.15	0.10	0.47	3.15	4.87	79.92	0.19	0.00043	22.56
129	0.13	0.23	0.06	1.75	0.15	0.01	0.78	4.06	4.88	41.50	0.18	0.00036	24.22
130	0.02	0.18	0.22	1.10	0.19	0.04	0.75	6.60	3.18	48.08	0.12	0.00051	21.22
131	0.01	0.13	0.31	1.36	0.20	0.20	0.62	4.59	5.19	54.51	0.12	0.00034	22.07
132	0.20	0.06	0.08	0.60	0.10	0.15	0.59	6.76	4.13	62.15	0.15	0.00060	21.00
133	0.06	0.08	0.14	1.69	0.15	0.02	0.71	2.09	3.41	53.14	0.13	0.00033	25.46
134	0.08	0.12	0.22	0.41	0.08	0.20	0.50	4.94	4.03	60.39	0.12	0.00051	24.74

135	0.24	0.02	0.03	0.72	0.15	0.13	0.66	7.49	3.40	69.68	0.19	0.00041	25.91
136	0.11	0.05	0.22	0.82	0.14	0.22	0.62	7.17	4.68	56.30	0.13	0.00043	23.08
137	0.12	0.12	0.25	1.24	0.14	0.25	0.44	3.33	4.98	40.88	0.12	0.00030	22.59
138	0.08	0.01	0.08	0.98	0.13	0.04	0.68	3.68	3.68	65.81	0.11	0.00040	22.15
139	0.13	0.04	0.16	0.75	0.20	0.02	0.57	2.04	4.92	43.32	0.20	0.00056	24.44
140	0.18	0.14	0.26	0.64	0.10	0.24	0.71	5.79	4.85	78.82	0.14	0.00044	24.29
141	0.21	0.17	0.11	0.39	0.09	0.16	0.62	7.77	5.41	62.94	0.17	0.00044	24.14
142	0.10	0.04	0.23	0.43	0.15	0.14	0.75	2.55	3.88	51.27	0.14	0.00044	23.03
143	0.02	0.06	0.24	0.44	0.02	0.11	0.60	2.38	4.41	87.15	0.15	0.00051	24.09
144	0.05	0.25	0.16	1.62	0.07	0.02	0.71	5.24	3.58	51.37	0.18	0.00059	23.23
145	0.04	0.07	0.04	0.73	0.12	0.06	0.42	3.24	3.10	46.36	0.14	0.00037	24.99
146	0.18	0.14	0.11	0.83	0.01	0.24	0.41	3.36	5.55	69.50	0.18	0.00048	25.56
147	0.25	0.25	0.31	0.05	0.10	0.22	0.61	6.80	3.69	67.65	0.19	0.00042	25.93
148	0.23	0.20	0.19	1.42	0.18	0.18	0.47	2.80	5.02	58.04	0.11	0.00038	21.03
149	0.03	0.27	0.31	1.15	0.12	0.13	0.63	6.86	5.07	54.69	0.19	0.00042	21.73
150	0.07	0.09	0.19	0.13	0.12	0.07	0.73	3.63	4.80	75.06	0.13	0.00048	21.59
151	0.23	0.21	0.10	1.09	0.00	0.14	0.71	7.12	3.61	87.95	0.15	0.00038	24.85
152	0.05	0.16	0.02	0.35	0.04	0.23	0.74	4.99	3.21	86.89	0.16	0.00040	24.71
153	0.05	0.17	0.05	0.08	0.06	0.20	0.78	4.11	5.51	62.24	0.14	0.00041	21.18
154	0.04	0.25	0.21	1.27	0.18	0.23	0.78	3.55	4.02	67.15	0.13	0.00048	25.36
155	0.17	0.00	0.21	1.41	0.04	0.02	0.75	4.44	3.32	48.62	0.18	0.00043	25.87
156	0.19	0.06	0.09	1.25	0.21	0.02	0.68	5.06	3.19	71.65	0.19	0.00049	23.31
157	0.24	0.02	0.02	0.01	0.01	0.06	0.47	4.53	4.37	71.52	0.10	0.00059	22.49
158	0.19	0.21	0.18	1.23	0.05	0.18	0.48	5.04	4.44	70.44	0.18	0.00035	25.93
159	0.04	0.22	0.23	1.62	0.12	0.23	0.61	4.28	4.37	54.13	0.17	0.00059	22.64
160	0.19	0.08	0.05	0.22	0.11	0.07	0.73	6.15	3.76	61.93	0.18	0.00034	23.88
161	0.08	0.30	0.21	0.01	0.05	0.10	0.41	7.00	3.42	46.78	0.12	0.00032	25.34
162	0.15	0.20	0.25	0.18	0.16	0.21	0.64	6.02	5.37	44.15	0.15	0.00047	24.59

163	0.15	0.18	0.29	0.81	0.09	0.18	0.56	3.58	3.60	71.22	0.11	0.00038	21.84
164	0.04	0.14	0.33	0.81	0.05	0.24	0.42	5.55	5.21	69.00	0.11	0.00041	24.23
165	0.07	0.19	0.00	0.26	0.09	0.22	0.60	2.68	5.89	52.46	0.12	0.00045	25.31
166	0.24	0.17	0.21	1.79	0.16	0.11	0.43	4.09	5.12	75.40	0.13	0.00042	24.84
167	0.14	0.09	0.02	0.12	0.10	0.20	0.77	7.25	5.72	86.67	0.11	0.00053	21.98
168	0.11	0.10	0.25	1.07	0.09	0.04	0.69	2.19	5.25	59.90	0.18	0.00058	25.25
169	0.18	0.22	0.12	0.12	0.19	0.03	0.68	2.53	4.89	45.93	0.12	0.00031	22.86
170	0.13	0.16	0.02	1.04	0.04	0.17	0.48	2.62	3.76	51.83	0.20	0.00042	22.41
171	0.15	0.27	0.29	0.53	0.18	0.01	0.55	7.09	3.29	52.68	0.13	0.00044	24.98
172	0.07	0.19	0.04	1.16	0.19	0.20	0.70	2.47	5.26	86.01	0.14	0.00035	22.96
173	0.15	0.25	0.27	0.63	0.12	0.06	0.65	6.51	5.52	85.71	0.12	0.00049	24.88
174	0.16	0.12	0.12	1.26	0.16	0.05	0.56	6.90	3.59	59.70	0.11	0.00034	24.47
175	0.04	0.25	0.01	0.57	0.02	0.15	0.79	2.49	4.14	50.85	0.13	0.00045	21.30
176	0.06	0.27	0.29	0.27	0.13	0.02	0.58	6.75	5.00	70.60	0.16	0.00038	23.95
177	0.02	0.28	0.11	1.55	0.15	0.23	0.67	6.63	3.39	49.99	0.16	0.00049	23.93
178	0.10	0.22	0.28	0.14	0.08	0.13	0.59	5.42	4.04	51.15	0.12	0.00051	23.05
179	0.11	0.06	0.30	1.04	0.04	0.10	0.57	3.78	3.40	38.60	0.17	0.00058	22.72
180	0.03	0.13	0.25	1.60	0.15	0.07	0.69	2.24	4.57	38.14	0.18	0.00040	22.60
181	0.23	0.03	0.18	0.19	0.13	0.25	0.45	3.16	3.96	54.85	0.11	0.00040	24.63
182	0.15	0.22	0.03	0.70	0.13	0.15	0.60	7.23	3.81	76.39	0.18	0.00040	22.99
183	0.12	0.15	0.11	1.64	0.20	0.08	0.63	5.22	4.60	47.78	0.13	0.00056	23.38
184	0.19	0.28	0.15	0.01	0.01	0.16	0.40	6.42	5.00	59.57	0.18	0.00059	21.57
185	0.18	0.01	0.00	1.08	0.13	0.13	0.47	7.85	5.23	80.55	0.14	0.00055	22.24
186	0.06	0.02	0.18	1.21	0.11	0.09	0.50	2.95	5.53	72.63	0.13	0.00030	22.25
187	0.04	0.22	0.17	0.75	0.20	0.04	0.48	7.73	5.42	69.66	0.10	0.00043	25.74
188	0.05	0.07	0.16	1.47	0.03	0.20	0.41	3.51	5.57	86.44	0.15	0.00058	23.98
189	0.09	0.13	0.05	1.52	0.14	0.18	0.45	4.82	3.74	47.10	0.10	0.00059	24.20
190	0.05	0.17	0.31	0.32	0.19	0.21	0.54	4.38	5.10	54.40	0.16	0.00056	21.50

191	0.11	0.24	0.18	1.04	0.20	0.19	0.59	4.79	5.74	40.82	0.12	0.00034	21.68
192	0.10	0.20	0.17	0.49	0.07	0.04	0.62	7.31	3.93	81.93	0.12	0.00057	21.76
193	0.23	0.29	0.10	0.98	0.16	0.07	0.43	2.42	3.57	58.77	0.18	0.00057	21.84
194	0.20	0.27	0.02	0.57	0.13	0.04	0.45	2.32	5.50	82.63	0.18	0.00059	21.63
195	0.06	0.30	0.14	0.74	0.05	0.19	0.43	6.31	5.04	73.39	0.12	0.00040	25.96
196	0.17	0.18	0.06	1.29	0.02	0.10	0.77	5.27	5.67	74.59	0.11	0.00032	22.28
197	0.17	0.21	0.13	1.70	0.10	0.20	0.80	4.17	3.99	49.16	0.20	0.00057	24.50
198	0.13	0.10	0.19	0.57	0.13	0.22	0.57	5.73	5.66	51.85	0.11	0.00054	22.33
199	0.03	0.11	0.19	1.78	0.19	0.23	0.51	5.10	4.46	38.31	0.19	0.00042	24.39
200	0.06	0.00	0.25	0.78	0.17	0.01	0.49	2.78	3.28	89.26	0.17	0.00049	21.02
201	0.19	0.21	0.05	0.59	0.10	0.19	0.59	4.87	5.36	56.18	0.17	0.00051	24.91
202	0.13	0.23	0.30	0.85	0.20	0.16	0.55	3.84	4.54	58.00	0.14	0.00045	23.47
203	0.10	0.21	0.10	0.77	0.10	0.09	0.57	5.49	4.26	52.99	0.14	0.00055	22.26
204	0.18	0.16	0.12	0.52	0.12	0.06	0.46	6.54	4.61	74.91	0.15	0.00041	25.85
205	0.12	0.02	0.10	0.69	0.06	0.21	0.60	5.78	4.22	38.67	0.14	0.00030	25.51
206	0.05	0.14	0.29	1.41	0.03	0.03	0.49	6.89	5.18	73.79	0.17	0.00054	24.68
207	0.04	0.11	0.15	0.83	0.01	0.17	0.78	5.08	3.44	75.49	0.10	0.00046	24.10
208	0.06	0.06	0.21	1.38	0.16	0.22	0.45	4.59	4.78	73.58	0.15	0.00035	23.38
209	0.23	0.26	0.30	0.04	0.03	0.07	0.76	2.19	3.27	52.80	0.17	0.00050	23.19
210	0.24	0.10	0.33	0.89	0.04	0.05	0.76	6.32	5.40	44.16	0.12	0.00047	22.02
211	0.18	0.12	0.08	0.39	0.02	0.12	0.64	2.50	3.47	73.13	0.16	0.00049	24.89
212	0.05	0.14	0.05	0.33	0.03	0.05	0.61	5.88	5.58	74.27	0.12	0.00037	24.66
213	0.06	0.00	0.15	0.54	0.13	0.01	0.40	2.02	5.60	89.61	0.12	0.00049	22.73
214	0.24	0.24	0.20	1.07	0.10	0.15	0.70	6.11	5.20	66.89	0.15	0.00053	21.43
215	0.22	0.09	0.08	0.84	0.05	0.08	0.66	7.96	4.13	49.92	0.19	0.00048	23.59
216	0.02	0.03	0.28	0.35	0.01	0.07	0.49	7.58	3.36	73.74	0.20	0.00037	23.33
217	0.17	0.26	0.33	0.52	0.16	0.23	0.77	3.59	5.96	68.85	0.19	0.00050	22.23
218	0.13	0.15	0.13	1.64	0.14	0.25	0.66	5.81	3.28	85.67	0.19	0.00045	22.78

103

219	0.08	0.11	0.21	0.12	0.08	0.13	0.45	7.74	5.62	54.28	0.17	0.00058	23.07
220	0.11	0.23	0.26	1.46	0.13	0.18	0.63	2.41	4.66	76.07	0.10	0.00031	23.69
221	0.14	0.02	0.06	1.52	0.15	0.01	0.77	6.39	3.90	46.92	0.20	0.00055	21.43
222	0.14	0.17	0.31	1.49	0.11	0.09	0.72	7.00	5.59	74.72	0.19	0.00048	22.33
223	0.14	0.08	0.06	1.04	0.17	0.09	0.41	4.37	5.20	50.63	0.19	0.00054	24.10
224	0.17	0.21	0.23	1.11	0.11	0.03	0.74	4.67	5.84	50.44	0.10	0.00052	22.10
225	0.16	0.29	0.21	0.17	0.00	0.16	0.70	6.96	5.90	84.51	0.19	0.00042	22.87
226	0.01	0.02	0.10	0.38	0.16	0.22	0.52	2.93	4.33	88.35	0.16	0.00035	24.68
227	0.05	0.10	0.16	1.18	0.10	0.09	0.42	2.17	4.34	66.98	0.17	0.00035	22.89
228	0.17	0.30	0.20	1.26	0.20	0.10	0.66	3.34	3.43	46.97	0.14	0.00045	23.51
229	0.10	0.29	0.03	0.85	0.14	0.23	0.74	3.61	5.94	42.66	0.13	0.00050	23.59
230	0.13	0.24	0.13	0.28	0.11	0.20	0.68	2.71	5.01	71.39	0.17	0.00038	25.69
231	0.25	0.12	0.05	1.13	0.07	0.07	0.73	4.71	4.19	41.04	0.15	0.00053	23.01
232	0.02	0.15	0.11	1.03	0.08	0.03	0.63	2.50	4.01	75.26	0.14	0.00034	23.09
233	0.06	0.07	0.15	1.75	0.10	0.18	0.40	5.13	3.31	55.22	0.13	0.00055	22.39
234	0.08	0.27	0.24	0.13	0.06	0.24	0.69	4.96	3.60	38.05	0.13	0.00031	25.50
235	0.11	0.13	0.22	0.75	0.16	0.01	0.65	5.34	5.11	45.89	0.11	0.00035	24.24
236	0.13	0.02	0.01	1.09	0.17	0.24	0.44	4.78	5.03	76.44	0.13	0.00031	22.52
237	0.24	0.22	0.30	0.97	0.17	0.02	0.72	5.85	3.59	61.26	0.19	0.00049	24.07
238	0.07	0.06	0.33	0.58	0.09	0.11	0.75	5.57	3.25	55.04	0.16	0.00036	21.22
239	0.01	0.01	0.25	1.33	0.07	0.08	0.68	5.91	3.33	43.44	0.16	0.00045	21.07
240	0.17	0.22	0.26	1.12	0.09	0.07	0.79	7.37	3.81	55.29	0.16	0.00035	23.64
241	0.20	0.21	0.07	0.31	0.04	0.12	0.72	5.09	3.50	47.90	0.20	0.00056	25.01
242	0.08	0.08	0.13	0.07	0.17	0.17	0.41	4.01	3.03	41.28	0.11	0.00050	21.26
243	0.04	0.26	0.06	0.94	0.08	0.08	0.57	3.94	5.84	50.04	0.15	0.00055	24.34
244	0.19	0.06	0.17	1.72	0.17	0.15	0.54	7.06	5.76	81.85	0.10	0.00053	23.67
245	0.11	0.10	0.26	0.91	0.17	0.13	0.70	2.51	3.54	44.07	0.14	0.00040	23.24
246	0.12	0.25	0.01	0.31	0.17	0.22	0.45	6.47	5.19	48.16	0.20	0.00043	25.09

247	0.17	0.02	0.02	0.97	0.13	0.10	0.55	4.84	3.95	61.68	0.16	0.00049	25.37
248	0.19	0.14	0.21	1.39	0.20	0.24	0.50	7.98	5.94	73.95	0.15	0.00054	25.52
249	0.20	0.01	0.31	0.65	0.02	0.04	0.64	2.10	3.08	87.04	0.10	0.00057	21.40
250	0.17	0.10	0.06	0.79	0.00	0.22	0.64	2.91	4.41	76.31	0.15	0.00050	24.18
251	0.24	0.22	0.11	0.98	0.11	0.12	0.48	6.83	5.81	70.85	0.14	0.00048	21.65
252	0.01	0.12	0.17	0.53	0.02	0.10	0.65	5.01	5.25	79.29	0.20	0.00049	22.51
253	0.06	0.23	0.15	1.23	0.12	0.08	0.71	2.12	4.05	58.91	0.16	0.00060	23.75
254	0.05	0.16	0.19	1.61	0.07	0.17	0.44	2.69	4.31	58.23	0.11	0.00051	25.77
255	0.01	0.26	0.03	1.50	0.16	0.13	0.44	7.72	5.16	78.80	0.20	0.00049	21.41
256	0.19	0.25	0.26	0.32	0.15	0.07	0.78	6.22	4.96	48.85	0.12	0.00047	22.14
257	0.14	0.04	0.02	0.10	0.17	0.20	0.75	6.70	5.06	52.29	0.14	0.00054	23.58
258	0.11	0.08	0.11	1.60	0.04	0.19	0.74	3.08	4.43	68.42	0.19	0.00048	21.89
259	0.09	0.30	0.31	1.14	0.09	0.06	0.60	2.44	5.47	83.36	0.15	0.00038	23.32
260	0.19	0.28	0.06	0.90	0.12	0.16	0.51	7.84	5.95	73.92	0.19	0.00040	23.55
261	0.11	0.13	0.12	0.54	0.14	0.20	0.67	4.72	3.53	85.08	0.16	0.00058	24.06
262	0.23	0.29	0.05	0.36	0.13	0.03	0.74	2.14	3.92	71.89	0.16	0.00032	25.10
263	0.00	0.28	0.24	0.49	0.10	0.23	0.51	3.00	4.86	77.43	0.11	0.00060	24.74
264	0.14	0.04	0.33	0.18	0.01	0.06	0.64	7.60	5.09	81.02	0.12	0.00059	22.35
265	0.07	0.07	0.20	0.93	0.03	0.09	0.79	4.50	4.45	83.69	0.11	0.00032	22.51
266	0.17	0.26	0.26	1.35	0.09	0.11	0.50	4.13	3.72	80.85	0.17	0.00030	23.60
267	0.01	0.07	0.01	1.13	0.10	0.05	0.72	5.89	3.58	63.54	0.18	0.00044	25.39
268	0.06	0.20	0.21	1.15	0.21	0.01	0.51	2.77	4.51	38.97	0.14	0.00034	21.66
269	0.23	0.02	0.27	1.57	0.01	0.04	0.55	7.18	4.21	70.72	0.15	0.00031	24.02
270	0.09	0.24	0.04	1.59	0.14	0.21	0.60	6.53	5.86	76.56	0.13	0.00050	24.53
271	0.02	0.22	0.22	0.86	0.20	0.23	0.54	3.48	4.08	72.26	0.13	0.00031	23.46
272	0.03	0.29	0.30	1.55	0.05	0.23	0.55	3.75	3.08	43.56	0.15	0.00060	21.75
273	0.04	0.17	0.07	0.28	0.06	0.06	0.46	4.05	4.58	43.69	0.19	0.00030	25.61
274	0.14	0.29	0.24	0.44	0.03	0.11	0.46	2.92	5.54	87.74	0.12	0.00034	25.48

275	0.19	0.06	0.32	1.33	0.10	0.19	0.57	6.01	5.80	80.02	0.17	0.00056	21.99
276	0.16	0.01	0.29	0.06	0.15	0.17	0.80	4.58	4.09	52.56	0.11	0.00038	25.67
277	0.21	0.17	0.07	0.10	0.08	0.13	0.50	2.90	3.84	44.87	0.17	0.00050	21.23
278	0.19	0.14	0.16	0.16	0.05	0.03	0.47	7.27	3.68	56.38	0.17	0.00059	23.28
279	0.15	0.00	0.15	0.67	0.19	0.21	0.47	7.47	4.28	83.08	0.10	0.00046	21.86
280	0.21	0.10	0.24	0.88	0.12	0.01	0.53	4.73	3.79	72.47	0.10	0.00055	25.78
281	0.03	0.19	0.18	0.19	0.17	0.18	0.79	3.39	3.97	40.48	0.20	0.00039	26.00
282	0.17	0.02	0.22	0.34	0.17	0.13	0.62	2.83	4.06	56.98	0.13	0.00046	25.38
283	0.18	0.09	0.04	0.24	0.03	0.00	0.50	6.04	3.52	77.82	0.20	0.00046	22.45
284	0.07	0.10	0.33	0.76	0.01	0.01	0.71	3.07	4.63	50.38	0.14	0.00039	25.40
285	0.23	0.03	0.31	0.42	0.03	0.05	0.55	6.50	5.36	76.18	0.14	0.00035	22.43
286	0.13	0.16	0.15	1.19	0.13	0.03	0.76	3.45	4.50	58.60	0.18	0.00036	25.06
287	0.16	0.04	0.05	0.44	0.04	0.05	0.51	4.21	3.83	87.39	0.17	0.00055	24.48
288	0.00	0.21	0.23	0.92	0.16	0.11	0.69	3.22	4.15	80.33	0.19	0.00055	21.87
289	0.17	0.14	0.05	0.96	0.12	0.03	0.40	7.78	4.47	58.68	0.17	0.00038	24.05
290	0.15	0.29	0.31	0.82	0.01	0.22	0.45	3.27	3.63	85.79	0.19	0.00046	22.40
291	0.04	0.08	0.33	0.91	0.21	0.03	0.60	3.85	5.27	60.18	0.14	0.00056	25.08
292	0.01	0.29	0.24	1.69	0.20	0.06	0.45	2.52	3.17	81.16	0.10	0.00031	22.45
293	0.16	0.11	0.29	1.55	0.18	0.17	0.54	5.07	4.20	39.15	0.11	0.00043	24.75
294	0.04	0.24	0.02	1.67	0.15	0.16	0.50	4.29	4.19	57.56	0.17	0.00031	21.12
295	0.14	0.18	0.07	1.07	0.02	0.25	0.79	3.60	5.62	76.79	0.15	0.00059	22.68
296	0.05	0.28	0.18	0.02	0.04	0.08	0.80	2.39	3.01	86.08	0.15	0.00044	21.09
297	0.11	0.16	0.29	0.42	0.04	0.15	0.77	4.52	4.64	70.70	0.14	0.00052	23.20
298	0.08	0.08	0.05	0.86	0.09	0.10	0.66	2.70	4.75	83.27	0.15	0.00041	23.41
299	0.21	0.21	0.18	0.18	0.07	0.01	0.48	5.33	5.87	56.41	0.16	0.00059	21.15
300	0.02	0.23	0.29	1.56	0.19	0.19	0.49	5.01	4.64	85.55	0.14	0.00052	23.18
301	0.12	0.22	0.07	0.66	0.08	0.09	0.64	6.66	3.15	43.18	0.18	0.00043	21.49
302	0.16	0.28	0.23	0.30	0.02	0.17	0.43	7.57	5.98	88.46	0.16	0.00046	23.90

303	0.21	0.19	0.04	0.52	0.04	0.14	0.77	3.07	5.39	65.97	0.14	0.00056	24.22
304	0.07	0.25	0.31	0.63	0.08	0.07	0.71	3.01	3.78	43.06	0.16	0.00041	23.22
305	0.24	0.04	0.30	1.77	0.19	0.12	0.69	2.65	3.83	64.43	0.11	0.00051	22.43
306	0.15	0.22	0.09	0.51	0.08	0.12	0.52	6.21	5.27	41.03	0.11	0.00054	24.48
307	0.09	0.13	0.17	1.46	0.18	0.11	0.58	6.44	3.23	70.52	0.13	0.00051	21.11
308	0.10	0.00	0.09	1.50	0.01	0.03	0.73	4.92	4.32	44.36	0.17	0.00050	25.89
309	0.20	0.05	0.28	1.00	0.04	0.24	0.44	4.57	3.82	44.59	0.19	0.00058	24.38
310	0.25	0.07	0.20	0.51	0.17	0.24	0.52	5.35	4.51	70.36	0.14	0.00030	24.26
311	0.08	0.07	0.06	0.46	0.20	0.20	0.61	5.93	5.79	49.55	0.15	0.00036	22.54
312	0.21	0.13	0.26	0.03	0.18	0.21	0.54	2.25	3.56	84.19	0.14	0.00042	24.60
313	0.19	0.21	0.09	1.68	0.07	0.20	0.55	4.35	4.40	68.56	0.15	0.00048	23.26
314	0.12	0.21	0.16	1.69	0.14	0.09	0.46	5.87	5.15	68.17	0.15	0.00030	23.17
315	0.20	0.11	0.19	0.59	0.14	0.08	0.44	2.07	3.86	45.23	0.12	0.00031	23.53
316	0.07	0.18	0.12	1.54	0.11	0.01	0.43	6.73	5.49	57.40	0.17	0.00039	22.37
317	0.10	0.04	0.32	1.19	0.18	0.16	0.47	2.87	5.34	85.37	0.12	0.00051	21.36
318	0.06	0.11	0.20	0.97	0.08	0.15	0.41	7.64	5.29	53.67	0.13	0.00060	23.37
319	0.04	0.05	0.17	1.05	0.08	0.18	0.49	3.48	5.09	84.88	0.10	0.00051	25.33
320	0.17	0.26	0.24	0.37	0.07	0.08	0.52	7.43	3.95	62.36	0.19	0.00032	25.79
321	0.15	0.05	0.04	0.64	0.09	0.14	0.74	6.52	5.48	88.60	0.13	0.00031	23.78
322	0.17	0.09	0.16	0.37	0.16	0.18	0.58	5.53	5.93	42.26	0.11	0.00045	21.31
323	0.19	0.19	0.28	0.04	0.03	0.00	0.77	5.09	3.22	83.49	0.19	0.00051	23.07
324	0.18	0.02	0.23	1.13	0.02	0.22	0.50	2.66	4.65	40.38	0.16	0.00037	22.24
325	0.04	0.15	0.19	1.01	0.12	0.00	0.61	6.27	3.20	80.15	0.19	0.00055	24.57
326	0.08	0.22	0.23	0.17	0.02	0.16	0.49	7.62	5.75	78.71	0.15	0.00033	24.35
327	0.13	0.21	0.00	1.53	0.05	0.13	0.64	3.33	5.23	61.32	0.18	0.00055	22.57
328	0.13	0.06	0.14	0.65	0.16	0.19	0.58	5.98	4.70	40.02	0.19	0.00036	24.29
329	0.02	0.27	0.20	0.47	0.20	0.22	0.53	5.16	4.76	39.51	0.15	0.00037	22.60
330	0.21	0.30	0.20	1.70	0.02	0.21	0.52	2.97	3.79	38.20	0.17	0.00048	22.10

331	0.10	0.08	0.32	1.06	0.14	0.10	0.61	2.99	4.88	65.62	0.16	0.00049	21.83
332	0.07	0.23	0.01	1.39	0.07	0.02	0.70	2.05	3.06	42.43	0.14	0.00051	23.81
333	0.25	0.26	0.31	1.75	0.12	0.10	0.69	4.75	3.85	85.19	0.16	0.00036	21.19
334	0.23	0.26	0.28	0.89	0.06	0.09	0.73	2.88	3.45	56.05	0.17	0.00052	23.86
335	0.03	0.16	0.10	0.25	0.04	0.15	0.60	6.97	4.00	41.85	0.10	0.00031	25.21
336	0.23	0.10	0.15	1.25	0.14	0.11	0.56	3.49	5.51	79.66	0.15	0.00033	24.47
337	0.10	0.16	0.13	0.90	0.06	0.17	0.74	6.83	5.00	41.31	0.14	0.00054	25.26
338	0.24	0.08	0.26	0.25	0.04	0.19	0.78	5.44	3.22	66.55	0.12	0.00039	23.54
339	0.24	0.00	0.15	0.95	0.11	0.02	0.48	7.18	4.48	50.92	0.18	0.00051	25.27
340	0.08	0.15	0.22	0.13	0.02	0.03	0.79	7.08	4.39	52.22	0.12	0.00038	25.73
341	0.20	0.20	0.29	0.46	0.06	0.23	0.53	5.56	4.52	55.16	0.16	0.00057	23.84
342	0.24	0.18	0.09	1.78	0.13	0.10	0.66	6.96	4.99	59.07	0.18	0.00055	25.64
343	0.17	0.28	0.27	0.08	0.19	0.08	0.80	3.57	4.46	71.96	0.11	0.00049	21.24
344	0.25	0.18	0.21	1.69	0.04	0.16	0.75	6.67	5.77	80.78	0.18	0.00039	25.48
345	0.22	0.07	0.05	0.50	0.02	0.09	0.44	6.63	3.08	62.43	0.15	0.00046	22.93
346	0.05	0.03	0.12	1.72	0.02	0.18	0.41	7.48	3.27	41.99	0.15	0.00048	21.76
347	0.17	0.15	0.31	0.48	0.14	0.16	0.77	7.32	5.03	51.34	0.12	0.00059	23.55
348	0.03	0.27	0.05	0.74	0.18	0.07	0.78	5.94	5.25	63.63	0.20	0.00034	24.00
349	0.21	0.29	0.26	0.17	0.06	0.20	0.51	5.23	3.29	45.82	0.13	0.00047	24.46
350	0.01	0.24	0.13	0.22	0.13	0.13	0.55	6.35	3.26	53.77	0.17	0.00046	23.52
351	0.11	0.04	0.20	0.70	0.16	0.19	0.64	7.67	5.66	44.49	0.12	0.00040	21.01
352	0.09	0.09	0.24	0.20	0.06	0.16	0.62	3.39	5.49	40.26	0.14	0.00046	23.21
353	0.00	0.07	0.19	0.38	0.19	0.09	0.59	4.24	3.75	73.32	0.13	0.00037	25.14
354	0.15	0.19	0.05	0.04	0.10	0.16	0.56	7.69	5.34	82.20	0.13	0.00054	24.63
355	0.09	0.23	0.33	1.71	0.09	0.15	0.68	4.76	5.27	87.34	0.13	0.00040	23.39
356	0.03	0.29	0.30	1.58	0.05	0.20	0.58	6.29	5.45	73.26	0.19	0.00054	25.13
357	0.12	0.28	0.00	1.27	0.02	0.14	0.54	7.39	3.06	84.00	0.20	0.00044	23.15
358	0.14	0.30	0.30	0.93	0.14	0.00	0.57	6.65	5.39	57.47	0.16	0.00050	21.34

359	0.01	0.06	0.11	0.70	0.18	0.10	0.72	3.88	4.26	79.54	0.17	0.00057	25.81
360	0.17	0.20	0.11	0.76	0.19	0.03	0.55	3.93	5.35	86.48	0.15	0.00058	24.41
361	0.10	0.25	0.10	0.92	0.00	0.24	0.64	6.16	5.04	89.18	0.19	0.00051	21.56
362	0.21	0.13	0.02	1.76	0.01	0.20	0.65	3.62	4.76	74.18	0.16	0.00057	23.88
363	0.18	0.10	0.15	0.96	0.01	0.01	0.48	3.37	5.97	42.22	0.15	0.00057	23.04
364	0.04	0.03	0.33	1.51	0.14	0.15	0.61	7.62	5.48	52.06	0.18	0.00054	24.06
365	0.07	0.25	0.18	0.09	0.05	0.16	0.50	4.54	3.64	78.17	0.15	0.00055	23.57
366	0.11	0.12	0.27	1.22	0.02	0.19	0.72	7.93	3.02	83.79	0.19	0.00052	23.94
367	0.12	0.02	0.32	0.91	0.13	0.06	0.63	5.00	4.73	87.78	0.17	0.00058	25.40
368	0.15	0.18	0.04	1.64	0.05	0.10	0.72	7.79	4.81	65.45	0.19	0.00039	21.94
369	0.24	0.04	0.11	0.39	0.07	0.16	0.53	4.70	4.31	82.99	0.16	0.00033	21.91
370	0.21	0.12	0.09	1.21	0.17	0.22	0.74	3.44	4.29	40.15	0.18	0.00048	24.84
371	0.02	0.04	0.27	1.67	0.20	0.11	0.76	6.47	4.07	55.90	0.11	0.00033	25.97
372	0.18	0.15	0.05	0.16	0.11	0.14	0.65	5.20	3.73	42.51	0.13	0.00034	22.17
373	0.06	0.26	0.00	1.15	0.17	0.05	0.73	4.62	3.07	45.10	0.13	0.00044	25.69
374	0.02	0.30	0.15	1.23	0.08	0.19	0.78	6.93	4.25	65.19	0.20	0.00042	23.29
375	0.10	0.23	0.30	1.03	0.12	0.05	0.65	6.34	4.11	81.66	0.10	0.00040	21.71
376	0.03	0.10	0.26	0.65	0.14	0.06	0.60	6.91	3.77	82.42	0.19	0.00054	22.62
377	0.07	0.05	0.24	1.17	0.04	0.19	0.72	5.72	5.05	57.22	0.18	0.00049	23.84
378	0.05	0.25	0.14	0.09	0.14	0.05	0.52	4.84	4.08	42.59	0.12	0.00059	25.68
379	0.16	0.25	0.12	0.15	0.09	0.14	0.65	3.53	4.91	49.73	0.18	0.00045	22.80
380	0.04	0.15	0.20	1.32	0.15	0.00	0.72	2.20	3.17	45.19	0.14	0.00048	21.52
381	0.09	0.19	0.07	0.74	0.18	0.07	0.46	7.56	5.28	41.82	0.19	0.00058	25.11
382	0.22	0.01	0.01	0.84	0.02	0.06	0.58	7.41	5.89	55.99	0.19	0.00052	22.27
383	0.09	0.19	0.07	0.25	0.01	0.19	0.76	4.56	5.29	67.78	0.12	0.00044	25.83
384	0.22	0.07	0.07	1.67	0.10	0.22	0.74	7.34	3.70	60.25	0.13	0.00038	25.54
385	0.18	0.09	0.09	0.87	0.18	0.01	0.65	5.32	5.93	44.69	0.11	0.00056	23.40
386	0.03	0.13	0.03	1.56	0.02	0.24	0.59	5.41	5.46	59.24	0.19	0.00035	24.82

387	0.11	0.06	0.08	1.70	0.07	0.04	0.44	5.38	3.00	39.32	0.20	0.00045	24.42
388	0.08	0.06	0.28	0.34	0.05	0.07	0.76	7.06	3.66	79.19	0.13	0.00032	23.50
389	0.19	0.20	0.27	0.24	0.02	0.20	0.45	7.30	4.30	77.25	0.19	0.00054	21.74
390	0.20	0.10	0.03	0.07	0.21	0.15	0.76	3.55	5.12	60.51	0.18	0.00036	21.09
391	0.23	0.25	0.09	1.78	0.03	0.00	0.51	2.22	5.46	66.88	0.12	0.00047	22.69
392	0.20	0.23	0.06	0.76	0.02	0.17	0.78	2.47	3.15	67.09	0.20	0.00036	25.94
393	0.15	0.05	0.12	0.07	0.20	0.08	0.41	4.51	5.53	54.43	0.17	0.00054	22.84
394	0.11	0.23	0.25	0.88	0.03	0.02	0.66	3.35	5.01	38.35	0.11	0.00058	23.03
395	0.17	0.10	0.00	0.32	0.06	0.00	0.61	3.76	3.12	38.84	0.17	0.00047	25.84
396	0.05	0.26	0.10	0.11	0.15	0.03	0.66	5.82	4.88	55.46	0.20	0.00034	25.28
397	0.22	0.02	0.05	1.44	0.10	0.05	0.79	5.19	4.94	84.08	0.13	0.00032	25.76
398	0.03	0.03	0.27	0.72	0.17	0.20	0.61	5.66	4.62	76.61	0.20	0.00044	25.52
399	0.18	0.17	0.10	0.90	0.19	0.02	0.79	7.87	3.14	86.75	0.16	0.00032	21.48
400	0.05	0.07	0.12	1.23	0.17	0.08	0.51	5.15	4.31	66.07	0.16	0.00045	24.25
401	0.07	0.03	0.29	0.79	0.06	0.04	0.53	5.72	5.33	71.28	0.18	0.00042	25.22
402	0.21	0.16	0.15	1.35	0.07	0.21	0.41	4.91	4.38	85.03	0.17	0.00056	24.53
403	0.03	0.28	0.03	0.50	0.07	0.20	0.60	5.94	3.18	88.52	0.19	0.00039	25.23
404	0.11	0.28	0.33	1.25	0.06	0.22	0.47	4.69	4.94	80.58	0.11	0.00042	21.25
405	0.22	0.14	0.26	1.15	0.16	0.08	0.69	5.36	3.89	42.74	0.13	0.00047	24.55
406	0.16	0.09	0.11	1.60	0.11	0.19	0.69	2.34	5.70	60.92	0.14	0.00043	21.06
407	0.11	0.17	0.07	0.74	0.16	0.01	0.40	2.42	4.91	61.40	0.14	0.00052	25.08
408	0.23	0.00	0.28	1.49	0.15	0.18	0.66	7.92	3.24	56.52	0.10	0.00032	23.71
409	0.01	0.28	0.28	1.45	0.20	0.15	0.75	3.26	5.28	72.96	0.17	0.00055	25.12
410	0.14	0.03	0.19	1.17	0.05	0.20	0.72	3.66	3.93	84.70	0.12	0.00054	24.05
411	0.21	0.19	0.32	1.77	0.11	0.05	0.73	5.36	3.48	53.21	0.16	0.00041	21.28
412	0.07	0.22	0.31	0.27	0.07	0.05	0.49	6.28	5.42	77.08	0.12	0.00050	24.61
413	0.24	0.19	0.24	0.02	0.11	0.11	0.61	4.15	4.74	75.16	0.14	0.00041	25.35
414	0.01	0.05	0.03	1.76	0.15	0.04	0.43	2.86	3.58	64.61	0.13	0.00059	23.44

415	0.08	0.09	0.13	1.28	0.07	0.25	0.76	4.67	3.41	54.03	0.17	0.00043	22.29
416	0.19	0.05	0.12	1.53	0.01	0.22	0.45	3.14	4.90	40.68	0.16	0.00040	25.24
417	0.06	0.20	0.02	0.69	0.05	0.23	0.66	7.50	5.32	38.76	0.15	0.00056	25.63
418	0.16	0.18	0.33	0.23	0.08	0.04	0.67	2.56	5.79	75.81	0.12	0.00036	25.66
419	0.06	0.18	0.28	0.33	0.17	0.24	0.54	3.21	4.53	73.46	0.19	0.00035	21.80
420	0.02	0.09	0.29	1.73	0.01	0.24	0.66	6.92	3.33	56.77	0.15	0.00038	24.64
421	0.12	0.06	0.21	0.27	0.08	0.02	0.44	2.74	5.67	61.10	0.11	0.00053	23.27
422	0.05	0.12	0.28	0.33	0.13	0.03	0.62	4.45	3.40	63.15	0.18	0.00034	22.61
423	0.02	0.12	0.01	1.43	0.03	0.07	0.77	5.63	4.15	64.28	0.11	0.00044	23.50
424	0.10	0.05	0.30	0.87	0.01	0.24	0.72	5.84	4.18	67.73	0.10	0.00050	25.32
425	0.17	0.29	0.01	0.61	0.03	0.01	0.72	3.65	4.58	44.45	0.13	0.00058	24.85
426	0.18	0.08	0.16	1.00	0.13	0.16	0.67	5.78	3.53	43.81	0.11	0.00037	21.91
427	0.14	0.17	0.21	0.32	0.08	0.13	0.49	3.04	3.62	81.44	0.13	0.00052	24.80
428	0.20	0.04	0.21	1.44	0.10	0.20	0.72	2.72	3.98	71.78	0.12	0.00054	23.85
429	0.16	0.18	0.32	0.13	0.11	0.16	0.47	5.17	3.98	49.23	0.17	0.00036	21.96
430	0.25	0.14	0.29	0.60	0.10	0.02	0.63	6.57	3.09	44.96	0.10	0.00041	23.82
431	0.15	0.07	0.16	1.43	0.16	0.14	0.62	2.38	3.48	41.12	0.19	0.00055	24.32
432	0.13	0.28	0.23	0.87	0.05	0.12	0.61	5.68	5.61	78.41	0.13	0.00054	25.88
433	0.25	0.05	0.10	1.45	0.02	0.14	0.70	2.74	4.97	84.36	0.12	0.00054	23.70
434	0.13	0.01	0.12	1.65	0.09	0.10	0.76	5.59	5.13	70.10	0.18	0.00051	23.73
435	0.06	0.27	0.18	1.11	0.20	0.15	0.63	5.76	4.59	79.76	0.10	0.00039	23.89
436	0.02	0.26	0.04	0.75	0.08	0.07	0.51	6.60	4.96	41.72	0.19	0.00037	22.97
437	0.23	0.26	0.07	0.36	0.11	0.14	0.68	5.65	5.31	63.41	0.16	0.00060	22.92
438	0.20	0.29	0.29	0.26	0.12	0.05	0.47	7.95	3.97	75.52	0.13	0.00045	25.96
439	0.03	0.14	0.06	0.15	0.04	0.10	0.78	3.11	4.17	82.53	0.15	0.00038	21.33
440	0.18	0.02	0.16	0.71	0.13	0.08	0.44	6.19	5.59	87.90	0.11	0.00035	21.85
441	0.05	0.00	0.20	1.24	0.01	0.08	0.58	5.13	5.07	38.55	0.16	0.00059	24.19
442	0.22	0.27	0.16	1.74	0.16	0.25	0.68	5.65	3.63	66.28	0.17	0.00031	21.88

443	0.22	0.16	0.13	1.31	0.19	0.12	0.57	4.81	3.16	42.86	0.11	0.00038	23.91
444	0.17	0.15	0.13	1.27	0.01	0.19	0.42	6.38	4.86	80.27	0.11	0.00038	25.23
445	0.03	0.23	0.23	1.09	0.01	0.08	0.57	2.59	5.99	48.48	0.20	0.00037	25.75
446	0.09	0.06	0.30	1.47	0.10	0.22	0.75	7.64	5.80	40.57	0.17	0.00032	23.42
447	0.03	0.05	0.15	1.76	0.00	0.16	0.41	2.81	4.98	70.27	0.14	0.00037	21.79
448	0.16	0.24	0.24	1.21	0.10	0.11	0.68	4.17	4.77	69.56	0.18	0.00047	21.38
449	0.20	0.08	0.07	1.34	0.07	0.17	0.59	3.96	4.81	61.70	0.11	0.00044	22.32
450	0.11	0.24	0.11	1.30	0.10	0.17	0.77	5.46	3.67	53.57	0.13	0.00052	21.53
451	0.04	0.28	0.01	1.68	0.00	0.00	0.45	7.02	4.24	42.38	0.13	0.00038	24.26
452	0.14	0.28	0.32	1.51	0.20	0.05	0.46	3.46	5.75	64.74	0.11	0.00053	23.65
453	0.06	0.21	0.02	0.63	0.08	0.12	0.68	3.25	4.16	87.11	0.18	0.00060	24.96
454	0.04	0.24	0.17	0.50	0.14	0.18	0.55	7.90	3.11	53.49	0.20	0.00057	21.73
455	0.08	0.13	0.00	1.47	0.03	0.22	0.79	3.73	4.95	46.32	0.14	0.00050	23.66
456	0.24	0.16	0.11	0.41	0.17	0.21	0.79	4.43	3.65	57.69	0.15	0.00042	24.43
457	0.24	0.22	0.20	1.41	0.06	0.22	0.69	3.71	4.90	39.42	0.13	0.00030	25.05
458	0.10	0.27	0.24	0.10	0.04	0.15	0.59	3.38	4.32	62.66	0.13	0.00036	24.37
459	0.08	0.27	0.19	0.97	0.03	0.13	0.76	6.68	3.70	50.10	0.11	0.00038	22.07
460	0.06	0.19	0.17	0.78	0.05	0.09	0.73	7.51	4.62	77.61	0.16	0.00044	23.06
461	0.07	0.30	0.17	0.42	0.11	0.18	0.46	4.61	4.83	63.04	0.18	0.00042	25.16
462	0.00	0.01	0.21	0.91	0.18	0.12	0.43	7.83	3.42	81.42	0.19	0.00033	23.75
463	0.12	0.23	0.09	0.88	0.03	0.05	0.53	7.10	5.11	88.14	0.12	0.00031	22.00
464	0.24	0.09	0.22	0.01	0.17	0.01	0.48	2.64	3.49	72.50	0.11	0.00053	21.60
465	0.00	0.14	0.24	0.78	0.03	0.22	0.65	2.16	3.71	74.85	0.14	0.00049	24.16
466	0.12	0.13	0.32	0.36	0.21	0.23	0.58	3.41	4.17	79.43	0.12	0.00058	22.63
467	0.08	0.03	0.20	0.78	0.20	0.24	0.78	4.38	5.47	88.68	0.12	0.00047	21.37
468	0.00	0.11	0.08	0.29	0.11	0.07	0.46	7.85	5.18	65.88	0.17	0.00045	24.32
469	0.02	0.21	0.27	0.94	0.19	0.22	0.75	6.48	3.74	80.22	0.13	0.00031	21.45
470	0.06	0.07	0.09	0.71	0.15	0.00	0.70	3.94	4.35	48.21	0.11	0.00037	22.80

471	0.11	0.16	0.09	0.09	0.08	0.20	0.71	3.04	3.22	81.59	0.11	0.00049	24.58
472	0.10	0.01	0.27	0.95	0.10	0.19	0.73	5.42	3.94	68.59	0.15	0.00051	23.92
473	0.19	0.26	0.21	0.65	0.01	0.16	0.62	7.44	3.04	43.38	0.12	0.00044	21.92
474	0.14	0.11	0.14	1.12	0.18	0.03	0.56	4.91	3.71	80.91	0.19	0.00036	22.74
475	0.25	0.23	0.23	0.82	0.08	0.11	0.41	5.92	4.02	51.94	0.14	0.00032	23.36
476	0.21	0.05	0.11	0.23	0.18	0.11	0.63	2.01	3.15	59.29	0.12	0.00042	23.02
477	0.21	0.21	0.13	1.57	0.20	0.02	0.75	7.21	4.90	50.74	0.19	0.00041	23.63
478	0.03	0.00	0.04	0.40	0.20	0.08	0.46	6.25	3.67	65.12	0.20	0.00039	22.18
479	0.14	0.01	0.03	1.60	0.00	0.12	0.47	5.80	5.73	58.99	0.17	0.00052	22.58
480	0.01	0.09	0.04	0.30	0.14	0.10	0.41	6.85	5.91	71.20	0.15	0.00046	25.85
481	0.20	0.18	0.10	1.32	0.08	0.14	0.42	6.03	3.39	86.31	0.13	0.00043	22.66
482	0.13	0.07	0.32	0.45	0.18	0.09	0.71	3.29	4.81	62.27	0.20	0.00039	21.69
483	0.15	0.11	0.24	1.63	0.19	0.14	0.67	5.39	5.64	89.44	0.15	0.00057	22.95
484	0.22	0.15	0.12	1.19	0.14	0.23	0.60	6.59	5.88	88.81	0.15	0.00044	23.11
485	0.25	0.15	0.07	1.37	0.15	0.01	0.60	7.10	5.64	68.67	0.18	0.00044	23.48
486	0.16	0.16	0.06	0.92	0.01	0.18	0.50	7.03	5.43	53.06	0.17	0.00057	21.34
487	0.14	0.20	0.12	1.62	0.08	0.18	0.43	3.18	5.93	60.76	0.17	0.00055	24.12
488	0.02	0.01	0.28	0.59	0.14	0.19	0.66	6.07	3.24	39.11	0.10	0.00037	24.80
489	0.14	0.07	0.31	1.28	0.02	0.13	0.57	3.70	4.98	78.50	0.10	0.00049	25.90
490	0.23	0.13	0.07	1.80	0.03	0.03	0.64	6.94	5.68	48.64	0.14	0.00032	24.83
491	0.24	0.04	0.02	1.06	0.06	0.02	0.72	4.23	3.56	40.16	0.15	0.00056	22.94
492	0.06	0.09	0.06	0.24	0.03	0.23	0.75	5.69	5.61	65.54	0.16	0.00040	21.61
493	0.05	0.27	0.26	1.71	0.05	0.13	0.46	7.55	5.72	47.42	0.18	0.00032	23.92
494	0.21	0.10	0.27	0.27	0.12	0.06	0.51	4.49	3.64	48.93	0.13	0.00032	23.55
495	0.15	0.05	0.16	0.72	0.14	0.02	0.68	7.76	3.91	57.32	0.12	0.00034	22.22
496	0.20	0.15	0.28	0.15	0.05	0.11	0.42	6.98	4.60	88.05	0.10	0.00034	22.81
497	0.21	0.28	0.08	1.30	0.10	0.21	0.46	5.29	3.14	58.14	0.16	0.00056	23.83
498	0.18	0.27	0.15	0.52	0.13	0.10	0.59	6.09	5.17	58.37	0.19	0.00036	23.28

499	0.07	0.08	0.09	0.56	0.09	0.21	0.55	4.65	3.09	45.32	0.15	0.00042	23.66
500	0.13	0.22	0.09	1.61	0.09	0.13	0.41	6.07	5.90	57.15	0.18	0.00049	25.26
501	0.19	0.01	0.10	0.31	0.07	0.19	0.55	4.88	4.45	66.15	0.15	0.00033	22.52
502	0.19	0.30	0.23	0.11	0.03	0.08	0.49	2.93	5.98	83.14	0.15	0.00052	23.25
503	0.04	0.15	0.20	0.29	0.04	0.02	0.65	4.36	4.49	72.85	0.18	0.00048	22.48
504	0.08	0.08	0.23	0.55	0.17	0.17	0.46	6.12	5.49	88.89	0.10	0.00046	24.70
505	0.20	0.09	0.19	0.80	0.04	0.21	0.62	7.30	5.65	70.01	0.13	0.00045	23.98
506	0.22	0.13	0.25	0.68	0.04	0.16	0.55	4.43	5.56	47.34	0.16	0.00035	25.98
507	0.14	0.29	0.19	0.09	0.02	0.01	0.52	2.30	5.78	82.80	0.11	0.00040	25.42
508	0.22	0.22	0.28	0.04	0.12	0.06	0.63	2.15	4.35	63.95	0.17	0.00036	23.16
509	0.01	0.06	0.09	1.37	0.06	0.21	0.64	6.78	3.91	40.78	0.17	0.00045	23.32
510	0.19	0.12	0.20	1.54	0.14	0.17	0.80	7.52	3.43	50.25	0.15	0.00038	22.01
511	0.03	0.25	0.32	0.12	0.15	0.02	0.50	3.43	3.55	53.42	0.10	0.00044	23.41
512	0.22	0.20	0.08	1.63	0.07	0.23	0.42	3.86	5.73	62.64	0.18	0.00047	21.64
513	0.17	0.20	0.30	1.74	0.21	0.00	0.56	3.72	4.17	43.00	0.18	0.00049	24.78
514	0.24	0.06	0.13	1.01	0.11	0.02	0.56	7.38	5.95	52.89	0.13	0.00031	25.61
515	0.16	0.16	0.23	1.52	0.11	0.21	0.74	4.77	4.48	84.32	0.14	0.00032	22.70
516	0.06	0.08	0.14	0.97	0.03	0.14	0.49	7.66	4.59	49.40	0.17	0.00053	25.71
517	0.13	0.16	0.12	0.69	0.09	0.20	0.41	3.82	5.44	69.77	0.14	0.00052	24.15
518	0.11	0.02	0.13	1.35	0.09	0.17	0.52	2.22	3.55	48.25	0.19	0.00043	22.46
519	0.20	0.11	0.02	0.96	0.11	0.14	0.71	5.41	4.28	89.48	0.11	0.00034	23.77
520	0.20	0.11	0.19	0.00	0.06	0.16	0.53	2.79	4.33	46.09	0.11	0.00032	23.12
521	0.02	0.09	0.23	0.34	0.07	0.03	0.48	6.08	4.35	46.85	0.16	0.00050	22.54
522	0.25	0.06	0.09	1.66	0.02	0.22	0.64	5.58	3.51	74.13	0.12	0.00043	25.51
523	0.18	0.28	0.02	1.55	0.04	0.01	0.77	4.31	3.84	39.82	0.19	0.00056	21.49
524	0.09	0.06	0.10	0.84	0.20	0.13	0.72	2.46	5.38	68.92	0.18	0.00053	23.79
525	0.20	0.03	0.11	0.61	0.20	0.12	0.44	4.42	3.63	78.26	0.18	0.00051	25.70
526	0.03	0.12	0.18	1.46	0.12	0.23	0.43	4.04	4.66	46.20	0.11	0.00058	24.87

527	0.22	0.01	0.26	1.61	0.04	0.23	0.64	5.87	3.44	74.78	0.19	0.00052	24.56
528	0.21	0.04	0.19	1.65	0.05	0.07	0.48	3.88	5.10	82.35	0.17	0.00055	21.32
529	0.17	0.08	0.25	1.40	0.16	0.15	0.80	4.47	4.18	55.40	0.16	0.00057	22.65
530	0.18	0.17	0.22	1.31	0.06	0.19	0.80	2.29	4.66	85.94	0.13	0.00038	23.31
531	0.18	0.27	0.23	0.22	0.11	0.16	0.48	5.53	4.55	61.17	0.15	0.00031	21.96
532	0.13	0.30	0.19	0.85	0.09	0.17	0.52	6.45	5.90	86.38	0.17	0.00031	25.59
533	0.09	0.03	0.13	1.66	0.14	0.24	0.44	4.52	4.10	76.71	0.16	0.00034	24.81
534	0.15	0.14	0.26	0.62	0.15	0.10	0.57	6.26	5.70	66.74	0.20	0.00041	25.20
535	0.24	0.15	0.10	0.87	0.11	0.09	0.49	2.11	3.35	46.70	0.16	0.00053	22.77
536	0.01	0.03	0.03	1.79	0.19	0.07	0.73	2.34	4.69	58.49	0.16	0.00041	22.89
537	0.21	0.04	0.06	0.56	0.16	0.23	0.76	2.26	5.69	73.05	0.12	0.00037	21.17
538	0.08	0.12	0.29	1.30	0.12	0.25	0.79	5.39	5.60	47.66	0.16	0.00035	24.94
539	0.07	0.18	0.22	0.02	0.13	0.14	0.42	7.66	5.98	77.45	0.11	0.00054	21.58
540	0.09	0.16	0.18	0.38	0.13	0.13	0.65	5.50	4.73	53.72	0.16	0.00034	24.70
541	0.21	0.21	0.06	1.53	0.00	0.13	0.74	4.10	5.08	82.32	0.13	0.00046	24.89
542	0.22	0.24	0.17	0.29	0.21	0.15	0.65	2.35	3.34	38.41	0.16	0.00040	24.31
543	0.24	0.12	0.30	0.63	0.06	0.11	0.67	4.03	4.23	49.01	0.20	0.00045	21.03
544	0.19	0.24	0.17	1.40	0.12	0.20	0.76	6.30	3.87	89.96	0.17	0.00041	23.86
545	0.21	0.03	0.05	1.39	0.13	0.17	0.79	6.17	4.78	42.13	0.19	0.00048	24.33
546	0.10	0.04	0.24	1.22	0.19	0.04	0.47	6.11	4.06	86.22	0.14	0.00043	22.88
547	0.18	0.11	0.04	1.25	0.08	0.05	0.43	3.87	5.86	78.92	0.11	0.00041	24.51
548	0.03	0.13	0.15	1.11	0.17	0.13	0.65	7.92	4.92	79.50	0.18	0.00030	22.98
549	0.08	0.22	0.22	0.99	0.12	0.11	0.58	3.13	3.90	46.57	0.15	0.00035	25.83
550	0.21	0.27	0.08	1.22	0.18	0.03	0.78	6.42	5.14	52.08	0.18	0.00031	25.54
551	0.15	0.17	0.26	1.18	0.18	0.15	0.59	4.41	3.31	49.45	0.15	0.00032	24.14
552	0.18	0.18	0.17	0.41	0.03	0.04	0.75	3.77	3.05	55.02	0.20	0.00049	22.85
553	0.01	0.06	0.18	0.56	0.13	0.22	0.79	3.14	5.38	87.21	0.19	0.00053	24.20
554	0.12	0.10	0.03	1.43	0.07	0.24	0.60	3.41	5.40	85.26	0.18	0.00050	22.55

555	0.22	0.05	0.16	1.63	0.10	0.07	0.76	7.87	5.71	63.78	0.17	0.00037	22.20
556	0.10	0.25	0.13	0.66	0.02	0.18	0.42	2.06	5.35	79.99	0.16	0.00044	22.71
557	0.00	0.02	0.22	0.22	0.15	0.12	0.71	3.84	3.54	53.90	0.13	0.00047	21.46
558	0.18	0.15	0.32	0.67	0.08	0.25	0.59	6.14	4.43	50.23	0.17	0.00056	21.64
559	0.18	0.29	0.06	1.71	0.11	0.24	0.78	2.40	3.66	40.43	0.13	0.00045	22.27
560	0.08	0.18	0.24	0.53	0.21	0.08	0.65	3.17	4.65	62.72	0.15	0.00036	22.32
561	0.22	0.08	0.16	0.07	0.05	0.11	0.68	5.15	3.69	67.36	0.13	0.00035	22.66
562	0.24	0.26	0.18	0.08	0.04	0.18	0.42	4.14	5.13	77.12	0.13	0.00058	22.36
563	0.02	0.05	0.20	1.29	0.15	0.06	0.69	6.13	3.51	66.24	0.14	0.00039	22.96
564	0.13	0.11	0.31	0.76	0.18	0.07	0.54	6.79	4.93	39.55	0.15	0.00032	25.58
565	0.04	0.09	0.22	1.16	0.19	0.12	0.66	4.26	3.74	59.61	0.16	0.00055	24.00
566	0.12	0.11	0.07	1.79	0.16	0.09	0.67	4.08	5.08	82.93	0.13	0.00033	24.62
567	0.10	0.11	0.03	0.48	0.19	0.09	0.63	7.51	4.34	87.52	0.19	0.00042	25.82
568	0.13	0.18	0.04	1.14	0.04	0.12	0.56	5.31	4.56	77.33	0.14	0.00055	23.49
569	0.02	0.19	0.32	0.95	0.15	0.10	0.52	5.90	4.12	61.83	0.18	0.00041	25.62
570	0.10	0.19	0.10	1.06	0.01	0.03	0.67	7.88	5.16	84.80	0.14	0.00047	21.14
571	0.01	0.28	0.18	1.77	0.09	0.14	0.62	2.61	4.25	54.20	0.15	0.00037	25.37
572	0.21	0.02	0.08	1.38	0.01	0.19	0.68	4.88	5.54	61.46	0.14	0.00059	25.62
573	0.05	0.10	0.15	0.82	0.12	0.23	0.42	4.62	5.56	73.68	0.18	0.00047	23.13
574	0.05	0.11	0.13	1.16	0.20	0.21	0.56	2.60	3.89	84.07	0.12	0.00046	24.36
575	0.05	0.13	0.05	0.81	0.11	0.09	0.41	7.19	3.37	63.01	0.17	0.00032	21.57
576	0.00	0.12	0.24	1.41	0.15	0.10	0.79	6.88	3.21	60.80	0.17	0.00046	23.65
577	0.05	0.12	0.21	1.36	0.19	0.12	0.53	3.06	4.36	52.61	0.12	0.00045	22.31
578	0.23	0.20	0.01	1.10	0.13	0.17	0.70	6.71	3.86	54.58	0.15	0.00033	24.03
579	0.14	0.01	0.07	1.18	0.06	0.05	0.49	5.97	5.58	48.77	0.16	0.00050	24.69
580	0.15	0.20	0.31	1.10	0.00	0.11	0.47	2.33	4.84	60.70	0.11	0.00039	24.66
581	0.01	0.12	0.25	0.70	0.11	0.06	0.59	5.18	3.52	62.49	0.10	0.00046	25.95
582	0.14	0.04	0.31	0.23	0.18	0.11	0.63	2.71	4.94	49.08	0.12	0.00034	21.39

583	0.05	0.07	0.17	0.85	0.16	0.18	0.52	4.48	4.77	72.21	0.14	0.00045	24.01
584	0.12	0.19	0.01	0.73	0.02	0.18	0.57	4.21	5.63	57.07	0.11	0.00046	24.42
585	0.16	0.25	0.03	1.62	0.09	0.09	0.57	2.87	4.47	78.09	0.19	0.00040	21.42
586	0.23	0.13	0.31	1.33	0.19	0.23	0.70	7.35	3.88	86.60	0.16	0.00046	24.97
587	0.16	0.15	0.05	1.40	0.07	0.25	0.51	2.98	4.75	83.87	0.18	0.00047	21.72
588	0.04	0.06	0.25	0.03	0.01	0.12	0.73	4.26	4.21	66.47	0.14	0.00053	21.05
589	0.10	0.17	0.25	0.71	0.16	0.04	0.44	4.83	5.99	75.34	0.19	0.00057	22.34
590	0.22	0.17	0.06	0.83	0.11	0.22	0.65	5.51	4.15	69.07	0.20	0.00056	25.43
591	0.12	0.24	0.27	0.18	0.07	0.21	0.41	6.05	5.22	89.88	0.14	0.00058	21.11
592	0.02	0.12	0.27	1.36	0.05	0.10	0.56	4.23	5.69	81.77	0.16	0.00033	25.44
593	0.01	0.01	0.29	1.03	0.06	0.20	0.55	2.96	5.38	88.76	0.18	0.00043	25.68
594	0.22	0.22	0.27	1.20	0.12	0.07	0.54	2.01	3.11	64.19	0.15	0.00031	23.76
595	0.23	0.26	0.14	1.45	0.03	0.23	0.63	4.98	4.79	63.89	0.20	0.00050	22.04
596	0.16	0.07	0.01	0.68	0.10	0.25	0.66	2.58	5.06	51.44	0.10	0.00036	24.36
597	0.23	0.21	0.03	1.68	0.14	0.14	0.63	6.72	3.50	64.12	0.15	0.00034	24.13
598	0.14	0.21	0.13	0.35	0.09	0.04	0.59	3.03	4.41	60.06	0.17	0.00055	21.20
599	0.07	0.19	0.17	1.31	0.18	0.15	0.47	2.10	4.55	87.68	0.19	0.00033	23.00
600	0.09	0.18	0.08	1.35	0.08	0.04	0.52	3.57	4.27	47.17	0.16	0.00058	23.78
601	0.02	0.26	0.26	0.93	0.19	0.12	0.52	6.40	3.73	50.68	0.20	0.00052	25.65
602	0.09	0.07	0.09	1.20	0.08	0.07	0.70	2.24	5.96	83.31	0.16	0.00044	21.68
603	0.08	0.14	0.32	0.14	0.13	0.09	0.61	6.23	3.72	59.79	0.15	0.00056	22.82
604	0.14	0.03	0.14	1.05	0.21	0.16	0.48	5.50	4.80	49.67	0.14	0.00043	21.13
605	0.20	0.24	0.27	0.40	0.21	0.04	0.71	3.28	3.92	67.59	0.13	0.00035	24.28
606	0.10	0.02	0.32	1.56	0.01	0.18	0.61	4.30	3.79	74.41	0.20	0.00033	25.47
607	0.13	0.17	0.18	0.46	0.18	0.24	0.74	7.15	3.61	51.05	0.15	0.00051	22.00
608	0.12	0.27	0.19	0.15	0.08	0.12	0.63	4.12	3.44	61.87	0.16	0.00041	23.10
609	0.17	0.19	0.28	1.28	0.02	0.07	0.53	7.04	5.92	45.55	0.13	0.00040	22.20
610	0.02	0.16	0.13	1.02	0.18	0.22	0.76	3.97	3.13	59.50	0.13	0.00042	22.75

611	0.08	0.08	0.00	0.49	0.03	0.11	0.64	3.18	3.07	46.07	0.12	0.00050	24.78
612	0.09	0.19	0.16	1.74	0.15	0.13	0.64	3.99	5.22	78.96	0.19	0.00042	25.72
613	0.07	0.03	0.03	0.62	0.06	0.06	0.68	3.50	3.99	51.62	0.14	0.00035	23.34
614	0.25	0.01	0.25	0.43	0.06	0.00	0.54	5.67	5.57	48.51	0.13	0.00047	21.53
615	0.02	0.14	0.29	0.21	0.06	0.05	0.53	6.94	4.87	65.71	0.18	0.00052	23.61
616	0.02	0.11	0.06	1.73	0.13	0.04	0.69	3.53	5.82	47.96	0.12	0.00033	24.51
617	0.16	0.29	0.32	0.59	0.17	0.08	0.70	7.13	5.80	74.34	0.19	0.00060	25.45
618	0.20	0.16	0.06	0.08	0.04	0.02	0.54	2.75	4.83	41.64	0.13	0.00052	21.30
619	0.12	0.04	0.31	0.39	0.09	0.15	0.63	6.55	5.50	46.44	0.13	0.00056	21.78
620	0.19	0.01	0.01	0.33	0.12	0.15	0.67	5.25	4.71	39.89	0.14	0.00039	25.92
621	0.11	0.29	0.11	0.47	0.16	0.14	0.69	7.53	3.35	44.79	0.18	0.00047	22.05
622	0.14	0.27	0.08	1.64	0.12	0.23	0.67	2.57	5.43	51.52	0.18	0.00050	22.63
623	0.20	0.03	0.03	1.58	0.13	0.18	0.51	6.78	6.00	89.04	0.14	0.00058	23.11
624	0.20	0.13	0.29	1.42	0.01	0.06	0.62	4.80	4.72	51.02	0.11	0.00057	21.67
625	0.24	0.03	0.28	0.21	0.00	0.09	0.45	3.80	5.45	47.50	0.13	0.00053	24.75
626	0.16	0.06	0.08	1.08	0.03	0.06	0.44	5.96	5.08	76.88	0.16	0.00048	22.90
627	0.00	0.09	0.12	0.20	0.05	0.18	0.52	3.43	4.57	76.08	0.11	0.00053	22.11
628	0.10	0.20	0.00	1.56	0.19	0.22	0.74	5.62	3.30	85.33	0.15	0.00048	24.98
629	0.09	0.14	0.30	1.44	0.20	0.15	0.78	4.97	5.76	56.66	0.13	0.00058	25.29
630	0.07	0.13	0.02	1.50	0.13	0.15	0.75	6.87	4.99	53.94	0.19	0.00034	25.43
631	0.05	0.29	0.22	0.80	0.10	0.08	0.77	3.90	3.81	81.69	0.10	0.00033	25.88
632	0.06	0.15	0.01	1.45	0.07	0.02	0.45	4.39	4.53	79.72	0.20	0.00051	21.15
633	0.22	0.19	0.04	0.23	0.15	0.02	0.42	7.14	4.40	52.34	0.16	0.00060	25.16
634	0.15	0.20	0.02	0.56	0.16	0.12	0.55	5.99	4.36	66.67	0.12	0.00048	21.40
635	0.15	0.27	0.17	1.57	0.06	0.21	0.63	5.96	5.14	55.62	0.14	0.00052	23.72
636	0.24	0.17	0.27	0.49	0.11	0.25	0.48	2.83	5.82	65.40	0.19	0.00031	25.15
637	0.03	0.24	0.22	1.54	0.17	0.10	0.71	2.98	3.85	43.66	0.15	0.00034	22.76
638	0.01	0.08	0.28	0.64	0.07	0.04	0.78	2.45	5.77	85.46	0.18	0.00030	24.77

639	0.02	0.19	0.01	0.69	0.16	0.07	0.46	4.19	4.26	44.26	0.13	0.00036	21.44
640	0.05	0.17	0.26	1.66	0.18	0.06	0.51	4.00	4.29	82.01	0.11	0.00058	22.77
641	0.20	0.00	0.27	1.21	0.18	0.06	0.53	2.85	5.97	47.69	0.16	0.00057	21.81
642	0.09	0.18	0.26	0.60	0.08	0.17	0.69	3.74	5.04	41.40	0.19	0.00042	23.45
643	0.12	0.16	0.24	1.67	0.14	0.14	0.60	6.69	3.13	60.08	0.13	0.00053	24.93
644	0.09	0.21	0.02	1.49	0.04	0.17	0.74	2.54	4.38	82.70	0.10	0.00053	22.12
645	0.07	0.02	0.23	0.80	0.19	0.09	0.71	3.69	5.84	69.13	0.12	0.00040	24.57
646	0.12	0.14	0.30	1.32	0.09	0.06	0.57	7.74	3.48	50.52	0.12	0.00039	21.08
647	0.02	0.05	0.16	0.06	0.15	0.06	0.71	6.37	5.65	39.63	0.16	0.00043	25.02
648	0.04	0.06	0.12	0.48	0.00	0.17	0.69	4.33	4.29	66.58	0.12	0.00035	23.73
649	0.08	0.09	0.27	1.72	0.01	0.21	0.56	7.94	5.21	75.69	0.18	0.00057	25.14
650	0.09	0.10	0.12	0.37	0.11	0.15	0.73	5.86	4.48	89.33	0.19	0.00048	21.77

Appendix 2. The building material details

Exterior Surface Construction		
Construction Type	**Layers**	**Material Properties**
Walls	20 mm plaster outside + 200 mm concrete block + 20 mm plaster inside	**20mm plaster:** • Roughness: Smooth • Thickness: 0.02 m • Conductivity: 0.25 W/m.K • Density: 900 kg/m^3 • Specific Heat: 830 J/kg.K • Thermal Absorptance: 0.9 • Solar Absorptance: 0.5 • Visible Absorptance: 0.4 **200 mm concrete blocks:** • Roughness: MediumRough • Thickness: 0.2 m • Conductivity: 0.19 W/m.K • Density: 600 kg/m^3 • Specific Heat: 840 J/kg.K • Thermal Absorptance: 0.9 • Solar Absorptance: 0.6 • Visible Absorptance: 0.5
Floors	MAT-CC05 4 HW Concrete + CP02 Carpet Pad	**MAT-CC05 4 HW CONCRETE:** • Roughness: Rough • Thickness: 0.1016 m • Conductivity: 01.311 W/m.K • Density: 2240 kg/m^3 • Specific Heat: 836.8 J/kg.K • Thermal Absorptance: 0.9 • Solar Absorptance: 0.85 • Visible Absorptance: 0.85 **CP02 CARPET PAD:**

		• Roughness: Smooth • Thermal Resistance: 0.1 m^2.K/W • Thermal Absorptance: 0.9 • Solar Absorptance: 0.8 • Visible Absorptance: 0.8
Roofs	10 mm built-up roofing + 150 mm concrete roof slab + 12.7 mm plaster inside	**10m built-up roofing** • Roughness: Very Rough • Thickness: 0.001 m • Conductivity: 0.16 W/m.K • Density: 1121.29 kg/m^3 • Specific Heat: 1460 J/kg.K • Thermal Absorptance: 0.9 • Solar Absorptance: 0.7 • Visible Absorptance: 0.7 **ROOF CONCRETE:** • Roughness: Rough • Thickness: 0.15 m • Conductivity: 01.311 W/m.K • Density: 2240 kg/m^3 • Specific Heat: 836.8 J/kg.K • Thermal Absorptance: 0.9 • Solar Absorptance: 0.85 • Visible Absorptance: 0.85 **12.7 mm plaster:** • Roughness: Smooth • Thickness: 0.01270 m • Conductivity: 0.25 W/m.K • Density: 900 kg/m^3 • Specific Heat: 830 J/kg.K • Thermal Absorptance: 0.9 • Solar Absorptance: 0.5 • Visible Absorptance: 0.4
Interior Surface Construction		

| Interior Walls | 13mm Lightweight Plaster + 100mm uninsulated concrete block | **13mm Lightweight Plaster:**

• Roughness: MediumSmooth
• Thickness: 0.013 m
• Conductivity: 0.16 W/m.K
• Density: 600 kg/m^3
• Specific Heat: 1090 J/kg.K
• Thermal Absorptance: 0.9
• Solar Absorptance: 0.4
• Visible Absorptance: 0.4
100mm uninsulated concrete block:

• Roughness: MediumRough
• Thickness: 0.1 m
• Conductivity: 0.19 W/m.K
• Density: 600 kg/m^3
• Specific Heat: 840 J/kg.K
• Thermal Absorptance: 0.9
• Solar Absorptance: 0.6
• Visible Absorptance: 0.5 |
| Interior floor | F16 Acoustic Tile+ F05 Ceiling airspace resistance + M11 100mm lightweight concrete | **F 16 Acoustic Tile**

• Roughness: MediumSmooth
• Thickness: 0.0191m
• Conductivity: 0.8 W/m.K
• Density: 1700 kg/m^3
• Specific Heat: 590 J/kg.K
• Thermal Absorptance: 0.9
• Solar Absorptance: 0.3
• Visible Absorptance: 0.3
F 05 Ceiling air space resistance

• Thermal Resistance: 0.18 m^2.K/W
M11 150mm lightweight concrete:

• Roughness: MediumRough
• Thickness: 0.15 m
• Conductivity: 2.30 W/m.K
• Density: 1280 kg/m^3 |

		• Specific Heat: 840 J/kg.K • Thermal Absorptance: 0.9 • Solar Absorptance: 0.5 • Visible Absorptance: 0.5
Ceilings	M11 150mm lightweight concrete + F 05 Ceiling air space resistance + F 16 Acoustic Tile	**M11 150mm lightweight concrete:** • Roughness: MediumRough • Thickness: 0.15 m • Conductivity: 2.30 W/m.K • Density: 1280 kg/m^3 • Specific Heat: 840 J/kg.K • Thermal Absorptance: 0.9 • Solar Absorptance: 0.5 • Visible Absorptance: 0.5 **F 05 Ceiling air space resistance** • Thermal Resistance: 0.18 m^2.K/W **F 16 Acoustic Tile** • Roughness: MediumSmooth • Thickness: 0.0191m • Conductivity: 0.6 W/m.K • Density: 368 kg/m^3 • Specific Heat: 590 J/kg.K • Thermal Absorptance: 0.9 • Solar Absorptance: 0.3 • Visible Absorptance: 0.3
Ground Contact Surface Construction		
Walls/Floors	MAT-CC05 4HW CONCRETE + CP02 CARPET PAD	**MAT-CC05 4HW CONCRETE:** • Roughness: Rough • Thickness: 0.101600 m • Conductivity: 1.311 W/m.K • Density: 2240 kg/m^3 • Specific Heat: 836.8 J/kg.K • Thermal Absorptance: 0.9 • Solar Absorptance: 0.85 • Visible Absorptance: 0.85

		CP02 CARPET PAD
		- Roughness: Smooth - Thermal Resistance: 0.1 m^2.K/W - Thermal Absorptance: 0.9 - Solar Absorptance: 0.8 - Visible Absorptance: 0.8
Exterior Subsurface Constructions		
Windows	Theoretical Glass	**Theoretical Glass:** - Optical Data Type: SpectralAverage - Thickness: 0.006 m - Conductivity: 0.0108 W/m.K - Solar Transmittance at Normal Incidence: 0.2374 - Front Side Solar Reflectance at Normal Incidence: 0.712600 - Back Side Solar : 0 - Visible Transmittance at Normal Incidence: 0.251200 - Front Side Visible Reflectance at Normal Incidence: 0.698800 - Front Side Infrared Hemispherical Emissivity: 0.985 - Back Side Infrared Hemispherical Emissivity: 0.985 - Dirt Collection Factor For Solar and Visible Transmittance: 1 - Solar Diffusing: Off
Exterior Door	F08 Metal Surface + IO1 25mm insulation board	**F08 Metal Surface:** - Roughness: Smooth - Thickness: 0.0008 m - Conductivity: 45.28 W/m.K - Density: 7824 kg/m^3 - Specific Heat: 500 J/kg.K - Thermal Absorptance: 0.9 - Solar Absorptance: 0.7 - Visible Absorptance: 0.7 **IO1 25mm insulation board:** - Roughness: Medium Rough - Thickness: 0.0254 m - Conductivity: 0.03 W/m.K - Density: 43 kg/m^3

		• Specific Heat: 1210 J/kg.K
		• Thermal Absorptance: 0.9
		• Solar Absorptance: 0.6
		• Visible Absorptance: 0.6
Interior Window and Door Construction		
Interior Window	Clear 3mm	**Clear 3mm:** • Optical Data Type: SpectralAverage • Thickness: 0.003 m • Conductivity: 0.0108 W/m.K • Solar Transmittance at Normal Incidence: 0.837 • Front Side Solar Reflectance at Normal Incidence: 0.075 • Back Side Solar : 0 • Visible Transmittance at Normal Incidence: 0.898 • Front Side Visible Reflectance at Normal Incidence: 0.08100 • Front Side Infrared Hemispherical Emissivity: 0.84 • Back Side Infrared Hemispherical Emissivity: 0.84 • Dirt Collection Factor For Solar and Visible Transmittance: 1 • Solar Diffusing: Off
Interior door	G025 25mm wood	**G025 25mm wood:** • Roughness: MediumSmooth • Thickness: 0.0254 m • Conductivity: 0.15 W/m.K • Density: 608 kg/m^3 • Specific Heat: 1630 J/kg.K • Thermal Absorptance: 0.9 • Solar Absorptance: 0.5 • Visible Absorptance: 0.5

Appendix 3. 48 cases randomly generated for meta-model verification

Number	Roof Insulation U Value	Wall U Value	Window U Value	Window SHGC	Equipment power density	Lighting power density	Occupancy density	Infiltration	Ventilation	Cooling Setpoint
1	0.14	0.16	0.99	0.12	5.29	4.65	66.54	0.15	0.00046	23.74
2	0.18	0.21	1.29	0.15	6.29	5.15	75.19	0.17	0.00051	24.58
3	0.15	0.18	1.08	0.13	5.62	4.81	69.34	0.16	0.00048	24.01
4	0.14	0.16	0.98	0.11	5.27	4.63	66.33	0.15	0.00046	23.72
5	0.11	0.13	0.76	0.09	4.54	4.27	60.03	0.14	0.00043	23.12
6	0.16	0.19	1.16	0.14	5.88	4.94	71.59	0.16	0.00049	24.23
7	0.11	0.13	0.79	0.09	4.63	4.31	60.75	0.14	0.00043	23.19
8	0.22	0.27	1.61	0.19	7.35	5.68	84.37	0.19	0.00057	25.46
9	0.24	0.29	1.73	0.20	7.78	5.89	88.11	0.20	0.00059	25.82
10	0.10	0.12	0.69	0.08	4.30	4.15	57.94	0.14	0.00042	22.92
11	0.20	0.24	1.43	0.17	6.75	5.38	79.17	0.18	0.00054	24.96
12	0.13	0.16	0.95	0.11	5.17	4.59	65.50	0.15	0.00046	23.64
13	0.14	0.17	1.02	0.12	5.41	4.70	67.54	0.16	0.00047	23.84
14	0.23	0.28	1.67	0.19	7.55	5.78	86.13	0.19	0.00058	25.63
15	0.02	0.02	0.13	0.01	2.43	3.21	41.69	0.11	0.00032	21.36
16	0.02	0.03	0.16	0.02	2.52	3.26	42.53	0.11	0.00033	21.44
17	0.21	0.25	1.50	0.17	7.00	5.50	81.30	0.18	0.00055	25.16
18	0.19	0.23	1.40	0.16	6.67	5.33	78.46	0.18	0.00053	24.89
19	0.22	0.26	1.57	0.18	7.22	5.61	83.24	0.19	0.00056	25.35
20	0.24	0.29	1.76	0.21	7.87	5.94	88.89	0.20	0.00059	25.89
21	0.20	0.24	1.44	0.17	6.79	5.40	79.56	0.18	0.00054	25.00
22	0.12	0.14	0.83	0.10	4.77	4.38	62.00	0.15	0.00044	23.31

23	0.20	0.23	1.40	0.16	6.68	5.34	78.59	0.18	0.00053	24.90
24	0.03	0.04	0.21	0.02	2.71	3.35	44.15	0.11	0.00034	21.59
25	0.16	0.19	1.15	0.13	5.84	4.92	71.28	0.16	0.00049	24.20
26	0.04	0.04	0.26	0.03	2.86	3.43	45.45	0.11	0.00034	21.72
27	0.24	0.28	1.70	0.20	7.67	5.83	87.12	0.19	0.00058	25.72
28	0.13	0.16	0.94	0.11	5.13	4.57	65.14	0.15	0.00046	23.61
29	0.10	0.12	0.75	0.09	4.49	4.24	59.56	0.14	0.00042	23.07
30	0.07	0.08	0.48	0.06	3.59	3.79	51.76	0.13	0.00038	22.32
31	0.19	0.23	1.39	0.16	6.65	5.32	78.26	0.18	0.00053	24.87
32	0.11	0.14	0.82	0.10	4.74	4.37	61.72	0.15	0.00044	23.28
33	0.14	0.17	1.02	0.12	5.41	4.71	67.56	0.16	0.00047	23.84
34	0.15	0.19	1.11	0.13	5.71	4.85	70.12	0.16	0.00049	24.09
35	0.15	0.18	1.10	0.13	5.67	4.84	69.83	0.16	0.00048	24.06
36	0.15	0.19	1.11	0.13	5.70	4.85	70.08	0.16	0.00049	24.08
37	0.24	0.28	1.70	0.20	7.66	5.83	87.07	0.19	0.00058	25.72
38	0.17	0.20	1.23	0.14	6.09	5.05	73.45	0.17	0.00050	24.41
39	0.09	0.11	0.65	0.08	4.16	4.08	56.69	0.14	0.00041	22.80
40	0.11	0.13	0.79	0.09	4.62	4.31	60.73	0.14	0.00043	23.19
41	0.17	0.21	1.26	0.15	6.19	5.09	74.28	0.17	0.00051	24.49
42	0.02	0.02	0.11	0.01	2.36	3.18	41.13	0.11	0.00032	21.30
43	0.17	0.20	1.20	0.14	6.00	5.00	72.67	0.17	0.00050	24.33
44	0.17	0.20	1.21	0.14	6.02	5.01	72.87	0.17	0.00050	24.35
45	0.05	0.06	0.38	0.04	3.26	3.63	48.94	0.12	0.00036	22.05
46	0.03	0.04	0.23	0.03	2.77	3.39	44.70	0.11	0.00034	21.64
47	0.08	0.09	0.57	0.07	3.89	3.95	54.40	0.13	0.00039	22.58
48	0.09	0.11	0.65	0.08	4.18	4.09	56.91	0.14	0.00041	22.82